MASTER THESIS

Title: Spectral Amplitude and Phase Characterization of Optical Devices by RF scan

Author: Giuseppe Pecere

Supervisors: Andrea Carena, Politecnico di Torino

Maria C. Santos Blanco, UPC Barcelona

Telecommunication Engineering, UPC, Barcelona

Master of Science in Telecommunication Engineering, Third School of Engineering: Information Technology, Politecnico di Torino

A mio padre

INDEX

TABLE OF CONTENTS

I. INTRODUCTION pag. 9

1.1 OBJECTIVES pag. 11

1.1.1 General

1.1.2 Specific

1.2 ORGANIZATION pag. 11

II. BASIC CONCEPTS pag. 13

2.1 DISPERSION THEORY pag. 15

2.2 MACH-ZEHNDER DEVICES pag. 21

2.2.1 Mach-Zehnder Interferometer: Modulator and Optical Filter pag.21

2.2.1.1 MZI Optical Filter pag.22

2.2.1.2 MZI Modulator pag. 26

III. MATHEMATICAL ANALYSIS pag. 30

3.1 MATHEMATICAL ANALYSIS WITH MAZI MODULATOR IN PUSH-PULL CONFIGURATION pag. 33

3.2 MPSM ANALYSIS pag. 34

3.3 PEUCHERET'S METHOD ANALYSIS pag. 36

3.4 ANALYSIS WITH MZI MODULATOR IN ASYMMETRIC CONFIGURATION pag. 40

3.5 MZSM ANALYSIS pag. 47

3.6 RF SCAN ANALYSIS CONSIDERING PHASE DISTORTION pag. 48

3.7 ANALYSIS WITH MZI MODULATOR IN ASYMMETRIC CONFIGURATION (PHASE AND AMPLITUDE DISTORTION) pag. 51

3.8 RF SCAN ANALYSIS CONSIDERING PHASE AND AMPLITUDE DISTORTION pag. 58

IV. VPI SIMULATIONS pag. 63

4.1 THE SIMULATOR VPI pag. 65

4.1.1 Hierarchy of simulator pag. 65

4.1.2 Signal representation pag.66

4.1.3 Global parameters pag. 67

4.1.4 Modules parameters pag. 68

4.1.5 Sweep configuration pag. 69

4.2 MODULUS AND PHASE COMPARISON BETWEEN MATLAB AND VPI pag. 72

4.2.1 Modulus transfer function pag. 72

4.2.1.1 Matlab (analytic model) pag. 72

4.2.1.2 VPI (numerical simulation of standard measurement setup) pag. 74

4.2.2 Phase transfer function pag. 80

4.2.2.1 Matlab (analytic model) pag. 80

4.2.2.2 VPI (numerical simulation of standard measurement) pag. 80

4.3 SIMULATION OF THE METHOD RF SCAN pag. 84

V. CONCLUSIONS AND FUTURE LINES pag. 92

ANNEX pag. 95

LIST OF FIGURES

Figure 1. Dispersion effect pag. 15

Figure 2. Intermodal or Modal dispersion pag. 15

Figure 3. Chromatic dispersion pag. 20

Figure 4. MZ Interferometer scheme pag. 21

Figure 5. MZI Filter Optical scheme pag. 22

Figure 6. MZI as composed of two optical couplers and two optical delay lines pag.23

Figure 7. Modulus of MZI Filter with Matlab pag. 25

Figure 8. Phase of MZI Filter with Matlab pag. 25

Figure 9. MZI Modulator scheme pag. 26

Figure 10. MZI Modulator pag. 26

Figure 11. Transfer Function of MZI Modulator in Push-Pull configuration pag. 28

Figure 12. Transfer Function of MZI Modulator in Asymmetric configuration pag. 28

Figure 13. Scheme of the system under studying pag. 32

Figure 14. Effect of the RF modulation pag.35

Figure 15. MZI Modulator with the two voltages on the same arm pag. 41

Figure 16. MZI Modulator with the two voltage on the different arms pag. 41

Figure 17. Effect of the Second harmonic pag. 48

Figure 18. VPI Hierarchy pag. 66

Figure 19. Parameter Editor pag. 69

Figure 20. Define Control Window pag. 70

Figure 21. Assign Control Window pag. 71

Figure 22. Master Control Window pag. 72

Figure 23. Optical Filter Modulus obtained with Matlab pag. 73

Figure 24. Optical Filter Modulus obtained (dB) with Matlab **pag. 74**

Figure 25. Optical Filter Modulus scheme with VPI **pag. 74**

Figure 26. Parameter Editor of Optical Filter Modulus (VPI) **pag. 75**

Figure 27. Laser source Parameter Editor **pag. 76**

Figure 28. Ramp and chop Parameter Editor **pag.76**

Figure 29. Optical filter block and its Parameter Editor **pag. 77**

Figure 30. Result of VPI simulation: Modulus of the Optical Filter **pag. 77**

Figure 31. Modulus of Filter obtained by VPI with Matlab **pag. 78**

Figure 32. Overlop between the Modulus obtained with Matlab and VPI **pag.79**

Figure 33. Cosine scheme with VPI **pag. 80**

Figure 34. Output of cosine file **pag. 81**

Figure 35. Sine scheme with VPI **pag. 82**

Figure 36. Output of sine file **pag. 82**

Figure 37. Overlop between the phase obtained with Matlab and VPI **pag. 83**

Figure 38. Scheme of system under simulation **pag. 83**

Figure 39. RF signal Parameters Editor **pag. 84**

Figure 40. Source laser Parameter Editor **pag. 84**

Figure 41. Modulator Parameter Editor **pag. 85**

Figure 42. Look Inside of the Optical Filter **pag. 85**

Figure 43. Network Analyzer Parameter Editor **pag. 86**

Figure 44. Photodiodo Parameter Editor **pag. 86**

Figure 45. Parameter Editor of the system. **pag. 87**

Figure 46. Amplitude graphic of the primer harmonic **pag. 87**

Figure 47. Phase graphic of the primer harmonic **pag. 88**

Figure 48. Amplitude graphic of the second harmonic **pag. 88**

Figure 49. Phase graphic of the second harmonic **pag. 89**

Figure 50. Parameter values obtained with Matlab and VPI with f=2.2 GHz **pag. 89**

Figure 51. Parameter values obtained with Matlab and VPI with f=2 GHz pag. 90

BIBLIOGRAPHY

[1] Maria C. Santos, Santa P. De Bernardo-Rodi, Marco A. Mitre-Gutierrez, (2007), *New Modulation Zero-Shift Method to Characterize Fast Group Delay Ripple of Dispersion-Compensating Fiber Bragg Gratings,* Articulo, IEEE Photonics Technology Letters.

[2] Obando Velazco, C. A. (2010), *New Methods for Measuring and Monitoring Chromatic Dispersion in Optical Communication Systems*, Master Thesis, Escola Tècnica Superior d'Enginyeria de Telecomunicació de Barcelona, Universitat Politècnica de Catalunya.

[3] Rongqing Hui, Maurice O'Sullivan, (2009), *Fiber optic Measurement Techniques,* book, Elsevier Academic Press.

[4]De Bernardo Rodi, Santa P,(2007), *Group Delay Measures at Optical Frequencies standard MPSM and new BASM,* Escola Tecnica Superior d'Enginyera de Telecomunicacio de Barcelona, Universitat Politecnica de Catalunya.

[5]Aleix Tresseras, Arnau Sarri, (2009), *Mesures de dispersion cromatica a frequencies optiques amb deteccio de segon harmonic,* Escola Tecnica Superior d'Enginyera de Telecomunicacio de Barcelona, Universitat Politecnica de Catalunya.

[6] C. Peucheret, F. Liu and R.J.S. Pedersen,(1999) *Measurement of small dispersion values in optical components*, Electronics Letters, Vol. 35, No. 5, pp. 409 – 411.

[7] VPI Transmission Marker - VPI Component Marker, *User's Manual*.

[8] P. Hernday, (2002) *Measuring the group delay characteristics of narrow – band devices by the modulation phase shift method*, Agilent Technologies.

[9] S. Toledo, (2006) *Análisis y Desarrollo experimental de los métodos MPSM y de control de polarización para lacaracterización del retardo de grupo en dispositivos ópticos*.

I. INTRODUCTION

Today the information has a main rule in the society; its creation, distribution and manipulation are becoming a significant economic and cultural activity. We can see around us that all is the result of modern telecommunications technologies that allow instantaneous communications between people almost anywhere in the planet.

With the increase of data flow to travel through communication networks all around the world, high-capacity and low-loss physical media are an urgent and important need. In this purpose, optical fibre appears as an exceptional choice due to its large bandwidth and low attenuation features.

If on the one hand the path towards next generation optical networks increases bit rates and complexity, on the other hand the compensation of fibre optic transmission impairments turns into a critical issue. Problems as stress, small variations due to temperature, aging or dynamic path reconfiguration, may have an important negative impact in performance. Therefore it is essential to have an estimate as accurate as possible in order to undertake some action to compensate for impairments. Moreover these countermeasures should be based on high-precision real-time on-line monitoring data

Chromatic Dispersion (CD) is one of the most limiting problems. Great research efforts have been exerted aiming at measuring and compensating this problem. Recent studies are now increasingly targeting an expansion of the existing knowledge on dispersion and are elaborating accurate techniques for its real-time on-line resolution.

In this regard, the use of radiofrequency (RF) pilot tones added at the emitter is advantageous because it offers good sensitivity, high dynamic range and reconfigurability, it also simplifies the receiver and allows monitoring at any given point in the network without the need to recover the data, and finally because the tones are useful for other network management issues such as channel identification. In this thesis RF-modulated test signal methods are reviewed.

We start with the CD measurement methods that use a Mach Zehnder (MZ) Modulator in its standard push-pull configuration, the Modulation Phase Shift Method (MPSM) and Peucheret's method. We evaluate their performance in the presence of amplitude distortions.

Then we analyze the performance of a MZ modulator in asymmetric configuration in the same setup as that for the previous methods. We lay the basis of a new dispersion measurement method that we call Modulation Zero Shift Method (MZSM) and see that the MPSM can also work with an asymmetric MZ modulator.

By combining the MPSM and MZSM using a MZ modulator in asymmetric configuration we will show that we can measure the CD spectral characteristic in a certain optical bandwidth by scanning the RF modulating frequency over a fixed optical carrier. We will show that this method is vulnerable against amplitude distortions.

A new method will be derived here both analytically and numerically through Virtual Photonics (VPI) simulations that allows for measurement of the spectrum of the optical transfer function of devices both in

phase and in amplitude by scan of the modulating frequency applied over a fixed carrier. The method uses a MZ modulator in asymmetric configuration and requires measurement of amplitude and phase of the second harmonic generated through beating of the upper and lower first-order sidebands in absence of the carrier (biasing the MZ modulator in its null transmission point).

As a Device Under Test suitable to test the validity of the new RF-scan method for the optical characterization of the spectral transfer function of devices both in amplitude and in phase, we will study the Mach Zehnder Optical filter.

1.1 OBJETIVES

1.1.1 General

Study and evaluate through both theoretic analysis and simulations with the program VPI the performance of the method which uses a RF scan to determinate the phase difference and the amplitude difference (in dB) in order to calculate the dispersion value D.

1.1.2 Specific

- Study dispersion and related concepts.
- Study theoretically and numerically the Mach-Zehnder Interferometer Modulator in its different configurations, as a key component in the four methods we use in this project: MPSM, Peucheret, MZSM, RF scan.
- Study theoretically and numerically the Mach-Zehnder Interferometer Optical Filter which we use as our Device Under Test and its importance in MZSM y RF scan.
- Plot the phase and the modulus of MZI Optical Filter with Matlab and VPI and verify that the graphics are similar.
- Though the VPI, simulate, using the method RF scan, the system which we consider the base of our thesis.

.1.2 ORGANIZATION

This master thesis has been divided into 3 Chapters, plus Introduction and Conclusions:

- ✓ ***Chapter II, Basic Concepts***: In this chapter we introduce the basic concepts related to dispersion. Moreover we explain two important devices which we use in our system: MZI Modulator with its configurations, standard push-pull and asymmetric, and the MZI Optical Filter

- ***Chapter III, Mathematical Analysis***: We derive the equations which define the MZI Modulator and we present the basis of MPSM and Peucheret's method, which consider the MZ modulator in the standard Push-pull configuration. Moreover we derive the expression for the asymmetr*ic configuration and we explain th*e methods which use it: MZSM and RF scan.

- ***Chapter IV, VPI Simulation:*** The first part of the chapter presents the VPI program, with its features and functions. In the second part there is a comparison between the modulus and the phase graphics obtained with Matlab and those obtained with VPI using standard methods. In the third part we pre**s**ent the simulation of the new RF-scan method of spectral phase and amplitude characterization of optical devices. Asoutputs we have the modulus and phase graphics for the first and for the second harmonic. We will take these values and we will use them to determine the spectral phase and amplitude transfer function of the MZ filter that will be compared with the previous results .

II. BASIC CONCEPTS

The aim of this chapter is to introduce the field of study of this thesis: the amplitude and phase characterization of optical devices by RF scan. Before we enter the specific matter of this study, we review and clarify the fundamental concepts required to develop and understand the subject matter of this research.

The chapter is divided in two paragraphs.

In paragraph 2.1, we recall some basic concepts of the dispersion theory. In particular, we introduce the concept of dispersion, with its two manifestations: the Intermodal or Modal dispersion and the Intramodal or Chromatic dispersion. Once we specify the expression of the electric field which travels along the fibre, we concentrate on the expression of the phase constant of the fundamental propagating mode β. This parameter, by using a Taylor approximation, can be viewed as the sum of three parts (the underlying assumption here is that the higher parts are neglected). Consequently, we explain the physical concepts behind these new three parameters, i.e. phase velocity v_f, group velocity v_g and group delay dispersion *(GDD)*. As a conclusion to the paragraph, some features of the Chromatic Dispersion are discussed.

In paragraph 2.2, we focus on Mach-Zehnder Devices. In paragraph 2.2.1 we describe the Mach-Zehnder Modulator with its behaviour and its different possible configurations (push-pull or asymmetric). In paragraph 2.2.2 we briefly discuss the transfer function of MZ Interferometer (MZI) and then, delve deeper into the transfer function of MZ Modulator and MZ Optical Filter. In this section, we also define two important concepts related to the transfer function: the Sensitivity of the electrodes (V_c) and the half-wave voltage (V_π) and we finally show that the transfer functions of the MZ modulator, interferometer and optical filter do not largely differ from each other.

2.1 Dispersion Theory

An optical signal is distorted when it travels along the fibre. This is mainly a consequence of ***dispersion,*** which is one of the most important problems in the optical fibre. The dispersion effect causes a different delay to each of the optical signal's components, so that, at the detector, these components are registered with different arrival times. All this produces a distorted signal with respect to the transmitted one. The phenomenon is illustrated in the figure 1 below, where each pulse broadens and overlaps with its neighbours becoming indistinguishable at the receiver.

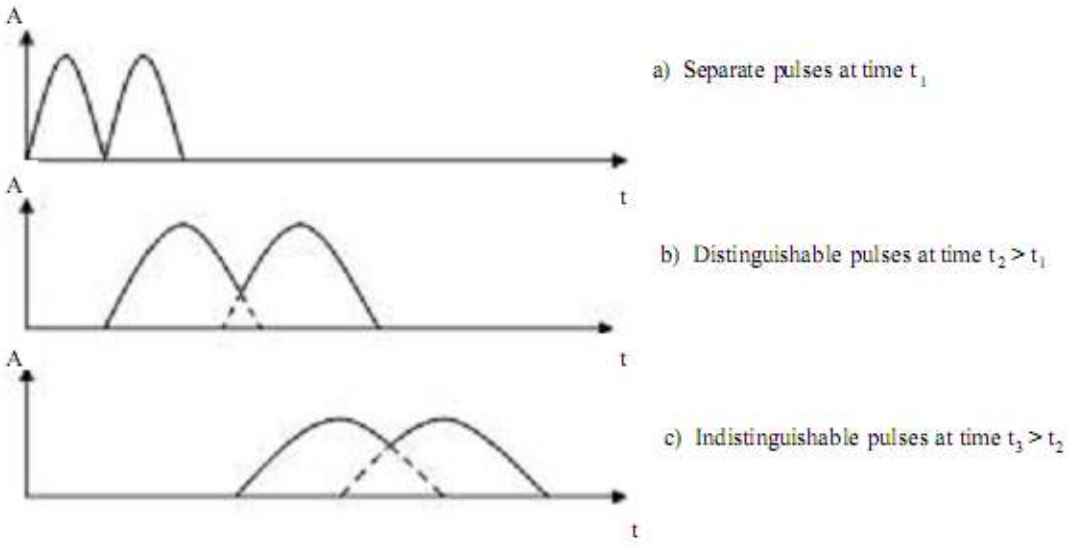

Figure 1. Dispersion effect

The phenomenon of dispersion consists of two different types:

Intermodal or Modal dispersion, appears in multi-mode fibres where the optical signal propagates in many "modes", each one following a different trajectory inside the fibre's core, as following from rays theory, see Figure 2 . In this way, all the modes, from a single pulse, experience different delays generating a pulse spread. The strength of this effect strongly depends on the refractive index profile of the fibre in and around the fibre core.

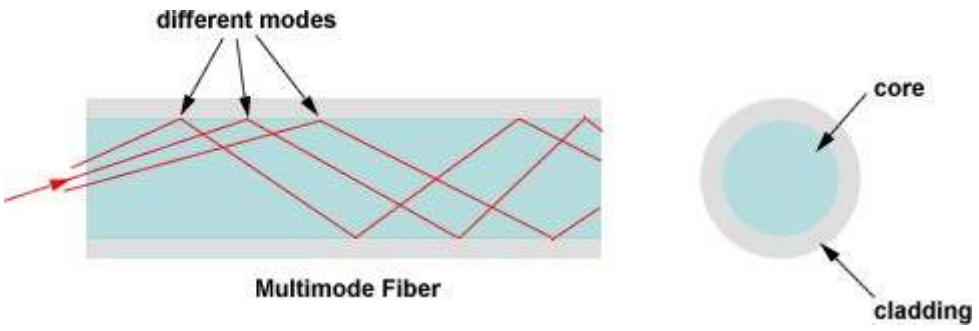

Figure 2. Intermodal or Modal dispersion

Intramodal or Chromatic Dispersion. Since the optical propagating signal is limited in time its energy is spread over a frequency band. Therefore, the energy into each propagating mode suffers additional differential delays for every frequency component over the signal's band. This is known as intramodal dispersion. The propagation delay differences between the different spectral components of the transmitted signal cause intramodal dispersion.

In this PFC we will be only considering monomode optical fibres and therefore we will be dealing exclusively with chromatic dispersion.

In order to present the chromatic dispersion effect, we introduce the expression of a pulse which travels along the fibre and analyze its components.

$$V(\omega, z) = V(\omega,0)e^{-j\beta(\omega)z} \tag{1}$$

$V(\omega,0)$ refers to the pulse value at the input of the fibre. The term $e^{-j\beta(\omega)z}$ reflects the phase constant of the fundamental propagating mode, which depends on frequency (the minus sign indicates propagation along the 'z' axis positive direction).

The expression above relates *β* and *ω,* and takes into account the chromatic dispersion as the main limiting effect in fibre propagation. In this case other phenomena (such as losses, nonlinear effects and so on) are considered of lower order. This approximation is relevant to several practical applications and allows to simplify the study of dispersion.

We now concentrate on the phase constant represented by $e^{-j\beta(\omega)z}$. In an ideal case, the phase constant suffers a linear dependency on frequency, so all spectral components experience the same delay and, at reception, there will be the same signal without distortion but only delayed. In a real case, as it happens in a dispersive channel, the dispersion relation is not linear; this effect leads to different arrival times of different frequency components. The signal recovered in reception will differ from the transmitted signal. An exact solution can be difficult to treat analytically, so in view of the fact that the phase constant slowly varies in the signal frequency bandwidth, it is possible to use a Taylor approximation to express *β(ω)* in a valid way:

$$\begin{aligned}\beta(\omega) &= \beta(\omega_0) + (\omega-\omega_0)\frac{\partial\beta}{\partial\omega}\Big|_{\omega=\omega_0} + \frac{(\omega-\omega_0)^2}{2}\frac{\partial^2\beta}{\partial\omega^2}\Big|_{\omega=\omega_0} + \frac{(\omega-\omega_0)^3}{6}\frac{\partial^3\beta}{\partial\omega^3}\Big|_{\omega=\omega_0} + \ldots \\ &= \beta_0 + \Delta\omega\beta_1 + \frac{\Delta\omega^2}{2}\beta_2 + \frac{\Delta\omega^3}{6}\beta_3 + \ldots\end{aligned} \tag{2}$$

where the third and higher terms can be neglected if we suppose that $\Delta\omega = \omega - \omega_0 << \omega_0$. In this way, the (2) expression can be rewritten as:

$$\beta(\omega) \approx \beta_0 + \Delta\omega\beta_1 + \frac{\Delta\omega^2}{2}\beta_2 \tag{3}$$

We will now delve deeper into the relations between the three β parameters (β_0, β_1, β_2) and their related physical concepts.

The first term, β_0, does not cause any effect over the envelope, but yields a phase shift on the optical carrier which travels with a velocity established by β_0, called ***phase velocity*** v_f. In fact, the phase velocity refers to a monochromatic wave. In vacuum, the phase velocity is independent on the optical frequency and equals the light velocity; in a medium of refractive index *n,* the phase velocity is smaller by a factor *n*. β_0 can be expressed as:

$$\beta_0 = \frac{2\pi}{\lambda}|_{\omega_0} = \frac{\omega_0}{v_f} \tag{4}$$

where the phase velocity v_f represents the propagation velocity of the optical carrier at frequency ω_0 , i.e. it is the velocity needed for an external agent to see the wave's phase constant.

β_1 is related to the ***group velocity*** v_g of the pulse and generates a time delay on the envelope without modifying the wave form, so that the information transmitted is kept unaltered. In this case each spectral component has a different phase velocity. Thus, while β_0 influences the optical carrier propagating velocity, the envelope propagates with the resulting velocity of all spectral components, called *group velocity* v_g, which depends on β_1. When the signal travels in the vacuum, the group velocity has the same value than the phase velocity. In a dispersive medium, instead, they are not equal, due to the fact that the phase velocity varies as a function of the frequency. In a pass-band signal, the group velocity is the velocity of the envelope, and, therefore, it gives the real delay of the signal, known as group delay (τ_g). As a consequence, this velocity does have a physical sense and can never be greater than the velocity of light in vacuum.

$$\beta_1 = \frac{\partial\beta(\omega)}{\partial\omega}|_{\omega_0} \tag{5}$$

The last term, β_2, causes both amplitude reduction and spread of the envelope, unlike previous parameters that do not modify the pulse form. It is worthwhile to notice that, despite this, the signal's energy is kept constant. β_2 is also responsible for altering the carrier's phase shift causing a chirp effect on it, i.e. a kind of acceleration and deceleration in frequency.

β_2 relates to the ***Group Delay Dispersion (GDD)*** which represents the frequency dependency of the group delay, i.e. the corresponding derivative with respect to angular frequency, and is specified in ps^2

$$\beta_2 = \frac{\partial\beta_1}{\partial\omega} = \frac{1}{c}\left(2\frac{\partial n}{\partial\omega} + \omega\frac{\partial^2 n}{\partial\omega^2}\right) = \frac{\partial\tau_g}{\partial\omega} \tag{6}$$

Drawing from this, it is possible to get to the definition of ***Group Velocity Dispersion (GVD)***. The latter, responsible for pulse broadening, is given by (6) and can be defined as the frequency (or wavelength) dependence of the group velocity in a medium. It is usually meant to be a term for the phenomenon, rather than used as a precisely defined quantity

$$\frac{\partial v_g}{\partial \omega} = \frac{\partial}{\partial \omega}\left(\frac{1}{\partial \beta / \partial \omega}\right) = -\frac{\partial^2 \beta / \partial \omega^2}{(\partial \beta / \partial \omega)^2} = -\beta_2 v_g^2 \tag{7}$$

With the scope to analyze in details the dispersion and its parameters we can study the propagation of a Gaussian pulse through a lossless transmission line. We suppose that at the input of a infinite line, a generator transmits a signal *v(0,t)*

$$v(0,t) = \underbrace{e^{-\frac{t^2}{2\tau^2}}}_{A(t)} e^{j\omega_0 t} \tag{8}$$

With τ a parameter related to the pulse width and ω_0 the optical carrier frequency. The Fourier Transformation of our expression is

$$V(0,\omega) = \int_{-\infty}^{\infty} v(0,t) e^{-j\omega t} \partial t = \int_{-\infty}^{\infty} e^{-\frac{t^2}{2\tau^2}} e^{-j(\omega-\omega_0)t} \partial t \tag{9}$$

$$V(0,\omega) = \sqrt{2\pi}\tau e^{-\frac{(\omega-\omega_0)^2 \tau^2}{2}} \tag{10}$$

and in a generic point of the line is

$$V(z,\omega) = V(0,\omega) e^{-j\beta(\omega) z} \tag{11}$$

After a mathematical development [5] we arrive to the expression which describes the dispersion through the parameter β

$$v(z,t)=\frac{1}{\sqrt[4]{1+\frac{\beta_2^2 z^2}{\tau^4}}}e^{-\frac{(t-\beta_1 z)^2}{2\tau^2\left(1+\frac{\beta_2^2 z^2}{\tau^4}\right)}}e^{j\left(\omega_0 t-\beta_0 z+\frac{(t-\beta_1 z)^2}{2\beta_2 z\left(1+\frac{\tau^4}{\beta_2^2 z^2}\right)}+\frac{\arctan\left(-\frac{\beta_2 z}{\tau^2}\right)}{2}\right)} \tag{12}$$

We observe a broadening of the pulse in a factor $\sqrt{1+\frac{\beta^2 z^2}{\tau^4}}$ accompanied by the corresponding decrease in amplitude so to keep the total pulse energy constant. Although the pulse is distorted we still see that the envelope essentially propagates at the group velocity while the phase travels at the phase velocity. In addition we see that the chromatic dispersion causes a temporal dependence of the phase which is known as chirp.

Chromatic Dispersion in fibre is usually defined by the dispersion parameter, D, which is the variation in group delay with wavelength. D is given by:

$$D=\frac{d\tau_g}{d\lambda}=\frac{d\omega}{d\lambda}\beta_2 \tag{13}$$

with:

$$d\omega=-\frac{2\pi c}{\lambda^2}d\lambda \tag{14}$$

It is possible to write:

$$D=-\frac{2\pi c}{\lambda^2}\beta_2=-\frac{2\pi c}{\lambda^2}\frac{d\tau_g}{d\omega} \tag{15}$$

The dispersion parameter has units of picoseconds per kilometer per nanometer (*ps/(Km*nm)*), so its influence depends on propagated length and spectral bandwidth with a linear relation.

In order to complete this section about dispersion theory, we should bring to mind that chromatic dispersion results from two phenomena:

1. variation in the reflective index of the constituent material of the fibre with the frequency;
2. variation in the waveguide properties of the fibre with frequency.

The expression (16) represents the dispersion parameter as the sum of these two effects, which are described by the frequency dependence of β.

$$D = -\frac{2\pi c}{\lambda^2}\beta_2 = -\frac{2\pi c}{\lambda^2}\frac{d^2}{d\omega^2}\beta = -\frac{2\pi}{\lambda^2}\frac{d}{d\omega}(n + \omega\frac{dn}{d\omega}) = \frac{-2\pi}{\lambda^2}(2\frac{dn}{d\omega} + \omega\frac{d^2n}{d\omega^2}) \quad (16)$$

The first component corresponds to material dispersion and the second to waveguide dispersion.

Material dispersion is caused by the variation of the index of refraction as a function of the optical wavelength. Because the group delay depends on the index of refraction, the various spectral components of a given mode will travel at different speeds, depending on the wavelength.

Waveguide dispersion results from the variation in group velocity with wavelength for a particular mode. It occurs because in a single mode fibre only about 80 percent of the optical power can arrive to the core. Hence, the dispersion arises, since the 20 percent of the light propagating in the cladding travels faster than the light confined to the core and since this percentage is dependent on wavelength. In this type of fibre, material and waveguide dispersion are correlated; the total dispersion can be minimized by choosing material and waveguide properties depending on the wavelength of operation. In multimode fibre, material and waveguide dispersion have different properties; waveguide is generally smaller compared to material dispersion, so it is usually neglected.

Figure 3 shows the chromatic dispersion value as the sum of material dispersion and waveguide dispersion.

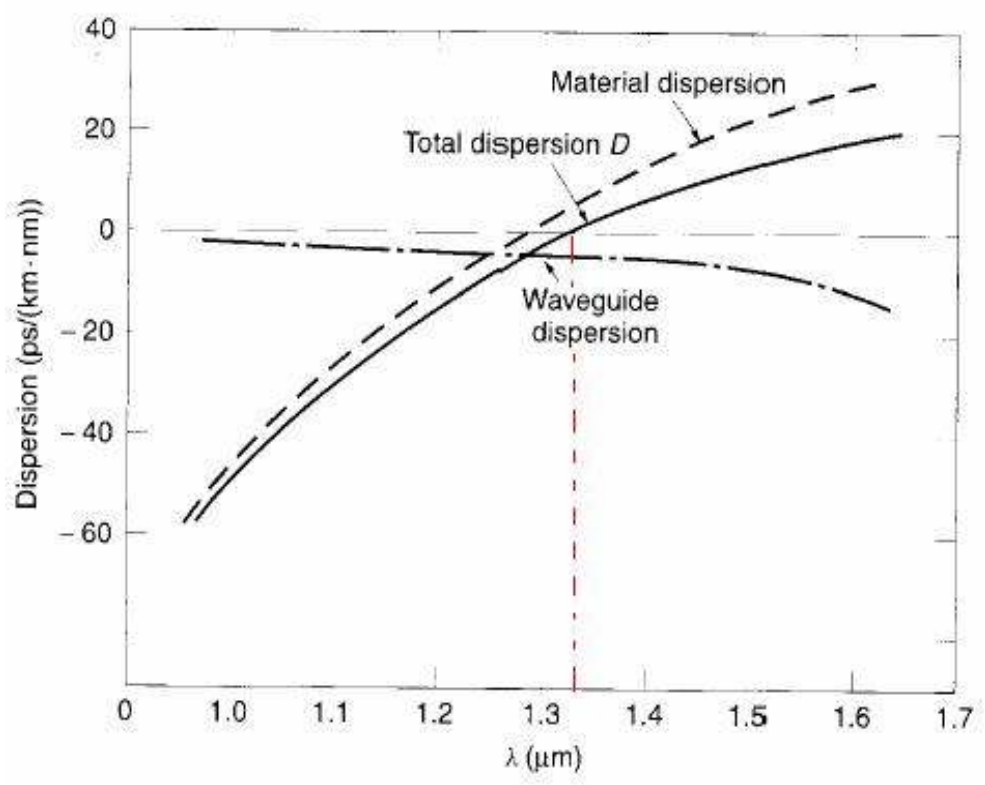

Figure 3. Chromatic Dispersion

From the figure we see that the second window of communications has zero dispersion coefficient while in the third window of minimum losses the total dispersion coefficient amounts to 17 ps/nmKm approximately.

It is important to clarify that the above has used the typical description of Dispersion in optical fiber which is based on the frequency dependence of the propagation constant. The group delay, the dispersion and other related parameters are then usually specified in a per –unit-length basis so that in order to know their precise value for a certain fiber length we have to take the unit-length value times the length. In a generic dispersive device where dispersion is not proportional to any length and there's not a defined phase constant, dispersion will be considered through a term such as $e^{j\phi(\omega)}$. Simple identification of phi(w)=-b(w)z and consideration of total, instead of per-unit-length basis parameters, will allow to extend the analysis to the generic case.

2.2 Mach-Zehnder devices

In this section we analyze the most important device of our system of measurement: the Mach-Zehnder Interferometer (MZI). Firstly we explain the MZI as an optical filter with its characteristics and transfer function; then, we focus our attention on MZI as a modulator with its transfer function and its behaviour.

In our system the MZI modulator is used as the device to obtain the RF modulated test signal to inject in the devices that are to be characterized, Devices Under Test (DUT), while the MZI filter will be used as the DUT yielding both a known amplitude and phase response used as a benchmark to test and prove the validity of the characterization method proposed.

The goal is to study the signal before and after its passage in these components.

2.2.1 Mach-Zehnder Interferometer: Modulator and Optical Filter

The basic principle of this device is the Interferometer effect: the signal in input is divided between the two arms; each arm applies a phase change to the signal and at the output the two signals, which come from the two paths, are joined, see Figure 4.

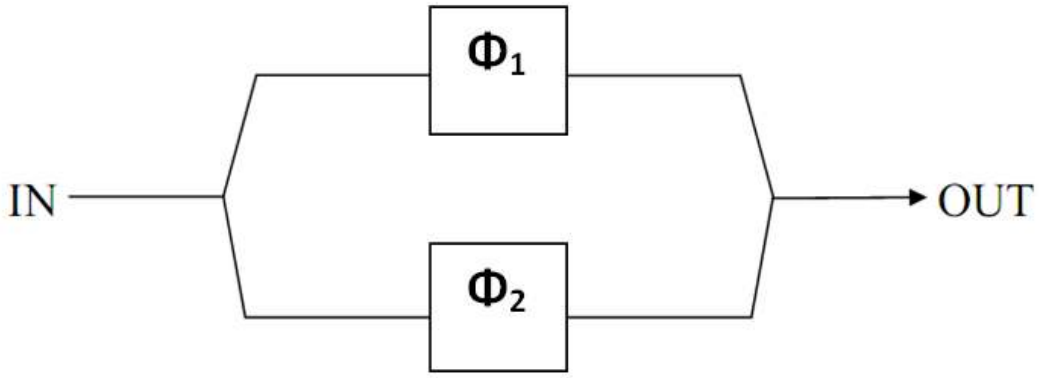

Figure 4. MZ Interferometer scheme

Starting from figure above, we can characterize the MZI devices, which we use in this thesis, modifying the values of ϕ_1 and ϕ_2.

2.2.1.1 MZI Optical Filter

Firstly we see the MZI as optical filter. As shown in Figure 5, the relative phase change between the interferometric arms is due to the different fibre lengths. The values of the phases are:

$$\phi_1 = 2\pi \frac{L}{\lambda} \qquad (17)$$
$$\phi_2 = 0$$

Since the phase change is different for each wavelength we obtain a transfer function which alternates transmission maxima and minima as a function of wavelength and therefore a filtering function.

A scheme that represents this type of filter can be

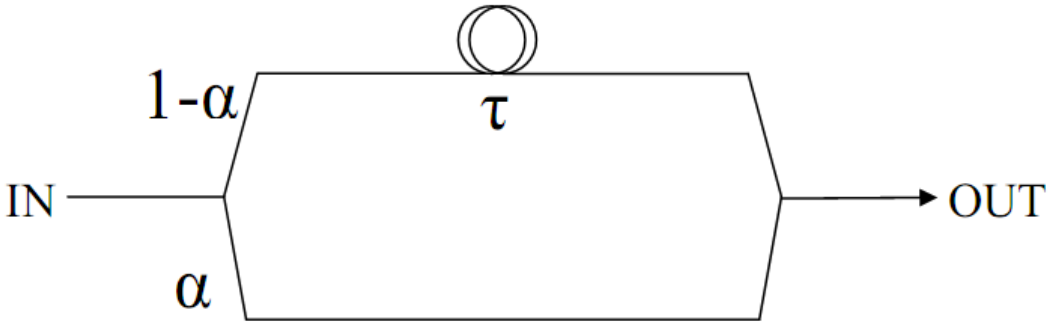

Figure 5. MZI Filter Optical scheme

Mathematically:

$$E_{out} = E_{in}((1-\alpha)e^{-j\omega_0\tau} - \alpha) \qquad (18)$$

With alpha the power splitting ratio which is ½ in the ideal case.

The normalized detected power in a photodiode will be

$$
\begin{aligned}
P_d &= \frac{|E_{out}|^2}{2} = \frac{|E_{in}((1-\alpha)e^{-j\omega_0\tau}-\alpha)|^2}{2} = E_{in}^2\frac{|((1-\alpha)e^{-j\omega_0\tau}-\alpha)|^2}{2} \\
&= \frac{E_{in}^2}{2}|(1-\alpha)(\cos(\omega_0\tau)-j\sin(\omega_0\tau))-\alpha|^2 = \frac{E_{in}^2}{2}(((1-\alpha)\cos(\omega_0\tau)-\alpha)^2+((1-\alpha)\sin(\omega_0\tau))^2) \\
&= \frac{E_{in}^2}{2}((1-\alpha)^2\cos^2(\omega_0\tau)+\alpha^2-2\alpha(1-\alpha)\cos(\omega_0\tau)+(1-\alpha)^2\sin^2(\omega_0\tau) \\
&= \frac{E_{in}^2}{2}((1-\alpha)^2+\alpha^2-2\alpha(1-\alpha)\cos(\omega_0\tau))
\end{aligned}
\tag{19}
$$

A practical MZI filter can be viewed as composed of two optical couplers and two optical delay lines connected to them. It can be made by free space optics and guided-wave optics. If we use a 2 X 2 coupler, we can represent a MZI with two inputs and two outputs, as in Figure 6.

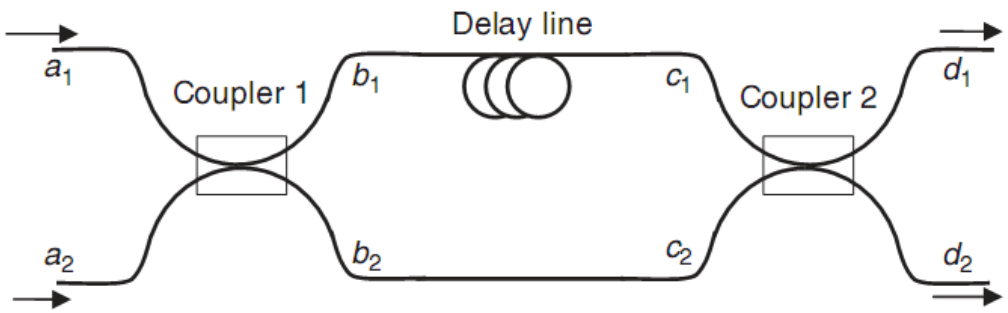

Figure 6. MZI as composed of two optical couplers and two optical delay lines

We can get the transfer function of a MZI by cascading the transfer function of two optical couplers and that of the optical delay lines. The transfer matrix of two delay lines is

$$
\begin{bmatrix} c_1 \\ c_2 \end{bmatrix} = \begin{bmatrix} \exp(-j\phi_1) & 0 \\ 0 & \exp(-j\phi_2) \end{bmatrix} \begin{bmatrix} b_1 \\ b_2 \end{bmatrix} \tag{20}
$$

where $\phi_1 = (2\pi/\lambda)n_1L_1$ and $\phi_2 = (2\pi/\lambda)n_2L_2$ are the phase delays of the two delay lines. To simplify the expressions, we set the two optical couplers identical with a power splitting ratio of α,

$$
\begin{bmatrix} d_1 \\ d_2 \end{bmatrix} = \begin{bmatrix} \sqrt{1-\alpha} & j\sqrt{\alpha} \\ j\sqrt{\alpha} & \sqrt{1-\alpha} \end{bmatrix} \begin{bmatrix} e^{-j\phi_1} & 0 \\ 0 & e^{-j\phi_2} \end{bmatrix} \begin{bmatrix} \sqrt{1-\alpha} & j\sqrt{\alpha} \\ j\sqrt{\alpha} & \sqrt{1-\alpha} \end{bmatrix} \begin{bmatrix} a_1 \\ a_2 \end{bmatrix} \tag{21}
$$

We now introduce an important parameter of MZI: the *Extinction Ratio* value. This value is defined as the relation between the maximum and the minimum power levels of the transfer function. So, if we have a

minimum power equal to “0”, we will have an infinite extinction ratio. To achieve the highest extinction ratio, we require α= 0.5, i.e. a 50 percent of power splitting ratio for optical couplers. In our analysis we will consider ideal couplers so the equation can be simplified as

$$\begin{bmatrix} d_1 \\ d_2 \end{bmatrix} = \frac{1}{2}\begin{bmatrix} (e^{-j\phi_1} - e^{-j\phi_2}) & j(e^{-j\phi_1} + e^{-j\phi_2}) \\ j(e^{-j\phi_1} + e^{-j\phi_2}) & -(e^{-j\phi_1} - e^{-j\phi_2}) \end{bmatrix}\begin{bmatrix} a_1 \\ a_2 \end{bmatrix} \tag{22}$$

We consider input port 1 in Figure 6 as the input of out MZI filter and that input port 2 is disconnected, i.e. a_2=0, the optical power at the output port 1 and at the output port 2 will be respectively

$$d_1 = \frac{1}{2}(e^{-j\phi_1} - e^{-j\phi_2})a_1 = -e^{-j\phi_0}\sin(\frac{\Delta\phi}{2})a_1 \tag{23}$$

and

$$d_2 = \frac{j(e^{-j\phi_1} + e^{-j\phi_2})}{2}a_1 = je^{-j\phi_0}\cos(\frac{\Delta\phi}{2})a_1 \tag{24}$$

where $\phi_0 = (\phi_1 + \phi_2)/2$ is the average phase delay and $\Delta\phi = (\phi_1 - \phi_2)$ is the differential phase shift of the two MZI arms.

Consequently, the optical power transfer function from input port 1 to output port 1 will be

$$H_{11} = \left.\frac{d_1}{a_1}\right|_{a_2=0} = \sin^2[\frac{\pi f}{c}(n_2L_2 - n_1L_1)] \tag{25}$$

and the optical power transfer function from input port 1 to output port 2 will be

$$H_{12} = \left.\frac{d_2}{a_1}\right|_{a_2=0} = \cos^2[\frac{\pi f}{c}(n_2L_2 - n_1L_1)] \tag{26}$$

With Matlab we can obtain the transfer function of the filter interferometer; we have plotted the modulus and the phase for different values of *alpha*, i.e. the coupling factor, which determines the part of signal which travels in every interferometer path. Due to the fabrication of the filter by fusion of two optical fibres there is a delay between optical paths which is obtained as

$$\tau = \frac{\lambda_1\lambda_2}{c(\lambda_2 - \lambda_1)} \tag{27}$$

where λ_1 represents the wavelength corresponding to a maximum and λ_2 refers to the wavelength of a minimum of the filter transfer function. The difference between the two wavelength is defined as the period of the optical filter transfer function.

Considering the low pass equivalent of the expression of detected power the modulus and the phase are presented respectively in Figures 7 and 8.

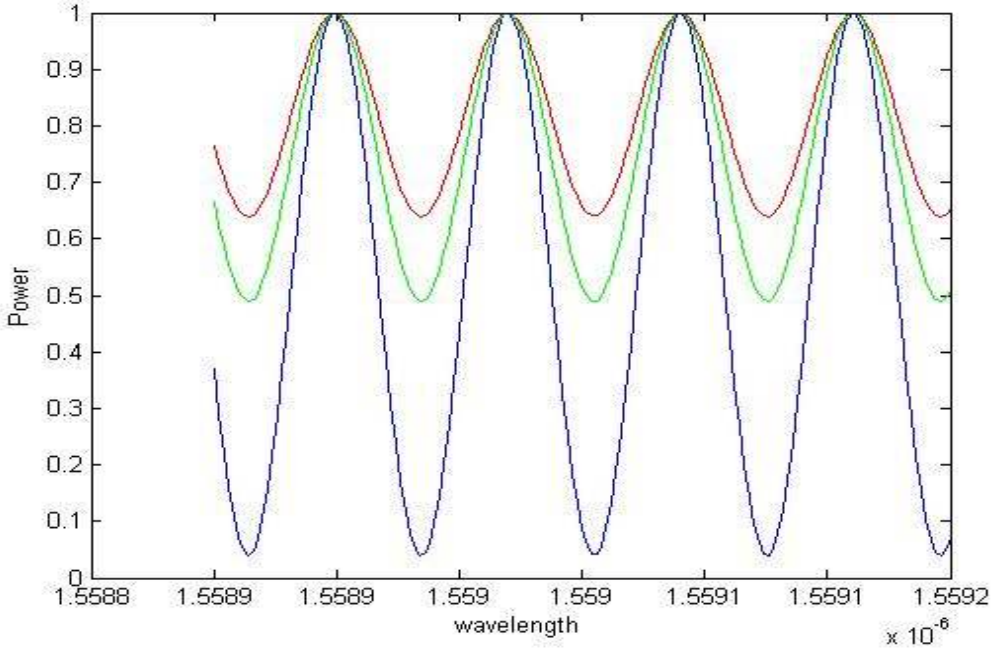

Figure 7. Modulus of MZI Filter with Matlab

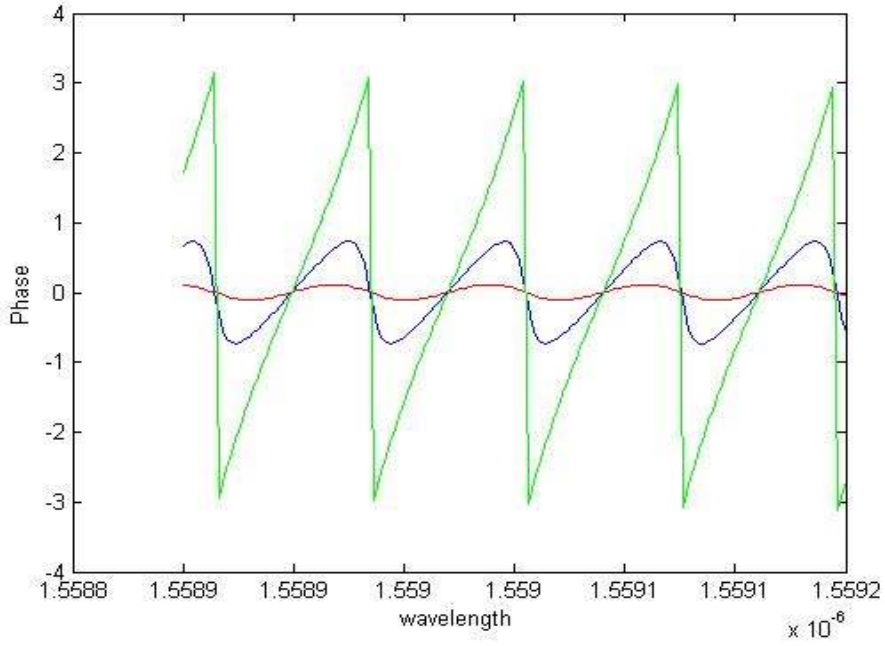

Figure 8. Phase of MZI Filter with Matlab

In Chapter 4 we will obtain the modulus and the phase transfer function of the MZ Optical Filter by using a simulation setup in VPI which follows the standard measurement method and will compare it with the analytical expressions.

2.2.1.2 MZI Modulator

Now we introduce the MZI modulator. The phase change, in this case, is due to the voltage applied to each arm. The scheme is presented in Figure 9.

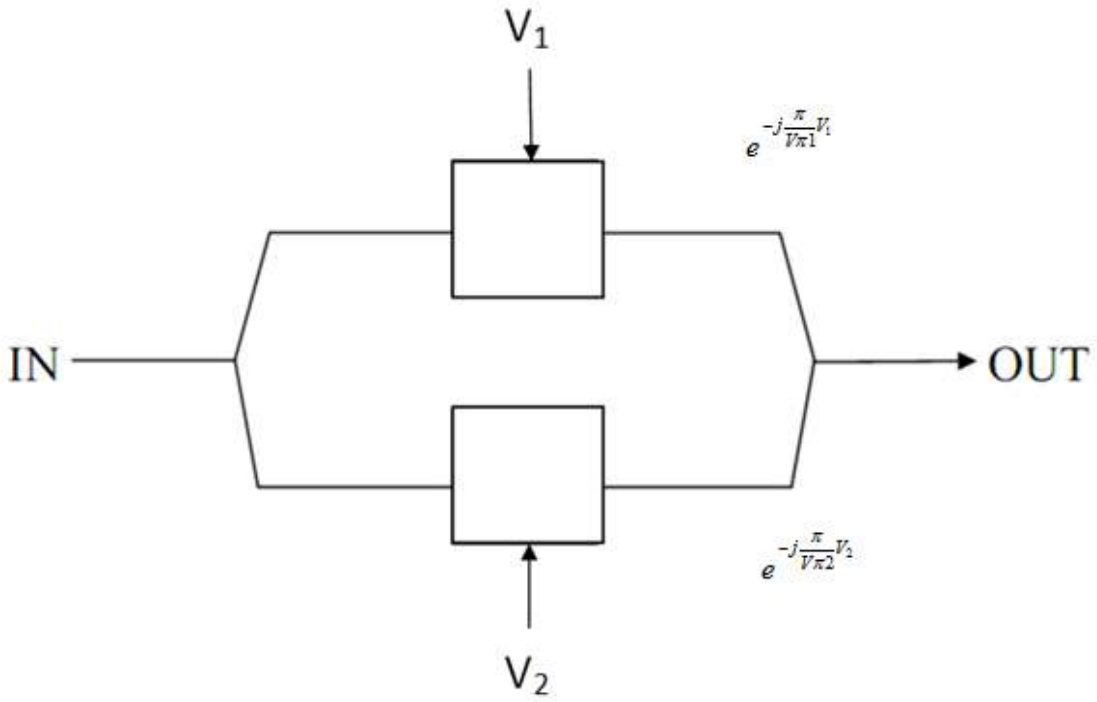

Figure 9. MZI Modulator scheme

In Mach-Zehnder modulators, the incoming light is split into two waveguides under the influence of conducting electrodes, as shown in Figure 10. The electro-optical effect induces a change in the refractive index of each interferometer arm and phase-modulates the light propagating into that arm according to the electric voltage applied to each electrode. By combining the two paths with different phase modulations, this phase modulation is turned into an intensity modulation.

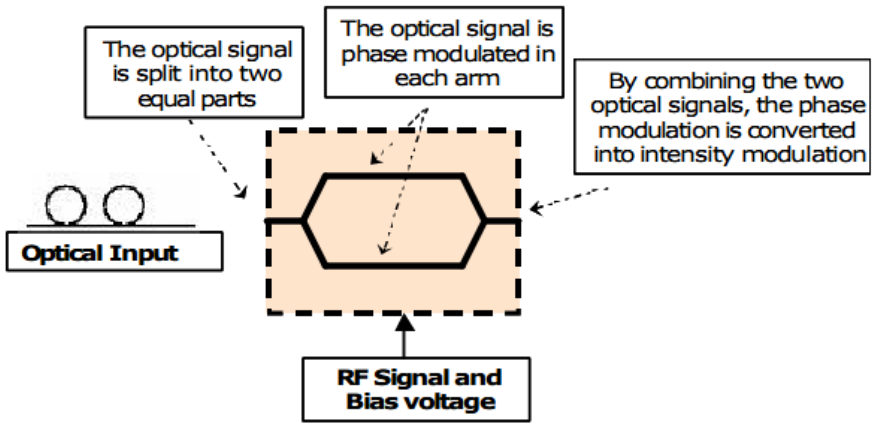

Figure 10. Mach-Zehnder interferometer modulator

Mathematically:

$$E_{out} = E_{in}((1-\alpha)e^{-j\frac{\pi}{V_{\pi_1}}V_1} + \alpha e^{-j\frac{\pi}{V_{\pi_2}}V_2}) \tag{28}$$

where again, alpha is the interferometric splitting ratio, ½ in the ideal case.

The fotodetected power will be, with the substitutions $\theta_1 = \frac{\pi}{V_{\pi_1}}V_1$ and $\theta_2 = \frac{\pi}{V_{\pi_2}}V_2$

$$P_d = \frac{1}{2}|E_{out}|^2 = \frac{1}{2}E_{in}^2\{[(1-\alpha)\cos\theta_1 + \alpha\cos\theta_2]^2 + [-(1-\alpha)\sin\theta_1 - \alpha\sin\theta_2]^2\} \tag{29}$$

This device has been reported in the literature as an electro-optic modulator for high digital bit-rate and RF transmission over optical fibre communication systems. The main operation of Electro-Optic Modulators (EOM) is based on the linear electro-optical effect (Pockels effect) where the refractive index of a medium is modified in proportion to the strength of the applied electric field.

We define two basic types of configurations of the Mach-Zehnder Modulator:

- ***Push-Pull Configuration***

This configuration is obtained by applying data and bias voltage in one arm and inverted data and inverted bias voltage in the other arm., i. e.

$$V_1 = -V_2 \tag{30}$$

This increases the relative phase shift in one path and decreases it in the other path. Since phase changes are equal in magnitude but opposite in sign in each arm a chirp free intensity modulation is obtained.

Following from expression (29), using alpha=1 and the condition in (30), the corresponding transfer function is shown in Figure 11

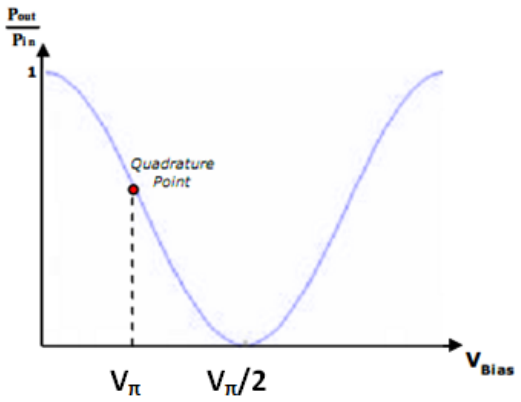

Figure 11. Transfer function of MZI Modulator in Push-Pull configuration

The above transfer function assumes an equal power split between the two interferometric branches (alpha=1) and therefore an infinite Extinction Ratio between the maximum and minimum power at the MZM. In practice it is very difficult to obtain an equal power split between branches and therefore we get a finite ER at the MZM output. A typical value is between 20-40 dB.

- ***Asymmetric Configuration***

In this thesis, we utilize this type of configuration, where the modulating signal and the bias voltage are applied to only one of the interferometric branches, either to the same or to different branches.

In this case using the above condition in expression (29), the transfer function is as shown in Figure 12.

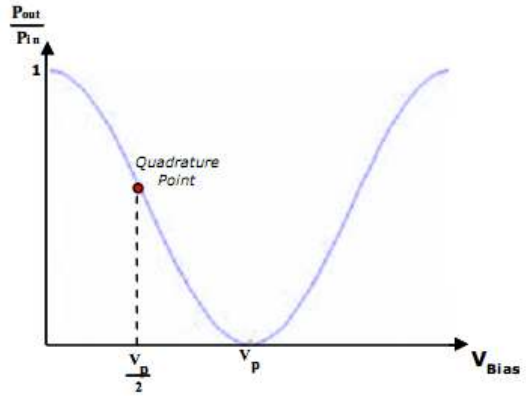

Figure 12. Transfer function of the MZI Modulator in Asymmetric configuration

As shown in the Figure above, we should underline three points:

- Quadrature Point (QP) is located at the centre of the linear zone where the modulator offers the maximum linearity. A V_π /2 voltage is required between the branches.
- Minimum Transmission Point (mTP): in an ideal situation there is no power at the output. Between branches there is a voltage difference equal to V_π. In practice, the carrier contribution at the output is not completely cancelled, because the power split over the two branches will never be exactly the same.
- Maximum Transmission Point (MTP): where the output power is maximum. The relative phase shift between branches is equal to 0.

Important for the transfer function definition are the Sensitivity of the electrodes (V_c) and the half-wave voltage (V_π).

The *Sensitivity* is independent on the configuration and represents the voltage into each electrode required to achieve a phase change of π in the optical signal. Even though each branch can have a different V_c value, in order to simplify the calculations, we treat them as equal.

The *half-wave voltage* is defined as the voltage needed to go from a maximum to a minimum of amplitude in the modulated signal

$$V_\pi = mTP - MTP \tag{32}$$

Its value depends on the modulator configuration.

We work with asymmetric configurations, so in this case the relation between these two magnitudes is

$$V_\pi = V_c \tag{33}$$

To obtain a phase shift of 180 degrees between the two branches, a voltage equal to the sensitivity of the electrodes that we are using is necessary.

About the push-pull configuration, the relation is

$$V_\pi = \frac{V_c}{2} \tag{34}$$

The transfer function with the two different configurations is the same; the only difference is that, in the asymmetric case, since only one arm is used, a double voltage with respect to the symmetric case is required to cancel the signal at the output.

III. MATHEMATICAL ANALYSIS

In this chapter first of all we introduce a scheme which represents the system which we will use and which is the base of our study. All the methods dealt with in this work are based on injection upon the Device Under Test (DUT) of a test signal obtained through modulation of an RF pure tone over the optical carrier and evaluation of the detected signal after going through the DUT. The MZI modulator is the device that imposes such RF modulation and therefore its mathematical description in section 3.1 plays a crucial role.

In section 3.2 we explain the Modulation Phase Shift Method MPSM [9]; this method recovers the semi difference between the optical phase shifts at each of the RF-generated optical sidebands at each side of the carrier as the electrical phase detected at the modulating frequency using a Vectorial Network Analyzer. The problems with MPSM are mainly two; one is that the method needs a tunable laser with a stable wavelength step size and the other is the incapability of the method to work with spectral amplitude distortions.

In section 3.3 we introduce Peucheret's method [6]. This method uses the same setup of MPSM; but, instead of measuring the detected signal's phase, Peucheret bases the analysis on the amplitude term. The concept is to obtain the zeros in the amplitude term and to arrive, from these, to the dispersion value. The analysis will be done first in absence of significant spectral amplitude distortions and then considering them. The problem of this method is related with the amount of dispersion introduced by DUT. It may happen that the RF frequency, which we need to change until we reach a dip, can be too high. The solution proposed is the introduction of a constant dispersion offset.

In Section 3.4 we present the mathematical analysis of MZI Modulator in Asymmetric configuration. In the first part the detected power expression is obtained without DUT, then in the second part we insert the DUT contribution.

Section 3.5 introduces the MZSM (Modulation Zero Shift Method) which is based on a MZ modulator in asymmetric configuration. The mathematical analysis will reveal that the amplitude dips of the detected signal will be dependent on the level of bias applied to only one of the interferometric arms so that dispersion can be measured in a similar way as in Peucheret's method but changing the bias value instead of the modulating frequency. In Section 3.6 we introduce a method which consist of use, together, the MPSM with Asymmetric configuration and MSZM [1]. The RF scan of modulating frequencies over the same optical carrier allows us to determine the optical dispersion spectrum.

In section 3.7 we carry out the same analysis of section 3.4, but this time considering amplitude distortions besides phase distortions. Here we will explain how the amplitude values can change the detected power expression and we will present the basis of the new method we will introduce in section 3.8 .

In the last Section 3.8 we introduce a technique which uses a RF scan to determine both the optical phase and the optical amplitude spectrum of the DUTs transfer function. While previously explained methods are able to measure only the optical phase spectrum , with this method we can build the optical phase and amplitude spectrum through RF scan without tuning the carrier. This method will be numerically tested through the Virtual Photonics (VPI) program in Chapter 4.

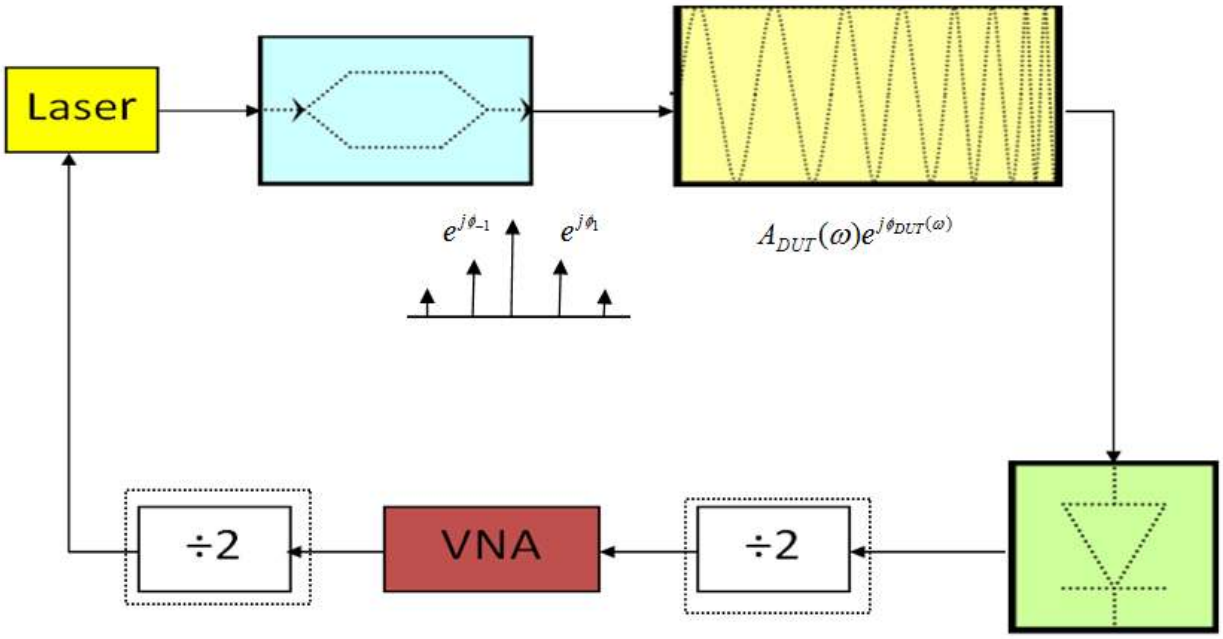

Figure 13. Scheme of the system under study

We have decided to put the scheme above out of any sections of this chapter, i.e. in the introduction, because we want to highlight that this system is the base of our study. From this we start and we study how to determine the Dispersion value through four methods.

In the scheme it is possible to see the laser, which can be tunable or fixed. It is our source which emits a signal towards the next block which is the MZI Modulator. We use this device with the two possible configurations presented in Chapter 2: Push-Pull and Asymmetric. In this block the signal is modulated by a RF, and a bias voltage is added. After the modulation, the signal enters the DUT which may introduce amplitude and phase distortions. As explained in Chapter 2 the DUT used in this project is the MZI Optical Filter. At the output there is the Optical Detector which determines the detected signal power of our system. Then there is the Network Analyzer, configured to make electrical transmission measurements both in amplitude and phase. The last two blocks represent two frequency dividers, we use them when we want, at the output, to measure the second harmonic.

3.1 Mathematical analysis with MZI Modulator in Push-Pull configuration

Now we can start with the analysis.

The signal enters the modulator where an RF signal and a bias are combined and applied with different sign to each electrode.

We have θ_b which is represented by

$$\theta_b = \frac{V_b}{V_\pi}\pi \tag{35}$$

And θ_{RF} which is represented by

$$\theta_{RF} = \frac{\pi}{2V_\pi}V_{RF}(t) \tag{36}$$

In a general case, the RF signal will be of much lower intensity than the bias level and therefore $\theta_{RF} << \theta_b$ and then we use a Taylor for $e^{j\theta_{RF}} \approx 1 + j\theta_{RF}$, $A_{RF} << V_b$ and then the small signal approximation may be used and at the output we have, considering the low pass equivalent and the small signal approximation (considering (3))

$$E_{MZ} = \frac{A_0}{2}[2\cos\theta_b - A_m \sin\theta_b(e^{j\omega_m t} + e^{-j\omega_m t})] \tag{37}$$

In this case since we are only interested in the first harmonic components, only terms up to first order have been used

When the E_{MZ} passes through the DUT, the optical signal suffers different phase shifts at the carrier and the sidebands; these shifts can be represented as:

- ϕ_0 which represents the phase shift at the carrier
- ϕ^+ which represents the phase shift at the upper sideband
- ϕ^- which represents the phase shift at the lower sideband

Consequently the E_{DUT} will be

$$E_{DUT} = \frac{A_0}{2}[2\cos\theta_b e^{j\phi_0} - A_m \sin\theta_b (e^{j\omega_m t} e^{j\phi^+} e^{j\phi_0} + e^{-j\omega_m t} e^{j\phi^-} e^{j\phi_0})]$$
$$= A_0 \cos\theta_b e^{j\phi_0} - \frac{A_0 A_m}{2} 2\sin\theta_b \cos(\frac{\phi^+ + \phi^-}{2}) \cos(\omega_m t + \frac{\phi^+ - \phi^-}{2})] \quad (38)$$

When the signal passes through the photodetector there is the translation into the electrical domain; this change follows the square-law principle. So, the detector output will be given by

$$P_d = \frac{1}{2} | E_{DUT} |^2 \quad (39)$$

The modulus function, in this case, implies taking the field envelope, i.e. to eliminate all the components at optical frequencies.

The detected power, is

$$P_d = \frac{A_0^2}{4}\cos^2\theta_b - \frac{A_0^2 A_m}{2}\cos\theta_b \sin\theta_b \cos(\frac{\phi^+ + \phi^-}{2} - \phi_0)\cos(\omega_m t + \frac{\phi^+ - \phi^-}{2})) \quad (40)$$

From this expression we can draw the following conclusions: the first term refers to the DC component which has no relevance on the dispersion determination. The second term is the RF modulating frequency. It is important to underline that the values of optical phase shifts at each of the sidebands, which are related to the chromatic dispersion value, are presented in both the amplitude and the phase of the detected signal at the modulationg frequency , respectively as the semi sum and the semi difference.

3.2 MPSM analysis

Now we can explain the **MPSM (Modulation Phase Shift Method)** to calculate the dispersion value D. This method uses a RF modulation and applies, on the optical signal, an amplitude modulation which generates two major sidebands on the carrier. Each of them suffers a phase shift after the passage through the DUT; The network analyzer recovers the signal at the modulating frequency ω_m. Therefore the mathematical expression which represents this method is obtained from the RF component in the expression (40)

$$P_d = -\frac{A_0^2 A_m}{2}\cos\theta_b \sin\theta_b \cos(\frac{\phi^+ + \phi^-}{2} - \phi_0)\cos(\omega_m t + \frac{\phi^+ - \phi^-}{2})) \quad (41)$$

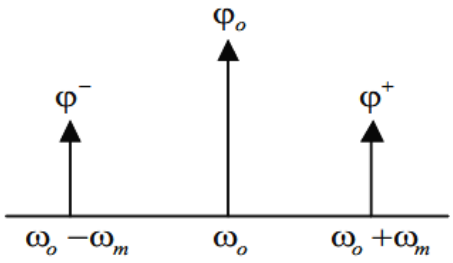

Figure 14. Effect of RF modulation

The network analyzer will recover the electrical phase as the semi difference between the optical phase shifts acquired by the two major sidebands.

$$\Delta\phi = \frac{\phi^{+} - \phi^{-}}{2} \tag{42}$$

After that, we approximate the group delay at the operating wavelength from this electrical phase, as explained below:

$$\frac{\phi^{+} - \phi^{-}}{\Delta\omega} \sim \frac{d\phi}{d\omega}$$

$$\tau_g = -\frac{d\phi}{d\omega} \approx -\frac{\Delta\phi}{360^{\circ}}\frac{1}{f_m} \tag{43}$$

where the first factor is defined as the fractional cycle of RF phase shift (expressed in degrees) and the second factor represents the period of the RF sine wave.

By sweeping the optical wavelength with the aid of a tuneable laser, we obtain the complete delay curve for the required bandwidth, and then, chromatic dispersion at the nominal wavelength is calculated by dividing the change of group delay by the wavelength change which stimulates it:

$$D = \frac{\tau_{g1} - \tau_{g2}}{\Delta\lambda} \approx \frac{\Delta\tau_g}{\Delta\lambda} \tag{44}$$

In order to achieve accurate measures it is important to have a stable wavelength step size, which completely depends on the tuneable laser stability.

We can notice how the group delay and the measured electrical phase present opposite slopes. The phase of a sinusoidal signal can be interpreted as the argument of this signal when the time variable is equal to zero. For example, if we have $\cos(\omega t + \theta)$, the phase of this signal is $+\theta$. The time delay presented in a sinusoidal signal can be defined as the time value which cancels the argument. For example, the time delay of $\cos(\omega t + \theta)$ is $-\theta / w$. Bearing these concepts in mind, it is of extreme importance to highlight that

when the group delay is estimated based in phase measurements, it is necessary to invert the sign of the phase before computing it.

To sum up, MPSM requires a tunable laser to obtain the dispersion because it measures the group delay value at a certain wavelength; it can be seen that this method fails in correctly determining the dispersion value whenever we have significant amplitude distortions.

Next section presents an alternative dispersion measure known as the Peucheret's Method.

3.3 Peucheret's Method analysis

The **Peucheret's Method** uses the same setup as MPSM, with the following difference: instead of measuring the detected signal's phase, Peucheret bases his analysis on the amplitude term in expression (39). As we know, chromatic dispersion is related with the phase shifts at the sidebands and, in this case, we will get the value D from the semi sum of these phase shift contained into the RF amplitude term.

To measure the exact amplitude value it is necessary an accurate equipment and a calibration procedure, because in the measurement the channel noise, the insertion loss and other signal attenuation factors have an effect on the detected amplitude. That is the reason why Peucheret's method focuses on determining the envelope's dips. In order to obtain these dips, Peucheret proposes to carry out a RF Frequency sweep on the setup. First we consider the mathematical analysis for the case where we do not have amplitude distortions from the DUT; then we will extend our study to the case where the amplitude distortions are relevant.

We start the analysis from expression (39):

$$P_d = -\frac{A_o^2 A_m}{2}\cos(\theta_B)\sin(\theta_B)\cos\left(\frac{\varphi^+ + \varphi^-}{2} - \varphi_o\right)\cos\left(\omega_m t + \frac{\varphi^+ - \varphi^-}{2}\right) \tag{45}$$

To obtain a "zero" in the amplitude term, we have:

$$\cos\left(\frac{\phi^+ + \phi^-}{2} - \phi_0\right) = 0 \tag{46}$$

$$\frac{\phi^+ + \phi^-}{2} - \phi_0 = \frac{(2n-1)\pi}{2} \tag{47}$$

$$\phi^+ + \phi^- - 2\phi_0 = (2n-1)\pi \tag{48}$$

Following the dispersion theory we have:

$$\sum \phi = \phi^{+} + \phi^{-} = 2\phi_0 + \frac{2\pi D\lambda^2 f_m^2}{c} \tag{48}$$

$$\phi^{+} + \phi^{-} - 2\phi_0 = \frac{2\pi D\lambda^2 f_m^2}{c} \tag{49}$$

Therefore, we can arrive to

$$\frac{2\pi D\lambda^2 f_m^2}{c} = (2n-1)\pi \tag{50}$$

$$D = \frac{(n-\frac{1}{2})c}{\lambda^2 f_m^2} \tag{51}$$

Where f_m is the modulating frequency at which we detect an amplitude null. Now we explain the case where the DUT inserts different amplitude attenuation levels at each frequency component. We will denote by A^+ the amplitude at the upper optical sideband, A^- the amplitude at the lower optical sideband. The mathematical analysis for this situation is developed as follows.

At the DUT's input, we receive the same optical signal from the modulator:

$$E_{MZ} = \frac{A_0}{2}[2\cos\theta_b - \frac{A_m}{2}\sin\theta_b(e^{j\omega_m t} + e^{-j\omega_m t})] \tag{52}$$

But now after it passes through the DUT we have:

$$E_{DUT} = \frac{A_0 \mathrm{A}^0}{2}\cos\theta_b(e^{j\phi_0} + e^{-j\phi_0}) - \frac{A_0 A_m}{4}\sin(\mathrm{A}^{+}(e^{j\omega_m t}e^{j\phi^{+}} + e^{-j\omega_m t}e^{-j\phi^{-}})\mathrm{A}^{-}(e^{-j\omega_m t}e^{j\phi^{-}} + e^{j\omega_m t}e^{-j\phi^{+}})) \tag{53}$$

At the optical detector's output, after applying the square-law,

$$P_d = \frac{|E_{out}|^2}{2} \tag{54}$$

we obtain:

$$P_d = \frac{1}{2}\left(\frac{A_0^2 \mathrm{A}_0^2}{2}\cos\theta_b - \frac{A_0^2 \mathrm{A}_0^2 A_m}{2}\cos\theta_b \sin\theta_b \left(\mathrm{A}^+\left(\frac{e^{j\omega_m t}e^{j\phi^+}e^{+j\phi_0} + e^{-j\omega_m t}e^{-j\phi^+}e^{-j\phi_0}}{2}\right) + \right.\right. \tag{55}$$

$$\left.\left. + \mathrm{A}^-\left(\frac{e^{j\omega_m t}e^{j\phi^-}e^{j\phi_0} + e^{-j\omega_m t}e^{-j\phi^-}e^{-j\phi_0}}{2}\right)\right)\right)$$

$$P_d = \frac{A_0^2 \mathrm{A}_0^2}{4}\cos^2\theta_b - \frac{A_0^2 \mathrm{A}_0^2 A_m}{4}\cos\theta_b \sin\theta_b \left(\mathrm{A}^+\cos(\omega_m t + \phi + \phi_0) + \mathrm{A}^-\cos(\omega_m t - \phi^- - \phi_0)\right) \tag{56}$$

Trough the following trigonometric identity:

$$A\cos(\omega + a) + B\cos(\omega + b) = \sqrt{\mathrm{A}^2 + \mathrm{B}^2 + 2\mathrm{AB}\cos(b-a)}\cos\left(\omega + a + \arctan\left(\frac{\sin(b-a)}{\frac{\mathrm{A}}{\mathrm{B}} + \cos(b-a)}\right)\right) \tag{57}$$

the detected power results:

$$P_d = \frac{A_0^2 \mathrm{A}_0^2}{4}\cos^2\theta_b - \frac{A_0^2 \mathrm{A}_0^2 A_m}{2}\cos\theta_b \sin\theta_b \sqrt{\mathrm{A}^{+2} + \mathrm{A}^{-2} + 2\mathrm{A}^+\mathrm{A}^-\cos(\phi^+ + \phi^- - 2\phi_0)}\cos(\omega_m t + \phi^+ - \phi_0$$

$$+ \arctan\left(\frac{\sin(\phi^+ + \phi^- - 2\phi_0)}{\frac{\mathrm{A}^+}{\mathrm{A}^-} + \cos(\phi^+ + \phi^- - 2\phi_0)}\right) \tag{58}$$

As before, we reach an amplitude dip when the cosine function takes its minimum value (-1), so we have:

$$\cos(\phi^+ + \phi^- - 2\phi_0) = -1 \tag{59}$$

$$\phi^+ + \phi^- - 2\phi_0 = (2n-1)\pi \tag{60}$$

We notice we are under the same condition than for the non-amplitude degradation DUT and therefore, expression (51) is still valid to calculate chromatic dispersion coefficient. Thus, this analysis confirms Peucheret's method robustness for characterizing this kind of devices, such as for example an MZI filter, in contrast to MPSM because as also seen from the above expression the electrical phase at the modulating frequency is affected by an error term.

This method presents an important problem, i.e. the fact that it depends on the amount of dispersion introduced by a determined DUT. Because of this amount the RF frequency which we need to reach a dip can be too high; therefore, to find the dispersion value a large sweep will be required. Moreover, the use of high frequencies on the setup presents two main inconveniences: it may occur that equipment available cannot operate at those frequencies; and the effect which is produced by the increase of the RF frequency

level, i.e. the moving of the sidebands even further from the carrier leads to loss of resolution and accuracy in calculations.

Peucheret tries to solve this problem by including a constant dispersion offset before the DUT in the setup. In this way the amount of total dispersion, which we want to measure, increases and the dip can be reached by using a lower RF frequency. Consequently the level of desired dispersion is now the change in the total dispersion (DUT and offset). However, this procedure is based on dispersion offset's stability during the entire process, which is hard to reach in highly dispersive channels[6].

Another feature steaming from expression (51) is an additional phase term which will give errors when trying to determine the dispersion through the MPSM.

3.4 Analysis with MZI Modulator in Asymmetric configuration

Once terminated the study of MPSM and Peucheret's Method with the MZI Modulator in Push-Pull configuration, it is the time to introduce a new technique: MZSM (Modulation Zero Shift Method)[2]. We determine the mathematical expression, without DUT and with DUT, of the first harmonic. With these expressions we will calculate the dispersion value.

First of all we have to change the MZI Modulator configuration, i.e. we will consider the asymmetric one. As we have already explained in Chapter 2, this configuration allows the RF voltage and the Bias voltage either to be applied to the different arms of the modulator or to the same one.

So, with the Figure 1 which represents our guide we are ready to start with the analysis. We will see this analysis more in detail because we have worked mainly with this configuration.

The signal enters the modulator where an RF signal and a bias are combined and applied with different sign to each electrode.

We have θ_b which is represented by

$$\theta_b = \frac{V_b}{V_\pi}\pi \tag{60}$$

And θ_{RF} which is represented by

$$\theta_{RF} = \frac{\pi}{2V_\pi}V_{RF}(t) \tag{61}$$

In a general case, the RF signal will be of much lower intensity than the bias level and therefore $\theta_{RF} << \theta_b$ and then we use a Taylor for $e^{j\theta_{RF}} \approx 1 + j\theta_{RF}$, $A_{RF} << V_b$ and then the small signal approximation may be used and at the output we have, considering the low pass equivalent and the small signal approximation (considering (3))

$$E_{MZ} = \frac{A_0}{2}[2\cos\theta_b - A_m \sin\theta_b(e^{j\omega_m t} + e^{-j\omega_m t})] \tag{62}$$

In this case since we are only interested in the first harmonic components, only terms up to first order have been used

Also a bias voltage V_b is applied, which brings the device under analysis into the transfer function region where we work; we will use

$$V_b = \frac{V_\pi \theta_b}{\pi} \tag{63}$$

First we will consider RF and Bias voltage applied to the same electrode.

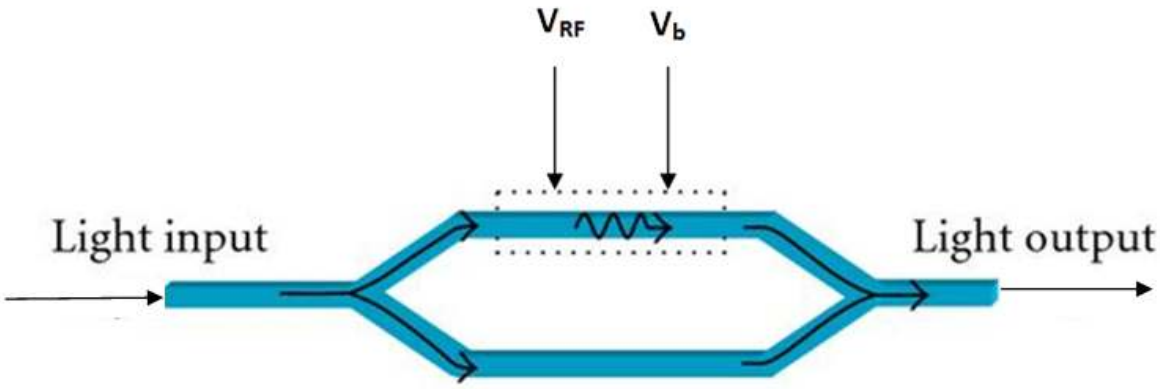

Figure 15. MZI Modulator with the two voltages on the same arm

The result is

$$E_{out} = e^{j\frac{\theta_b}{2}}\left[2\cos\frac{\theta_b}{2} + je^{+j\frac{\theta_b}{2}}\theta_{RF} - \frac{1}{2}e^{j\frac{\theta_b}{2}}\theta_{RF}^2\right] \tag{64}$$

The second configuration considers the Bias and RF voltage are applied to different arms

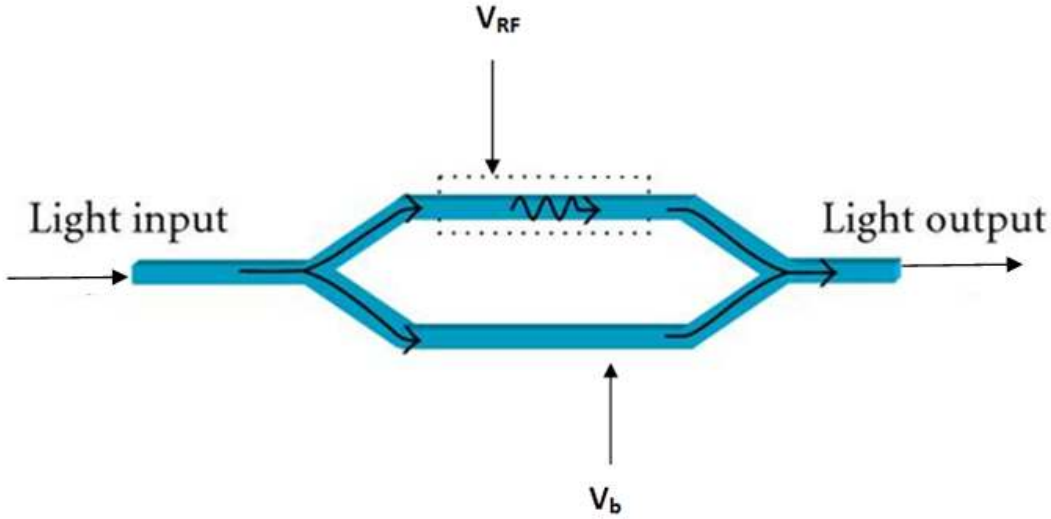

Figure 16. MZI Modulator with the two voltages on different arms

The output would be

$$E_{out} = e^{j\theta_b} + e^{j\theta_{RF}} \approx e^{j\theta_b} + 1 + j\theta_{RF} = e^{j\frac{\theta_b}{2}}\left(e^{j\frac{\theta_b}{2}} + e^{-j\frac{\theta_b}{2}}\right) \tag{65}$$

$$= e^{j\frac{\theta_b}{2}}\left[2\cos\frac{\theta_b}{2} + je^{-j\frac{\theta_b}{2}}\theta_{RF}\right] \tag{66}$$

It is possible to note that the only difference between the two expressions is the sign in the term $e^{\pm j\frac{\theta_b}{2}}$.

To continue with the analysis, we follow the signal which passes through the modulator with asymmetric configuration, RF and bias voltage in different electrodes. The electric field at the modulator output can be rewritten, using the relation

$$\theta_{RF} = m\cos(\omega t) \tag{67}$$

where

$$m = \frac{\pi V_{RF}}{V_\pi} \tag{68}$$

as

$$E_{out} = \frac{1}{2}A_0 e^{j\frac{\theta_b}{2}}[2\cos\frac{\theta_b}{2} + je^{-j\frac{\theta_b}{2}}\theta_{RF}] = \frac{1}{2}A_0\cos(\omega_0 t)e^{j\frac{\theta_b}{2}}[2\cos\frac{\theta_b}{2} + je^{-j\frac{\theta_b}{2}}m\cos(\omega t)] =$$
$$\frac{1}{2}A_0 e^{j\frac{\theta_b}{2}}[2\cos\frac{\theta_b}{2} + jme^{-j\frac{\theta_b}{2}}\cos(\omega t)]$$
$$= \frac{1}{2}A_0 e^{j\frac{\theta_b}{2}}[2\cos\frac{\theta_b}{2} + jme^{-j\frac{\theta_b}{2}}\cos(\omega t)] \tag{69}$$

Now we focus our attention on the term $\cos(\omega t)$, which represents the modulation applied to the signal which travels through the MZ modulator. In this case without DUT, we consider that the amplitudes are equal to each other, whereas the phase shifts are different. In other words, the phase of the upper sideband (positive sideband) is different from the phase of lower sideband (negative sideband). For this reason, we can rewrite the equation of detected power using a new nomenclature:

ϕ_0^+ : Phase shift of the optical carrier in the positive sideband

ϕ_0^- : Phase shift of the optical carrier in the negative sideband

We can rewrite the power expression considering the new nomenclature as

$$\cos(\omega t) - - > \frac{1}{2}[e^{j\omega t}e^{j\phi_0^+} + e^{-j\omega t}e^{j\phi_0^-}] \tag{70}$$

With this substitution the expression is

$$E_{out} = \frac{1}{2}A_0 e^{j\frac{\theta_b}{2}}\{2\cos\frac{\theta_b}{2} + je^{-j\frac{\theta_b}{2}}m\frac{1}{2}[e^{j\omega t}e^{j\phi_0^+} + e^{-j\omega t}e^{j\phi_0^-}]]\}$$
$$= \frac{1}{2}A_0\{2\cos\frac{\theta_b}{2} + jm\frac{1}{2}[e^{j\omega t}e^{j\phi_0^+}e^{-j\frac{\theta_b}{2}} + e^{-j\omega t}e^{j\phi_0^-}e^{-j\frac{\theta_b}{2}}]\} \tag{71}$$

The expression above represents the general analysis of our system, without DUT, at the output of MZI Modulator.

The first harmonic of this expression is

$$E_{out} = \frac{1}{2}A_0\{2\cos\frac{\theta_b}{2} + jm\frac{1}{2}[e^{j\omega t}e^{j\phi_0^+}e^{-j\frac{\theta_b}{2}} + e^{-j\omega t}e^{j\phi_0^-}e^{-j\frac{\theta_b}{2}}]\}$$
$$= \frac{1}{2}A_0\{2\cos\frac{\theta_b}{2} + jm\frac{1}{2}[\cos(\omega t + \phi_0^+ - \frac{\theta_b}{2}) + j\sin(\omega t + \phi_0^+ - \frac{\theta_b}{2}) +$$
$$+\cos(\omega t - \phi_0^- + \frac{\theta_b}{2}) - j\sin(\omega t - \phi_0^- + \frac{\theta_b}{2})]\}$$
$$= \frac{1}{2}A_0\{2\cos\frac{\theta_b}{2} + \frac{1}{2}m[-\sin(\omega t + \phi_0^+ - \frac{\theta_b}{2}) + \sin(\omega t - \phi_0^- + \frac{\theta_b}{2})] +$$
$$+ j\frac{1}{2}m[\cos(\omega t + \phi_0^+ - \frac{\theta_b}{2}) + \cos(\omega t - \phi_0^- + \frac{\theta_b}{2})]\} \tag{72}$$

We introduce new parameters

$$\phi_b^+ = \phi_0^+ - \frac{\theta_b}{2}$$
$$\phi_b^- = -\phi_0^- + \frac{\theta_b}{2} \tag{73}$$

$$E_{out} = \frac{1}{2} A_0 \{2\cos\frac{\theta_b}{2} + \frac{1}{2} m[-\sin(\omega t + \phi_b^+) + \sin(\omega t + \phi_b^-)] +$$
$$+ j\frac{1}{2} m[\cos(\omega t + \phi_b^+) + \cos(\omega t + \phi_b^-)]\} \tag{74}$$

When the signal passes through the photodetector there is the translation into the electrical domain; this change follows the square-law principle. So, the modulator output will be given by

$$P_d = \frac{|E_{out}|^2}{2} \tag{75}$$

The modulus function, in this case, implies taking the field envelope, i.e. to eliminate all the components at optical frequencies. So the detected power is

$$P_d = \frac{1}{2} |\frac{1}{2} A_0 \{2\cos\frac{\theta_b}{2} + \frac{1}{2} m[-\sin(\omega t + \phi_b^+) + \sin(\omega t + \phi_b^-)] +$$
$$+ j\frac{1}{2} m[\cos(\omega t + \phi_b^+) + \cos(\omega t + \phi_b^-)]\}|^2$$
$$= \frac{1}{8} A_0^2 \{[2\cos\frac{\theta_b}{2} - \frac{1}{2} m\sin(\omega t + \phi_b^+) + \frac{1}{2} m\sin(\omega t + \phi_b^-)]^2 +$$
$$+ \frac{1}{4} m^2 [\cos(\omega t + \phi_b^+) + \cos(\omega t + \phi_b^-)]^2\} \tag{76}$$

The calculation of the square of a complex number is

$$|a + jb|^2 = a^2 + b^2$$

$$P_d = \frac{1}{8} A_0^2 \{4\cos^2\frac{\theta_b}{2} + \frac{1}{4} m^2 \sin^2(\omega t + \phi_b^+) + \frac{1}{4} m^2 \sin^2(\omega t + \phi_b^-) - 2m\cos\frac{\theta_b}{2}\sin(\omega t + \phi_b^+) +$$
$$+ 2m\cos\frac{\theta_b}{2}\sin(\omega t + \phi_b^-) - 2m^2 \sin(\omega t + \phi_b^+)\sin(\omega t + \phi_b^-) + \frac{1}{4} m^2 \cos^2(\omega t + \phi_b^+) +$$
$$+ \frac{1}{4} m^2 \cos^2(\omega t + \phi_b^-)] + 2m^2 \cos(\omega t + \phi_b^+)\cos(\omega t + \phi_b^-)\} \tag{77}$$

Because we are ultimately interested in the first harmonic, the DC part and the part with *m* are extremely important to us, so

$$P_d = \frac{1}{8} A_0^2 \{4\cos^2\frac{\theta_b}{2} - 2m\cos\frac{\theta_b}{2}\sin(\omega t + \phi_b^+) + 2m\cos\frac{\theta_b}{2}\sin(\omega t + \phi_b^-)\}$$
$$= \frac{1}{4} A_0^2 \{2\cos^2\frac{\theta_b}{2} - m\cos\frac{\theta_b}{2}\sin(\omega t + \phi_b^+) + m\cos\frac{\theta_b}{2}\sin(\omega t + \phi_b^-)\} \tag{78}$$

Through mathematical development we arrive to

$$P_d = \frac{1}{2} A_0^2 \cos^2 \frac{\theta_b}{2} + m \frac{1}{2} A_0^2 \cos \frac{\theta_b}{2} \cos(\omega t + \frac{\phi_0^+ - \phi_0^+}{2}) \sin(\frac{\phi_0^+ - \phi_0^-}{2} - \theta_b)\} \tag{79}$$

The first term corresponds to the continuous wave component, which defines the transfer function of the modulator. On the other hand, the other term corresponds to the harmonic at the modulation frequency whose amplitude is a function of the bias voltage.

At this point we consider the signal at the MZI Modulator output; now we insert the signal in the DUT which has the effect to add a phase shift to each frequency component in E_{out}, as with the MZI Modulator. These phase shifts sum to the others derived by the Modulator.

φ_{DUT}^+ : Phase shift which corresponds to the upper band $\omega_0 + \omega_{RF}$

φ_{DUT}^- : Phase shift which corresponds to the lower band $\omega_0 - \omega_{RF}$

Considering the parameters above, the expression of electric field at the output of MZ Optical Filter and that of the detected power at the output of the detector changes.

$$\cos(\omega t) - - > \frac{1}{2}[e^{j\omega t} e^{j\phi_0^+} e^{j\phi_{DUT}^+} + e^{-j\omega t} e^{j\phi_0^-} e^{j\phi_{DUT}^-}] \tag{80}$$

The next step is expressing it in real and imaginary part

$$\begin{aligned} E_{out} &= \frac{1}{2} A_0 \{2\cos\frac{\theta_b}{2} + jm\frac{1}{2}[\cos(\omega t + \phi_0^+ + \phi_{DUT}^+ - \frac{\theta_b}{2}) + j\sin(\omega t + \phi_0^+ + \phi_{DUT}^+ - \frac{\theta_b}{2}) + \\ &+ \cos(\omega t - \phi_0^- - \phi_{DUT}^- + \frac{\theta_b}{2}) - j\sin(\omega t - \phi_0^- - \phi_{DUT}^- + \frac{\theta_b}{2})]\} \\ &= \frac{1}{2} A_0 \{2\cos\frac{\theta_b}{2} + \frac{1}{2} m[-\sin(\omega t + \phi_0^+ + \phi_{DUT}^+ - \frac{\theta_b}{2}) + \sin(\omega t - \phi_0^- - \phi_{DUT}^- + \frac{\theta_b}{2})] + \\ &+ m\frac{1}{2} j[\cos(\omega t + \phi_0^+ + \phi_{DUT}^+ - \frac{\theta_b}{2}) + \cos(\omega t - \phi_0^- - \phi_{DUT}^- + \frac{\theta_b}{2})]\} \end{aligned} \tag{81}$$

We simplify the expression with the following substitutions

$$\phi^+ = \phi_0^+ + \phi_{DUT}^+ - \frac{\theta_b}{2} \tag{82}$$

$$\phi^- = -\phi_0^- - \phi_{DUT}^- + \frac{\theta_b}{2} \tag{83}$$

And then calculate the detected power

$$P_d = \frac{1}{8} A_0^2 \{[2\cos\frac{\theta_b}{2} + m\frac{1}{2}[\sin(\omega t + \phi_0^+ + \phi_{DUT}^+ - \frac{\theta_b}{2}) + \sin(\omega t - \phi_0^- - \phi_{DUT}^- + \frac{\theta_b}{2})]^2 +$$
$$+ m^2 \frac{1}{4}[\cos(\omega t + \phi_0^+ + \phi_{DUT}^+ - \frac{\theta_b}{2}) + \cos(\omega t - \phi_0^- - \phi_{DUT}^- + \frac{\theta_b}{2})]\}$$
$$= \frac{1}{8} A_0^2 \{[4\cos^2\frac{\theta_b}{2} + m^2 \frac{1}{4}\sin^2(\omega t + \phi^+) + m^2 \frac{1}{4}\sin^2(\omega t + \phi^-) +$$
$$-\frac{1}{2} m^2 \sin(\omega t + \phi^+)\sin(\omega t + \phi^-) - 2m\cos\frac{\theta_b}{2}\sin(\omega t + \phi^+) +$$
$$+ 2m\cos\frac{\theta_b}{2}\sin(\omega t + \phi^-) + m^2 \frac{1}{4}[\cos(\omega t + \phi^+) + \cos(\omega t + \phi^-)]^2 \quad (84)$$

We are interested in the first harmonic, so we take only the terms DC and the terms with *m*

$$P_d = \frac{1}{8} A_0^2 \{4\cos^2\frac{\theta_b}{2} - 2m\cos\frac{\theta_b}{2}\sin(\omega t + \phi^+) + 2m\cos\frac{\theta_b}{2}\sin(\omega t + \phi^-)\}$$
$$= \frac{1}{4} A_0^2 \cos\frac{\theta_b}{2}\{2\cos\frac{\theta_b}{2} - m\sin(\omega t + \phi^+) + m\sin(\omega t + \phi^-)\} \quad (85)$$

With a mathematical development we arrive to

$$P_d = \frac{1}{2} A_0^2 \cos^2\frac{\theta_b}{2} - \frac{1}{2} A_0^2 m\cos\frac{\theta_b}{2}\cos(\omega t + \frac{\Delta\phi_0 + \Delta\phi_{DUT}^+}{2})\sin(\frac{\theta_b}{2} - \frac{\sum\phi_{DUT} + \sum\phi_0}{2})\} \quad (86)$$

Where the first term corresponds with the continuous wave component, which defines the transfer function of the modulator. The second term is the harmonic at the modulation frequency.

The phase is the same in MPSM, the conclusion is that we may use MPSM with a MZ Modulator in Asymmetric configuration.

We see that just as when we used the MZM in push-pull configuration the detected amplitude at the RF term contains the sum phase coefficient. The important feature here is that it is possible to use the bias value to cause detected amplitude nulls without changing the modulating frequency. We deepen into detail in the next section.

3.5 MZSM Analysis

The MZSM, object of analysis in this section, uses the Mach-Zehnder Modulator in asymmetric configuration and the Mach-Zehnder Optical Filter together with a fixed laser and a ideal detector. With

this method we measure the amplitude of the detected signal (i.e. the modulus of S21). Then we look for the bias value which brings to zero this amplitude. The goal of this method is to determine the sum of optical phase which, finally, is related with the dispersion parameter D.

To explain the basis of MZSM, we take the power expression in absence of amplitude distortion. The relation is

$$P_d = \frac{1}{2}A_0^2\cos^2\frac{\theta_b}{2} - \frac{1}{4}A_0^2 m\cos\frac{\theta_b}{2}\sin(\frac{\theta_b}{2} - \frac{\phi_{DUT}^+ + \phi_{DUT}^- + \sum\phi_0}{2})\cos(\omega t + \frac{\phi_{DUT}^+ - \phi_{DUT}^- + \Delta\phi_0}{2}) \tag{87}$$

To obtain a "zero" in the amplitude term, we have:

$$\sin(\frac{\theta_b}{2} - \frac{\sum\phi_{DUT}}{2} - \frac{\sum\phi_0}{2}) = 0 \tag{88}$$

$$\frac{\theta_b}{2} - \frac{\sum\phi_{DUT}}{2} - \frac{\sum\phi_0}{2} = (n-1)\pi \tag{89}$$

$$\sum\phi_{DUT} + \sum\phi_0 - \theta_b = -2(n-1)\pi \tag{90}$$

Following the dispersion theory we have

$$\sum\phi_{DUT} = \phi^+ + \phi^- = -\sum\phi_0 + \frac{2\pi D\lambda^2 f_m^2}{c} \tag{91}$$

$$\phi^+ + \phi^- + \sum\phi_0 = \frac{2\pi D\lambda^2 f_m^2}{c} \tag{92}$$

Therefore, we can arrive to

$$\frac{2\pi D\lambda^2 f_m^2}{c} = \theta_b - 2(n-1)\pi \tag{93}$$

3.6 RF scan analysis considering phase distortion

At this point, it is useful to insert a summary scheme to clarify what we have explained until now.

MODULATOR CONFIGURATION	METHOD	DETECTED PARAMETER	NUMBER OF λ NEEDED	VULNERABILITY
Asymmetric or Push-Pull	MPSM	Electrical phase	Two wavelength	Amplitude
Push-Pull	Peucheret	Amplitude	A wavelength	No vulnerability
Asymmetric	MZSM			

(99)

Now we introduce a method which is the result of the combination of two methods. In this section we calculate the Dispersion value with MZSM and MPSM; the benefit is that we determinate the phase difference $\Delta\phi$ through MPSM with Asymmetric configuration and the $\sum\phi$ through MZSM. The method needs two modulation frequencies in order to obtain the phase spectral without a tunable laser

We start from the detected power expression

$$P_d = \frac{1}{2}A_0^2\cos^2\frac{\theta_b}{2} - \frac{1}{4}A_0^2 m\cos\frac{\theta_b}{2}\sin\left(\frac{\theta_b}{2} - \frac{\phi_{DUT}^{+} + \phi_{DUT}^{-} + \sum\phi_0}{2}\right)\cos\left(\omega t + \frac{\phi_{DUT}^{+} - \phi_{DUT}^{-} + \Delta\phi_0}{2}\right) \quad (94)$$

As mentioned in the section 3.3 the MPSM can be implemented using a MZ in Asymmetric configuration and therefore by measuring the electrical phase we can measure the sidebands optical phases semi difference; on the other hand by varying the bias voltage the zeros in the amplitude response can be determined so to obtain the sidebands optical phases sum.

The method can be represented by the Figure 18

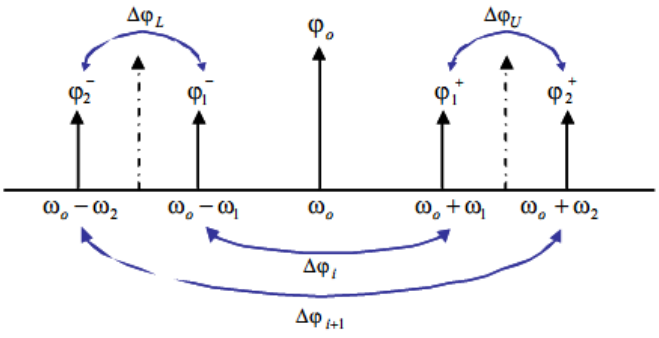

Figure 17. RF scan with MPSM and MZSM

Therefore, in order to obtain the group delay we need two measures:

1. The phase difference between the detected signal and the input signal for two modulation frequencies

$$\Delta\phi_1 = \frac{\phi_1^+ - \phi_1^-}{2} \tag{95}$$

2. The bias voltage which cancels out the detected signal in each frequency allowing us to determine $2\phi_0 - \phi^+ - \phi^-$ as follows

$$\sin\left(\frac{\theta_b}{2} - \frac{\phi_{DUT}^+ + \phi_{DUT}^- + \sum\phi_0}{2}\right) = 0 \Longrightarrow \quad \frac{\phi_{DUT}^+ + \phi_{DUT}^- + \sum\phi_0}{2} = \frac{\theta_b}{2} - n\pi \tag{96}$$

For each pair of frequencies we get

$$\theta_{b_1} = \phi_{DUT1}^+ + \phi_{DUT1}^- + \sum\phi_0 \tag{97}$$

Considering the difference of the bias obtained for cancellation at two different modulating frequencies, we have

$$\Delta\theta_b = \theta_{b_i+1} - \Delta\theta_{b_i} = \phi_{DUT1}^+ + \phi_{DUT1}^- + \sum\phi_0 - (\phi_{DUT2}^+ + \phi_{DUT2}^- + \sum\phi_0) \tag{98}$$

and the same for the detected phase

$$\Delta\phi_{DET} = \Delta\phi_2 - \Delta\phi_1 = \frac{\phi_2^+ - \phi_2^-}{2} - \frac{\phi_1^+ - \phi_1^-}{2} \tag{99}$$

Therefore for the upper band we have

$$\Delta\phi^+ = \phi_2^+ - \phi_1^+ = \Delta\phi_{DET} - \frac{\Delta\theta_b}{2} \tag{100}$$

The same for the lower band

$$\Delta\phi^- = \phi_1^- - \phi_2^- = \Delta\phi_{DET} + \frac{\Delta\theta_b}{2} \tag{101}$$

So, the group delays comes from

$$\tau_{g_l} \approx -\frac{\Delta\phi_l}{360^\circ}\frac{1}{\Delta f} \tag{102}$$

$$\tau_{g_u} \approx -\frac{\Delta\phi_u}{360^\circ}\frac{1}{\Delta f} \tag{103}$$

where Δf is the modulating frequency step ($\Delta f = f_{i+1} - f_i$).

The sum of the last two expressions leads to the final relation of the group delay, i.e.

$$D = \frac{d\tau_g}{d\lambda} \approx \frac{\Delta\tau_g}{\Delta\lambda} \tag{104}$$

3.7 Analysis with MZI Modulator in Asymmetric configuration (phase and amplitude distortion)

Now we focus our attention on the phase and the amplitude distortions of our signal when it enters in the DUT. In other words, the amplitude of the upper sideband (positive sideband) is different from the amplitude of the lower sideband (negative sideband); the same holds for the phase. For this reason, we can rewrite the equation of detected power using the same parameters of the previous analysis with the adding of new variables: $A_0^+, A_0^-, A_{DUT}^+, A_{DUT}^-$ where the first two represent the amplitude distortions, on the two sidebands, caused by the modulator or the whole measurement system in the absence of DUT and the last two refer to those caused by the DUT.

So we present first the analysis without the DUT in order to see the behaviour of the system and then we add the DUT to know its contribution to our study. So the parameters are:

φ_0^+ : Phase shift of the optical carrier in the positive sideband

φ_0^- : Phase shift of the optical carrier in the negative sideband

A_0^+ : Amplitude shift of the optical carrier in the positive sideband

A_0^- : Amplitude shift of the optical carrier in the negative sideband

We can write the power expression (69) considering the substitution

$$\cos(\omega t) --> \frac{1}{2}[A_0^+ e^{j\omega t} e^{j\phi_0^+} + A_0^- e^{-j\omega t} e^{j\phi_0^-}] \tag{105}$$

In order to present a complete analysis, we consider the approximation (70) up to the third term.

In this case we should consider the second harmonic because we need it, but the second harmonic we need is the mTP, it is the same because there is not the carrier and this does not bring contribution on the SH measured after the detector.

So the expression of electric field can be rewritten as

$$E_{out} = \frac{1}{2} A_0 e^{j\frac{\theta_b}{2}} [2\cos\frac{\theta_b}{2} + je^{-j\frac{\theta_b}{2}} \theta_{RF}] = \frac{1}{2} A_0 e^{j\frac{\theta_b}{2}} [2\cos\frac{\theta_b}{2} + je^{-j\frac{\theta_b}{2}} m\cos(\omega t)]$$
$$= \frac{1}{2} A_0 e^{j\frac{\theta_b}{2}} [2\cos\frac{\theta_b}{2} + je^{-j\frac{\theta_b}{2}} m\cos(\omega t)]$$
$$= \frac{1}{2} A_0 e^{j\frac{\theta_b}{2}} [2\cos\frac{\theta_b}{2} + je^{-j\frac{\theta_b}{2}} m\cos(\omega t)] \quad (106)$$

Substituting the relation with the different amplitudes and phases we obtain

$$E_{out} = \frac{1}{2} A_0 e^{j\frac{\theta_b}{2}} \{2\cos\frac{\theta_b}{2} + je^{-j\frac{\theta_b}{2}} m\frac{1}{2}[A_0^+ e^{j\omega t} e^{j\phi_0^+} + A_0^- e^{-j\omega t} e^{j\phi_0^-}]\}$$
$$= \frac{1}{2} A_0 \{2\cos\frac{\theta_b}{2} + jm\frac{1}{2}[A_0^+ e^{j\omega t} e^{j\phi_0^+} e^{-j\frac{\theta_b}{2}} + A_0^- e^{-j\omega t} e^{j\phi_0^-} e^{-j\frac{\theta_b}{2}}]\}$$
$$= \frac{1}{2} A_0 \{2\cos\frac{\theta_b}{2} + jm\frac{1}{2}[A_0^+ \cos(\omega t + \phi_0^+ - \frac{\theta_b}{2}) + jA_0^+ \sin(\omega t + \phi_0^+ - \frac{\theta_b}{2}) +$$
$$+ A_0^- \cos(\omega t - \phi_0^- + \frac{\theta_b}{2}) - jA_0^- \sin(\omega t - \phi_0^- + \frac{\theta_b}{2})]\} \quad (107)$$

We introduce some new parameters

$$\phi_b^+ = \phi_0^+ - \frac{\theta_b}{2}$$
$$\phi_b^- = -\phi_0^- + \frac{\theta_b}{2}$$

$$E_{out} = \frac{1}{2} A_0 \{2\cos\frac{\theta_b}{2} + jm\frac{1}{2}[A_0^+ \cos(\omega t + \phi_b^+) + jA_0^+ \sin(\omega t + \phi_b^+) + A_0^- \cos(\omega t - \phi_b^-) +$$
$$- jA_0^- \sin(\omega t - \phi_b^-)]\} \quad (108)$$

In this way the detected power is

$$P_d = \frac{1}{2}|\frac{1}{2}A_0\{2\cos\frac{\theta_b}{2}+\frac{1}{2}m[-A_0^+\sin(\omega t+\phi_b^+)+A_0^-\sin(\omega t+\phi_b^-)]+$$
$$+j\frac{1}{2}m[A_0^+\cos(\omega t+\phi_b^+)+A_0^-\cos(\omega t+\phi_b^-)]\}|^2$$
$$=\frac{1}{8}A_0^2\{[2\cos\frac{\theta_b}{2}-\frac{1}{2}mA_0^+\sin(\omega t+\phi_b^+)+\frac{1}{2}mA_0^-\sin(\omega t+\phi_b^-)]^2+$$
$$+\frac{1}{4}m^2[A_0^+\cos(\omega t+\phi_b^+)+A_0^-\cos(\omega t+\phi_b^-)]^2\} \quad (109)$$

$$P_d=\frac{1}{8}A_0^2\{4\cos^2\frac{\theta_b}{2}+\frac{1}{4}m^2(A_0^+)^2\sin^2(\omega t+\phi_b^+)+\frac{1}{4}m^2(A_0^-)^2\sin^2(\omega t+\phi_b^-)-2m\cos\frac{\theta_b}{2}A_0^+\sin(\omega t+\phi_b^+)+$$
$$+2m\cos\frac{\theta_b}{2}A_0^-\sin(\omega t+\phi_b^-)-2m^2A_0^+A_0^-\sin(\omega t+\phi_b^+)\sin(\omega t+\phi_b^-)+\frac{1}{4}m^2(A_0^+)^2\cos^2(\omega t+\phi_b^+)+$$
$$+\frac{1}{4}m^2(A_0^-)^2\cos^2(\omega t+\phi_b^-)]+2m^2A_0^+A_0^-\cos(\omega t+\phi_b^+)\cos(\omega t+\phi_b^-)\} \quad (110)$$

Because we are ultimately interested in the first harmonic, the DC part and the part with *m* are extremely important for us, so

$$P_d=\frac{1}{8}A_0^2\{4\cos^2\frac{\theta_b}{2}-2m\cos\frac{\theta_b}{2}A_0^+\sin(\omega t+\phi_b^+)+2m\cos\frac{\theta_b}{2}A_0^-\sin(\omega t+\phi_b^-)\}$$
$$=\frac{1}{4}A_0^2\{2\cos^2\frac{\theta_b}{2}-m\cos\frac{\theta_b}{2}A_0^+\sin(\omega t+\phi_b^+)+m\cos\frac{\theta_b}{2}A_0^-\sin(\omega t+\phi_b^-)\} \quad (111)$$

Now, we introduce a new relation:

$$A\sin(\omega+a)+B\sin(\omega+b)=\sqrt{A^2+B^2+2AB\cos(b-a)}\sin(\omega+a+\arctan(\frac{\sin(b-a)}{[\frac{A}{B}+\cos(b-a)]})) \quad (112)$$

From this relation, we can get two important parameters: the first is the amplitude A and the second is the phase PH in the detected first harmonic for this setup.

$$\mathrm{A}=\sqrt{(A_0^+)^2+(A_0^-)^2-2A_0^+A_0^-\cos(\phi_b^--\phi_b^+)}=\sqrt{(A_0^+)^2+(A_0^-)^2-2A_0^+A_0^-\cos(-\phi_0^-+\frac{\theta_b}{2}-\phi_0^++\frac{\theta_b}{2})}$$
$$=\sqrt{(A_0^+)^2+(A_0^-)^2-2A_0^+A_0^-\cos(-\sum\phi_0+\theta_b)}$$

(113)

$$PH=\phi_0^+-\frac{\theta_b}{2}+\arctan(\frac{\sin(-\phi_0^-+\frac{\theta_b}{2}-\phi_0^++\frac{\theta_b}{2})}{[-\frac{A_0^+}{A_0^-}+\cos(-\phi_0^-+\frac{\theta_b}{2}-\phi_0^++\frac{\theta_b}{2})]})$$
$$=\phi_0^+-\frac{\theta_b}{2}+\arctan(\frac{\sin(-\sum\phi_0+\theta_b)}{[-\frac{A_0^+}{A_0^-}+\cos(-\sum\phi_0+\theta_b)]})=\phi_0^+-\theta_b+\arctan(\frac{-\sin(\sum\phi_0-\theta_b)}{[-\frac{A_0^+}{A_0^-}+\cos(\sum\phi_0-\theta_b)]})$$
$$=\phi_0^+-\frac{\theta_b}{2}+\arctan(\frac{\sin(\sum\phi_0-\theta_b)}{[\frac{A_0^+}{A_0^-}-\cos(\sum\phi_0-\theta_b)]})$$

(114)

The phase can be rewritten as

$$PH=\frac{\Delta\phi_0}{2}+\frac{\sum\phi_0}{2}-\frac{\theta_b}{2}+\arctan\left(\frac{\sin(\sum\phi_0-\theta_b)}{[\frac{A_0^+}{A_0^-}-\cos(\sum\phi_0-\theta_b)]}\right)$$

(115)

where we have used the relation

$$\phi_0^+-\frac{\theta_b}{2}=\frac{\Delta\phi_0}{2}+\frac{\sum\phi_0}{2}-\frac{\theta_b}{2}$$

(116)

With these new expressions we get to the final detected power which can be written as follows

$$P_d = \frac{1}{4} A_0^2 \{2\cos^2 \frac{\theta_b}{2} - m\cos\frac{\theta_b}{2} \sqrt{(A_0^+)^2 + (A_0^-)^2 - 2A_0^+ A_0^- \cos(-\sum \phi_0 + \theta_b)}\}$$
$$\sin(\omega t + \frac{\Delta\phi_0}{2} + \frac{\sum \phi_0}{2} - \frac{\theta_b}{2} + \arctan(\frac{\sin(\sum \phi_0 - \theta_b)}{[\frac{A_0^+}{A_0^-} - \cos(\sum \phi_0 - \theta_b)]})) \quad (117)$$

To present a complete description of the MZ Modulator behaviour in the most interesting points, we should explain what happens in the mTP; in this way we can see the influence of the optical carrier in the second harmonic. Starting from the expression of the electrical field, we have to substitute the value $\theta_b = \pi$. Under the approximation (70) up to the second term, we obtain

$$E_{out} = \frac{1}{2} A_0 e^{j\frac{\theta_b}{2}} [2\cos\frac{\theta_b}{2} + je^{-j\frac{\theta_b}{2}} \theta_{RF}] = \frac{1}{2} A_0 e^{j\frac{\theta_b}{2}} [2\cos\frac{\theta_b}{2} +$$
$$+ m\cos(\omega t)\sin\frac{\theta_b}{2} + jm\cos(\omega t)\cos\frac{\theta_b}{2}] =$$
$$= \frac{1}{2} A_0 [m\cos(\omega t)] \quad (118)$$

With the substitution of the relation of $\cos(\omega t)$ we get the expression for the second harmonic

The detected power will be,

$$P_d = \frac{1}{8} A_0^2 m^2 \{[A_0^+ \cos(\omega t + \phi_0^+) + A_0^- \cos(\omega t - \phi_0^-)]^2 + [A_0^+ \sin(\omega t + \phi_0^+) - A_0^- \sin(\omega t - \phi_0^-)]^2\}$$
$$= \frac{1}{8} A_0^2 m^2 \{(A_0^+)^2 \cos^2(\omega t + \phi_0^+) + (A_0^-)^2 \cos^2(\omega t - \phi_0^-) + 2A_0^+ A_0^- \cos(\omega t + \phi_0^+)\cos(\omega t - \phi_0^-) +$$
$$+ (A_0^+)^2 \sin^2(\omega t + \phi_0^+) + (A_0^-)^2 \sin^2(\omega t - \phi_0^-) - 2AA\sin(\omega t + \phi_0^+)\sin(\omega t - \phi_0^-)\}$$
$$= \frac{1}{32} A_0^2 m^2 \{(A_0^+)^2 + (A_0^-)^2 + 2A_0^+ A_0^- \cos(\omega t + \phi_0^+)\cos(\omega t - \phi_0^-) - 2A_0^+ A_0^- \sin(\omega t + \phi_0^+)\sin(\omega t - \phi_0^-)$$
$$= \frac{1}{32} A_0^2 m^2 \{(A_0^+)^2 + (A_0^-)^2 + 2A_0^+ A_0^- [\frac{1}{2}\cos(\omega t + \phi_0^+ - \omega t + \phi_0^-) + \frac{1}{2}\cos(2\omega t + \phi_0^+ - \phi_0^-) +$$
$$- \frac{1}{2}\cos(\phi_0^+ + \phi_0^-) + \frac{1}{2}\cos(2\omega t + \phi_0^+ - \phi_0^-)]\}$$

$$P_d = \frac{1}{32} A_0^2 m^2 \{(A_0^+)^2 + (A_0^-)^2 + 2A_0^+ A_0^- \cos(2\omega t + \Delta\phi_0)\} \quad (119)$$

Now we move on to analyze the system with the DUT; therefore we consider the expression (125) which corresponds to the MZ Modulator output. This signal goes into the MZ Optical Filter which has the effect to add an amplitude and phase shift to each frequency component in E_{out}. These amplitudes and phase shifts sum to the others added by the experimental setup.

ϕ_{DUT}^{+} : Phase shift which corresponds to the upper band $\omega_0 + \omega_{RF}$

ϕ_{DUT}^{-} : Phase shift which corresponds to the lower band $\omega_0 - \omega_{RF}$

A_{DUT}^{+} : Amplitude shift which corresponds to the upper band $\omega_0 + \omega_{RF}$

A_{DUT}^{-} : Amplitude shift which corresponds to the lower band $\omega_0 - \omega_{RF}$

Considering the parameters above, the expression of electric field at the output of MZ Optical Filter and that of the detected power at the output of the detector change.

$$\cos(\omega t) --> \frac{1}{2} e^{j\frac{\theta_b}{2}} [A_0^+ A_{DUT}^+ e^{j\omega t} e^{j\phi_0^+} e^{j\phi_{DUT}^+} + A_0^- A_{DUT}^- e^{-j\omega t} e^{j\phi_0^-} e^{j\phi_{DUT}^-}]$$

$$\begin{aligned}
E_{out} &= \frac{1}{2} A_0 e^{j\frac{\theta_b}{2}} [2\cos\frac{\theta_b}{2} + je^{-j\frac{\theta_b}{2}} \theta_{RF}] = \frac{1}{2} A_0 \cos(\omega_0 t) \{2\cos\frac{\theta_b}{2} + \\
&+ j\frac{1}{2} m e^{j\frac{\theta_b}{2}} [A_0^+ A_{DUT}^+ e^{j\omega t} e^{j\phi_0^+} e^{j\phi_{DUT}^+} + A_0^- A_{DUT}^- e^{-j\omega t} e^{j\phi_0^-} e^{j\phi_{DUT}^-}]\} \\
&= \frac{1}{2} A_0 \{2\cos\frac{\theta_b}{2} + j\frac{1}{2} m[A_0^+ A_{DUT}^+ e^{j\omega t} e^{j\phi_0^+} e^{j\phi_{DUT}^+} e^{-j\frac{\theta_b}{2}} + A_0^- A_{DUT}^- e^{-j\omega t} e^{j\phi_0^-} e^{j\phi_{DUT}^-} e^{-j\frac{\theta_b}{2}}]\} \\
&= \frac{1}{2} A_0 \{2\cos\frac{\theta_b}{2} + jm\frac{1}{2}[A_0^+ A_{DUT}^+ \cos(\omega t + \phi_0^+ + \phi_{DUT}^+ - \frac{\theta_b}{2}) + jA_0^+ A_{DUT}^+ \sin(\omega t + \phi_0^+ + \phi_{DUT}^+ - \frac{\theta_b}{2}) + \\
&+ A_0^- A_{DUT}^- \cos(\omega t - \phi_0^- - \phi_{DUT}^- + \frac{\theta_b}{2}) - jA_0^- A_{DUT}^- \sin(\omega t - \phi_0^- - \phi_{DUT}^- + \frac{\theta_b}{2})]\} \\
&= \frac{1}{2} A_0 \{2\cos\frac{\theta_b}{2} + \frac{1}{2} m[-A_0^+ A_{DUT}^+ \sin(\omega t + \phi_0^+ + \phi_{DUT}^+ - \frac{\theta_b}{2}) + A_0^- A_{DUT}^- \sin(\omega t - \phi_0^- - \phi_{DUT}^- + \frac{\theta_b}{2})] + \\
&+ jm\frac{1}{2}[A_0^+ A_{DUT}^+ \cos(\omega t + \phi_0^+ + \phi_{DUT}^+ - \frac{\theta_b}{2}) + A_0^- A_{DUT}^- \cos(\omega t - \phi_0^- - \phi_{DUT}^- + \frac{\theta_b}{2})]\}
\end{aligned} \quad (120)$$

We use the following substitutions

$$\phi^+ = \phi_0^+ + \phi_{DUT}^+ - \frac{\theta_b}{2} \quad (121)$$

$$\phi^- = -\phi_0^- - \phi_{DUT}^- + \frac{\theta_b}{2} \quad (122)$$

$$P_d = \frac{1}{8}A_0^2\{[2\cos\frac{\theta_b}{2} + m\frac{1}{2}[-A_0^+A_{DUT}^+\sin(\omega t + \phi_0^+ + \phi_{DUT}^+ - \frac{\theta_b}{2}) + A_0^-A_{DUT}^-\sin(\omega t - \phi_0^- - \phi_{DUT}^- + \frac{\theta_b}{2})]^2 +$$
$$+ m^2\frac{1}{4}[A_0^+A_{DUT}^+\cos(\omega t + \phi_0^+ + \phi_{DUT}^+ - \frac{\theta_b}{2}) + A_0^-A_{DUT}^-\cos(\omega t - \phi_0^- - \phi_{DUT}^- + \frac{\theta_b}{2})]\}$$
$$= \frac{1}{8}A_0^2\{[4\cos^2\frac{\theta_b}{2} + m^2\frac{1}{4}(A_0^+)^2(A_{DUT}^+)^2\sin^2(\omega t + \phi^+) + m^2\frac{1}{4}(A_0^-)^2(A_{DUT}^-)^2\sin^2(\omega t + \phi^-) +$$
$$-\frac{1}{2}A_0^+A_{DUT}^+A_0^-A_{DUT}^-m^2\sin(\omega t + \phi^+)\sin(\omega t + \phi^-) - 2m\cos\frac{\theta_b}{2}A_0^+A_{DUT}^+\sin(\omega t + \phi^+) +$$
$$+ 2m\cos\frac{\theta_b}{2}A_0^-A_{DUT}^-\sin(\omega t + \phi^-) + m^2\frac{1}{4}[A_0^+A_{DUT}^+\cos(\omega t + \phi^+) + A_0^-A_{DUT}^-\cos(\omega t + \phi^-)]^2 \quad (123)$$

We are interested in the first harmonic, so we take only the terms DC and the terms with *m*

$$P_d = \frac{1}{8}A_0^2\{4\cos^2\frac{\theta_b}{2} - 2m\cos\frac{\theta_b}{2}A_0^+A_{DUT}^+\sin(\omega t + \phi^+) + 2m\cos\frac{\theta_b}{2}A_0^-A_{DUT}^-\sin(\omega t + \phi^-)\}$$
$$= \frac{1}{4}A_0^2\cos\frac{\theta_b}{2}\{2\cos\frac{\theta_b}{2} - mA_0^+A_{DUT}^+\sin(\omega t + \phi^+) + mA_0^-A_{DUT}^-\sin(\omega t + \phi^-)\} \quad (124)$$

As we did in the first section, we determine the amplitude A and phase with the relation (118)

$$\mathrm{A} = \sqrt{(A_0^+)^2(A_{DUT}^+)^2 + (A_0^-)^2(A_{DUT}^-)^2 - 2A_0^+A_{DUT}^+A_0^-A_{DUT}^-\cos(\phi^- - \phi^+)} =$$
$$= \sqrt{(A_0^+)^2(A_{DUT}^+)^2 + (A_0^-)^2(A_{DUT}^-)^2 - 2A_0^+A_{DUT}^+A_0^-A_{DUT}^-\cos(-\phi_0^- + \frac{\theta_b}{2} - \phi_{DUT}^- - \phi_0^+ + \frac{\theta_b}{2} - \phi_{DUT}^+)}$$
$$= \sqrt{(A_0^+)^2(A_{DUT}^+)^2 + (A_0^-)^2(A_{DUT}^-)^2 - 2A_0^+A_{DUT}^+A_0^-A_{DUT}^-\cos(\sum\phi_0 + \sum\phi_{DUT} - \theta_b)} \quad (125)$$

$$PH = \phi_0^+ - \frac{\theta_b}{2} + \phi_{DUT}^+ + \arctan(\frac{\sin(-\phi_0^- + \frac{\theta_b}{2} - \phi_{DUT}^- - \phi_0^+ + \frac{\theta_b}{2} - \phi_{DUT}^+)}{[-\frac{A_0^+A_{DUT}^+}{A_0^-A_{DUT}^-} + \cos(-\phi_0^- + \frac{\theta_b}{2} - \phi_{DUT}^- - \phi_0^+ + \frac{\theta_b}{2} - \phi_{DUT}^+)]})$$
$$= \phi_0^+ - \frac{\theta_b}{2} + \phi_{DUT}^+ + \arctan(\frac{\sin(-\sum\phi_0 - \sum\phi_{DUT} + \theta_b)}{[-\frac{A_0^+A_{DUT}^+}{A_0^-A_{DUT}^-} + \cos(-\sum\phi_0 - \sum\phi_{DUT} + \theta_b)]})$$
$$= \phi_0^+ - \frac{\theta_b}{2} + \phi_{DUT}^+ + \arctan(\frac{\sin(\sum\phi_0 + \sum\phi_{DUT} - \theta_b)}{[\frac{A_0^+A_{DUT}^+}{A_0^-A_{DUT}^-} - \cos(\sum\phi_0 + \sum\phi_{DUT} - \theta_b)]}) \quad (126)$$

The phase can be rewritten

$$PH = \frac{\Delta\phi_0}{2} + \frac{\sum\phi_0}{2} + \frac{\Delta\phi_{DUT}}{2} + \frac{\sum\phi_{DUT}}{2} - \frac{\theta_b}{2} + \arctan\left(\frac{\sin(\sum\phi_0 + \sum\phi_{DUT} - \theta_b)}{\left[\frac{A_0^+ A_{DUT}^+}{A_0^- A_{DUT}^-} - \cos(\sum\phi_0 + \sum\phi_{DUT} - \theta_b)\right]}\right) \tag{127}$$

with a new relation in the first part

$$\phi_0^+ - \frac{\theta_b}{2} + \phi_{DUT}^+ = \frac{\Delta\phi_0}{2} + \frac{\sum\phi_0}{2} + \frac{\Delta\phi_{DUT}}{2} + \frac{\sum\phi_{DUT}}{2} - \frac{\theta_b}{2} \tag{128}$$

The final expression of detected power is

$$P_d = \frac{1}{4}A_0^2\cos\frac{\theta_b}{2}\{2\cos\frac{\theta_b}{2} - m\sqrt{(A_0^+)^2(A_{DUT}^+)^2 + (A_0^-)^2(A_{DUT}^-)^2 - 2A_0^+A_{DUT}^+A_0^-A_{DUT}^-\cos(\sum\phi_0 + \sum\phi_{DUT} - \theta_b)}$$
$$\sin(\omega t + \frac{\Delta\phi_0}{2} + \frac{\sum\phi_0}{2} + \frac{\Delta\phi_{DUT}}{2} + \frac{\sum\phi_{DUT}}{2} - \frac{\theta_b}{2} + \arctan\left(\frac{\sin(\sum\phi_0 + \sum\phi_{DUT} - \theta_b)}{\left[\frac{A_0^+ A_{DUT}^+}{A_0^- A_{DUT}^-} - \cos(\sum\phi_0 + \sum\phi_{DUT} - \theta_b)\right]}\right)) \tag{129}$$

The first term corresponds to the continuous wave component which defines the transfer function of the modulator. The second term is the harmonic at the modulation frequency (the modulating signal).

Now we determine the expression for the mTP ($\theta_b = \pi$), so we have

$$E_{out} = \frac{1}{2} A_0 \cos(\omega_0 t) e^{j\frac{\theta_b}{2}} [2\cos\frac{\theta_b}{2} + je^{-j\frac{\theta_b}{2}} \theta_{RF}] = \frac{1}{2} A_0 \cos(\omega_0 t)[j(A_0^+ A^+ \cos(\omega t + \phi_0^+ + \phi_{DUT}^+) +$$
$$+ jA_0^+ A^+ \sin(\omega t + \phi_0^+ + \phi_{DUT}^+) + A_0^- A^- \cos(\omega t - \phi_0^- - \phi_{DUT}^-) - jA_0^- A^- \sin(\omega t - \phi_0^- - \phi_{DUT}^-))] =$$

$$P_d = \frac{1}{4} A_0^2 \{[A_0^+ A^+ \cos(\omega t + \phi_0^+ + \phi_{DUT}^+) + A_0^- A^- \cos(\omega t - \phi_0^- - \phi_{DUT}^-)]^2 + [-A_0^+ A^+ \sin(\omega t + \phi_0^+ + \phi_{DUT}^+) +$$
$$+ A_0^- A^- \sin(\omega t - \phi_0^- - \phi_{DUT}^-)]^2\}$$
$$= \frac{1}{4} A_0^2 \{(A_0^+ A^+)^2 + (A_0^- A^-)^2 + 2A_0^+ A_0^- A^+ A^- \cos(\omega t + \phi_0^+ + \phi_{DUT}^+)\cos(\omega t - \phi_0^- - \phi_{DUT}^-) +$$
$$- 2A^+ A^- A_0^+ A_0^- \sin(\omega t + \phi_0^+ + \phi_{DUT}^+)\sin(\omega t - \phi_0^- - \phi_{DUT}^-)\}$$
$$= \frac{1}{4} A_0^2 \{(A^+ A_0^+)^2 + (A^- A_0^-)^2 + 2A^+ A^- \cos(2\omega t + \Delta\phi_0 + \Delta\phi_{DUT})\} \quad (130)$$

3.8 RF scan Analysis considering phase and amplitude distortions

In this section we introduce a technique which uses the expressions obtained previously. We present the parameters which we need.

First of all we need the calibration of the required measurement.

For the first harmonic we have:

the amplitude expression for analysis with DUT is

$$\sqrt{(A_0^+)^2 (A_{DUT}^+)^2 + (A_0^-)^2 (A_{DUT}^-)^2 - 2A_0^+ A_{DUT}^+ A_0^- A_{DUT}^- \cos(\sum \phi_0 + \sum \phi_{DUT} - \theta_b)} \quad (131)$$

Whereas the amplitude expression for analysis without DUT

$$\sqrt{(A_0^+)^2 + (A_0^-)^2 - 2A_0^+ A_0^- \cos(\sum \phi_0 - \theta_b)} \quad (132)$$

From the first harmonic we want to obtain the parameter

$$\sum \phi_{DUT} \quad (133)$$

So, with DUT the amplitude depends on

$$\sum \phi_0 + \sum \phi_{DUT} = \theta_{bDUT} \quad (134)$$

and without DUT

$$\sum \phi_0 = \theta_{b\sin DUT} \quad (135)$$

Therefore the phase sum is

$$\sum \phi_{DUT} = \sum \phi_0 + \sum \phi_{DUT} - \sum \phi_0 = \theta_{bDUT} - \theta_{b\sin DUT} \tag{136}$$

Now we analyze the phase of the first harmonic

For the system without DUT

$$PH_{1H} = \frac{\Delta\phi_0}{2} + \frac{\sum \phi_0}{2} - \frac{\theta_b}{2} + \arctan\left(\frac{\sin(\sum \phi_0 - \theta_b)}{[\frac{A_0^+}{A_0^-} - \cos(\sum \phi_0 - \theta_b)]}\right) \tag{137}$$

For the system with DUT

$$\frac{\Delta\phi_0}{2} + \frac{\sum \phi_0}{2} + \frac{\Delta\phi_{DUT}}{2} + \frac{\sum \phi_{DUT}}{2} - \frac{\theta_b}{2} + \arctan\left(\frac{\sin(\sum \phi_0 + \sum \phi_{DUT} - \theta_b)}{[\frac{A_0^+ A_{DUT}^+}{A_0^- A_{DUT}^-} - \cos(\sum \phi_0 + \sum \phi_{DUT} - \theta_b)]}\right) \tag{138}$$

Now we have to suppose that $A_0^+ = A_0^-$

With this approximation we have

$$PH_{1H} = \frac{\Delta\phi_0}{2} + \frac{\sum \phi_0}{2} - \frac{\theta_b}{2} + \arctan\left(\frac{\sin(\sum \phi_0 - \theta_b)}{[1 - \cos(\sum \phi_0 - \theta_b)]}\right) = \frac{\Delta\phi_0}{2} + \frac{\sum \phi_0}{2} - \frac{\theta_b}{2} - \frac{\sum \phi_0}{2} + \frac{\theta_b}{2}$$

$$= \frac{\Delta\phi_0}{2} \tag{139}$$

Whereas in the system with DUT

$$PH_{1H} = \frac{\Delta\phi_0}{2} + \frac{\sum \phi_0}{2} + \frac{\Delta\phi_{DUT}}{2} + \frac{\sum \phi_{DUT}}{2} - \frac{\theta_b}{2} + \arctan\left(\frac{\sin(\sum \phi_0 + \sum \phi_{DUT} - \theta_b)}{[\frac{A_{DUT}^+}{A_{DUT}^-} - \cos(\sum \phi_0 + \sum \phi_{DUT} - \theta_b)]}\right) \tag{140}$$

From the expression above we take the value

$$\frac{A_{DUT}^+}{A_{DUT}^-} \tag{141}$$

using the values of

$$\sum \phi_{DUT} \, , \, \Delta\phi \tag{142}$$

taken from the other measurements.

Now we move on to the second harmonic:

The expression is

$$P_d = \frac{1}{4} A_0^2 \{(A^+ A_0^+)^2 + (A^- A_0^-)^2 + 2A^+ A^- \cos(2\omega t + \Delta\phi_0 + \Delta\phi_{DUT})\} \tag{143}$$

Then for the amplitude we have

$$P_{2H} = \frac{P_{2H-mTP-DUT}}{P_{2H-mTP-SINDUT}} = \frac{A_0^+ A_0^- A^+ A^-}{A_0^+ A_0^-} = A^+ A^- \tag{144}$$

For the phase of the second harmonic

$$PH_{2H} = PH_{2H-mTP-DUT} - PH_{2H-mTP-SINDUT} = \Delta\phi_0 + \Delta\phi_{DUT} - \Delta\phi_0 = \Delta\phi_{DUT} \tag{145}$$

The previous parameters will be determined with the VPI simulator for two difference modulating frequencies. Once done it, we calculate the phase difference for the upper sideband and for the lower sideband; the same for the amplitude.

We can explain the method with the following Figure

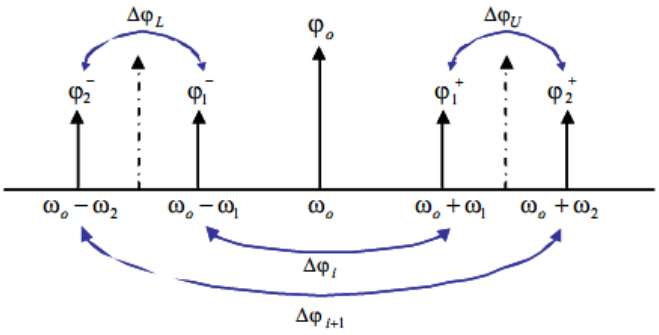

Figure 17. RF scan method

Now we determine the phase difference, for the upper band and for the lower band, between two subsequent frequencies, which we call f_1 and f_2

$$\Delta\phi_{21}^{+}=\frac{1}{2}(-\sum\phi_1+\sum\phi_2-\Delta\phi_1+\Delta\phi_2)=\frac{1}{2}(-\phi_1^{+}-\phi_1^{-}+\phi_2^{+}+\phi_2^{-}-\phi_1^{+}+\phi_1^{-}+\phi_2^{+}-\phi_2^{-})$$
$$=\frac{1}{2}(-2\phi_1^{+}+2\phi_2^{+}) \tag{146}$$

$$\Delta\phi_{21}^{-}=\frac{1}{2}(-\sum\phi_1+\sum\phi_2-\Delta\phi_2+\Delta\phi_1)=\frac{1}{2}(-\phi_1^{+}-\phi_1^{-}+\phi_2^{+}+\phi_2^{-}-\phi_2^{+}+\phi_2^{-}+\phi_1^{+}-\phi_1^{-})$$
$$=\frac{1}{2}(-2\phi_1^{-}+2\phi_2^{-}) \tag{147}$$

$$\Delta A_{21}^{+}=\frac{1}{2}(-\sum A_1+\sum A_2+\Delta A_2-\Delta A_1)=\frac{1}{2}(-A_1^{+}-A_1^{-}+A_2^{+}+A_2^{-}+A_2^{+}-A_2^{-}-A_1^{+}+A_1^{-})$$
$$=\frac{1}{2}(-2A_1^{+}+2A_2^{+}) \tag{148}$$

$$\Delta A_{21}^{-}=\frac{1}{2}(-\sum A_1+\sum A_2-\Delta A_2+\Delta A_1)=\frac{1}{2}(-A_1^{+}-A_1^{-}+A_2^{+}+A_2^{-}-A_2^{+}+A_2^{-}+A_1^{+}-A_1^{-})$$
$$=\frac{1}{2}(-2A_1^{-}+2A_2^{-}) \tag{149}$$

Where we have assumed that the amplitudes are in dB.

We continue considering another frequency f_3, which, with f_2, allows us to determine

$$\Delta\phi_{32}^{+}=\frac{1}{2}(-2\phi_2^{+}+2\phi_3^{+}) \tag{150}$$

In this way we can write a generic expression of the phase difference

$$\Delta\phi_{i+,i_}^{+}=\frac{1}{2}(-2\phi_1^{+}+2\phi_{i+1}^{+}) \tag{151}$$

All these values form a vector, which we can use to plot a graphic which represents the evolution of ϕ

$$\phi^{+}(\omega)=\phi_0+\Delta\phi_{10}^{+}+\Delta\phi_{21}^{+}+\Delta\phi_{32}^{+}+\Delta\phi_{43}^{+}+\ldots \tag{152}$$

There is a point where we have to do an approximation: is the Zero Point. In this point the determination of the phase needs a deeper investigation, because to know what happens close to the carrier is an information not so simple to obtain using this method.

IV. VPI SIMULATIONS

Section 4.1 presents the VPI as a program to test the new RF-scan method for amplitude and phase characterization of optical devices. We introduce the simulator with a general vision about its functions, features and types of use. We will see the Hierarchy where we explain the subsystems which compose the program; then we talk about the signal representation where the data exchange can be organized in two ways: in blocks or by transmitting individual samples. Then we focus the attention on the parameters of VPI, in particular the Global parameters and Module parameters. The formers are common to all modules in a simulation; the latters, when they are placed on a schematic, lead to the creation of an instance of the module. Each instance can carry unique values for the module's parameters. VPI offers the possibility of perform parameter sweeps and allows the monitoring of the system performance for different parameter settings. In this way is possible to detect the influence of specified parameters on the setup behaviour.

In section 4.2 we show the plots of thephase and modulus of the transfer function of our device under test (MZI Optical Filter) obtained in Matlab using the analytical model in chapter 2;. On the other hand, we simulated in VPI a standard measurement scheme to obtain the same phase and amplitude transfer function and thus we confirmed agreement between the analytical and the nummerical approaches.. In the section 4.3 we use Matlab and VPI to simulate the new RF-scan amplitude and phase characterization method of chapter 3.

4.1 The Simulator VPI

VPI is a powerful tool which allows to verify designs, to evaluate new components and also to investigate and to optimize new technologies. This program is quite complex, therefore in order to obtain and to understand the results, it is better to first explain its basic operation principles. The scope of this section is to introduce the reader to this simulator program and to present some terms that will be used in the development of the project. Moreover it is important to understand how the software is structured and how certain basic parameters should be defined to allow for successful simulations.

Additionally, VPI provides a set of applications to show how laboratory instrumentation is used in practice to measureactual components. These applications are located in the folder *WDM Demos →Test and Measurements*. Some of these applications illustrate interesting methods for measuring chromatic dispersion such as for example the MPSM.

4.1.1 Hierarchy of the Simulator

The VPI organization is hierarchical, it is organized in stars, galaxies and universes.

Stars are the lowest level in the simulation; they represent individual components, modules or instruments. As basic elements in the simulation, stars cannot be subdivided, reason why they are often referred to as "atomic" modules. At the same time, they cannot be run independently, meaning that in order to be run they have to be part of a universe. Stars have a series of parameters that can be manually configured, by double – clicking on the module.

Galaxies can be considered as schematics of stars linked among them or embedded galaxies; they can exist as separate schematics, but can only be simulated if they stay within a universe. Galaxies present input and output ports, and can thus act as elements in another schematic. Thanks to this characteristic, these ports allow the interconnection between galaxies. Galaxies are used to take stars together in order to keep simulation setups clear and make parameter handling easy. The contents of a galaxy can be viewed by dragging it onto the workspace but not onto a schematic or by making use of the Looking – Inside option obtained by right button clicking when the galaxy is a module on a schematic.

The last group is composed by universes, which constitute the complete simulation application. They are the highest layer of the hierarchy and outside them there is nothing since they have not external connections. They can be considered either as the support where the simulation runs or as the global schematic that can be run as a simulation. Thus, universes are, as we said before, the only level of a simulation that can be executed independently. A double – click on the schematic grants access to the global parameters corresponding with a universe. Due to their importance in this master thesis they will be detailed in section 4.1.3. Figure 18 shows the hierarchical structure of the simulator: a universe consists of a network of star and galaxies which are connected among them and represents the highest layer of the hierarchy; the galaxies contain stars and other galaxies and are connected to higher levels of the hierarchy using ports, and the stars are the lowest level in the simulation.

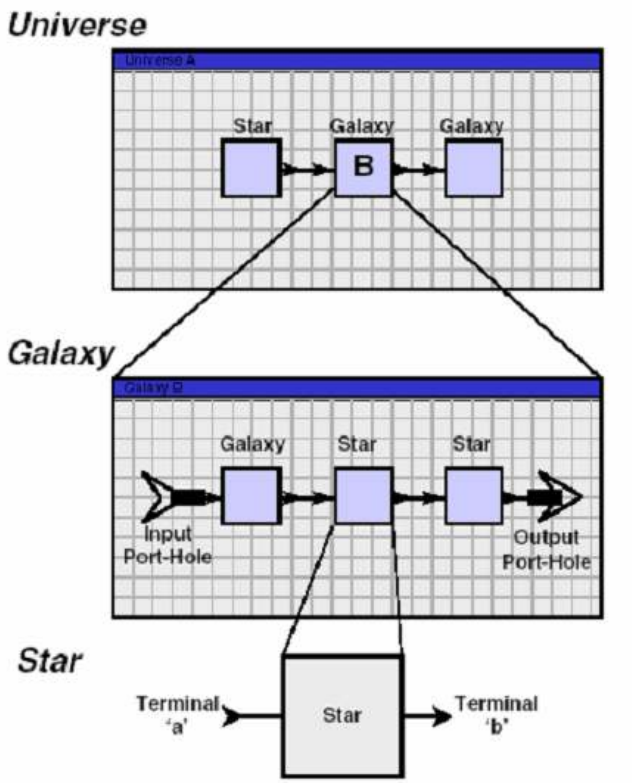

Figure.18 VPI hierarchy

4.1.2 Signal Representation

With VPI the data exchange can be organized in two ways: in blocks or by transmitting individual samples.

The *Block Mode* is the most efficient form of simulation, as modules only work when data passes through them. This is more suitable for system simulation where components are widely – spaced compared with the modelled time, or where the signals flow in a unidirectional way, from transmitter to receiver. Through this mode, each module generates samples which are packed into a block which, once completed, will be passed to the following module for its respective processing.

The *Sample Mode* needs more simulation's time, but it allows more flexibility when designing systems. In this case, each module passes the data to the following one in a sample – by – sample scheme, i.e. the different modules may be executed at the same time. In additional this mode is necessary when the delay between the modules is much shorter than a block length, when a fast communication between them is necessary in order to fully simulate their joint behaviour.

In this master thesis we used the Block Mode since signals flow in a unidirectional way from transmitter to receiver. Additionally, Block Mode can realize the duality between representations in the time and frequency domain which allows us to understand simulations results.

4.1.3 Global Parameters

The parameters can divided in two groups depending on its use: global parameters and module parameters.

The Global parameters are common to all modules in a simulation. A correct and efficient setting of these parameters is very important to have a good operation of the simulator. In this section, we explain the meaning of each one of the most used global parameters and then we describe some specifications about the setting of these global parameters.

VPI has the following already defined global parameters:

- *TimeWindow*: this value sets the period of real time in which the simulation takes place. Additionally, this time will fix the spectral resolution of the simulated signals setting, i. e., the resolution of spectral displays.

- *InBandNoiseBins:* this parameter has two states: ON and OFF. The first, ON, represents the noise within the sampled bands; since noise is a statistical parameter, it is used for deterministic BER estimation. The second, OFF, adds random noise to the sampled signal representations in their spectral range.

- *BoundaryConditions*: it allows to specify if the boundary conditions, within the simulated window, are periodic or aperiodic. Normally, a signal, which traverses a system, suffers transformations in the frequency domain and it is only later passed to the temporal domain. In order to make this domain change, when we are using periodic signals, the program applies the FFT algorithm, whereas when we are using aperiodic signals it applies the convolution.

  We have used only periodic signals in order to treat the simulation in isolation. Since the delays are circular, the signal power is assumed to be zero outside the simulated bandwidth. So, the filters and the spectrum, through periodic boundary, are represented exactly.

- *LogicalInformation*: it is a tool used by VPI to send information between modules within the same simulation. It removes the need for wires between the transmitters and some modules such as BER Estimators, Clock Recovery modules and the Channel Analyzer.

- *SampleModeCenterFrequency*: optical signals have a very high frequency compared with the frequency of the modulation signal; therefore, to correctly sample them it is necessary a very high sampling frequency. In order to avoid this problem, VPI treats signals in its baseband equivalent and uses this variable which sets a global centre frequency for all the signals in sample mode simulations. Since we worked with Block Mode this global parameter does not have effect over the simulations run during this project.

- *SampleModeBandwidth*: it specifies the sampling frequency when working in sample mode. Besides defining the temporary resolution, it also defines the simulation bandwidth. In this project we worked only with Block Mode, so this parameter was not used.

- *SampleRateDefault*: it specifies the sampling frequency when we work in block mode. It is defined as the number of samples taken by second and determines the maximum frequency that can be simulated.
- *BitRateDefault*: it defines the transmission bit rate which is set by the BitRate parameter of emitters, bit generators.

For all the parameters which we have used, except TimeWindow and SampleRateDefault, we use the default values;. As previously said, these parameters define the frequency and time resolution respectively; therefore, they will depend on the desired simulated frequencies, which vary depending on the experiment.

Since VPI works with the FFT algorithm, when we work with periodic signals, we have to consider a series of restrictions,. First, the number of samples by Time Window has to be a power of two. This condition sets a limitation when selecting the Time Window and the Sample Rate, since the product of these two variables results in the number of samples, as it appears in expression.

$$n°sample = TimeWindow * SampleRate = 2^n \tag{153}$$

The choice of TimeWindow and SampleRate will set the following nummerical resolution limits concerning respectively the minimum time and frequency

$$dt = \frac{1}{SampleRateDefault} \tag{154}$$

(155)

$$df = \frac{1}{TimeWindow} \tag{156}$$

4.1.4 Modules Parameters

When a module is placed on a schematic, an instance of the module is created. Each instance can carry unique values for the module's parameters. We can edit the values of the parameters with the *Parameter Editor* which can be opened either with a right – click on the icon of the module's instance and choosing *"Edit Parameter"* or with a double – click on the icon of the module instance. Figure 19 above shows the *Parameter Editor* for the instance *FuncSine*, which is a sine generator that we will use as a RF signal generator.

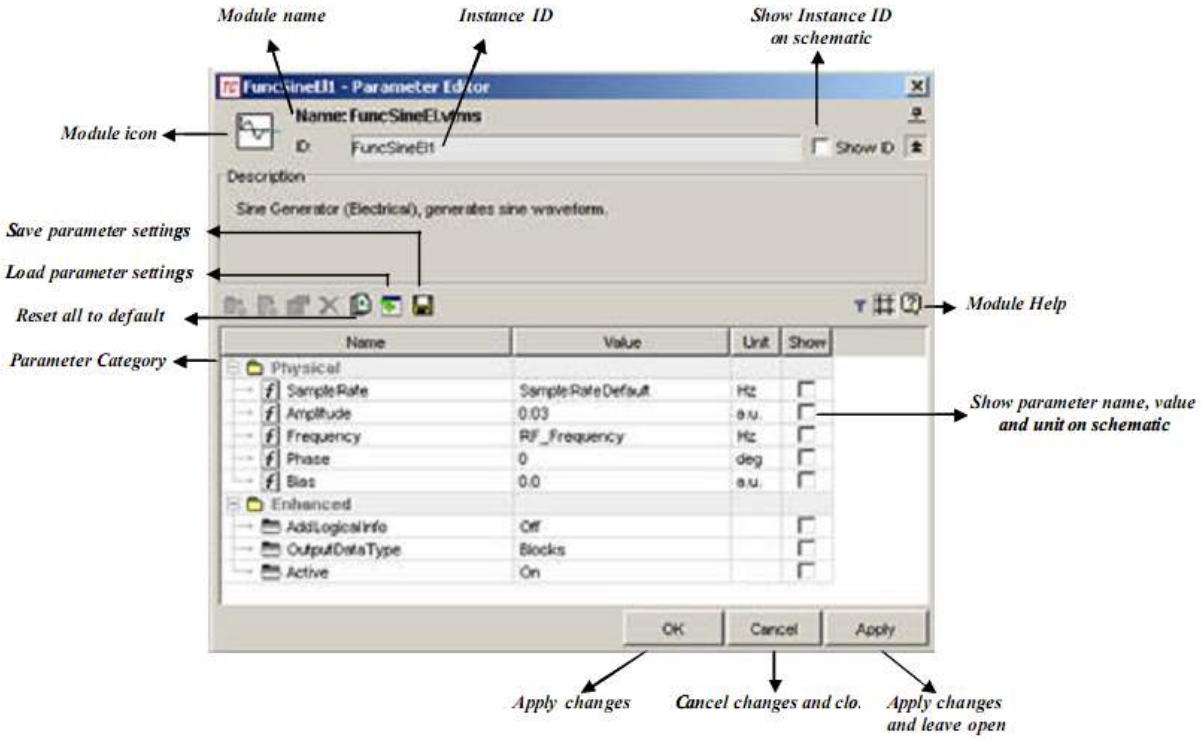

Figure 19. Parameter Editor window

As we can see from the Figure, in the *Parameter Editor* window, we can find the name, the value and the unit of any parameter. This information is displayed as text. The parameters are grouped in categories and every parameter belongs to a single category. Categories are displayed as folders within the parameter editing panel. In order to have a simulation with its own set of data the categories can be modified; for example to modified the device we should change the *Physical* parameters. To change the values is simple: it is only necessary to modify its value in the corresponding cell and to click the *Apply* button to make it valid. There is, also, the opportunity to open, during the simulation, a *Parameter Editor,* but the values cannot be modified. The update of the parameters is allowed only at the start of each simulation run.

4.1.5 Sweep Configuration

VPI offers the possibility of performing parameter sweeps and allows the monitoring of the system performance for different parameter settings. In this way it is possible to detect the influence of specified parameters on the setup behaviour. There are modules, called *"The Magic Modules"*, which are able to modify specific parameters of other modules within the simulation setup when these parameters are executed. In this way a control module is placed on the schematic to force part of the simulation to run multiple times. These new modules can be found within the *Simulation Tools* folder.

The Magic Modules take their input value and set a specified parameter of a specified module within the setup to this value before each run. VPI presents two types of magic modules: the *MagicPrefix* modules which modify a parameter of the module located after them, and the *MagicPostfix* modules which modify a parameter of the module located before them.

Additionally, VPI allows the creation of explicit parameter sweeps from the *Parameter Editor* of the module which contains the value we want to sweep. To create this type of sweep we have to open the *Parameter Editor* of the module which presents this parameter; after this we have to do a right – click on the desired parameter and finally we will select *" Create Sweep Control"*.

This will bring a *"Define Control"* window where it is possible to define the type and the range of the desired sweep. There are four different control modes: continuous, list, random and expression, but only one of them were used during this project, i.e. :

- Continuous Mode, Figure (20), where it is necessary to specify the control variable's name, the upper and lower limits of the sweep as well as the division type (Number of Steps, Step Width, or Percentage of the upper limit minus the lower limit) and the division value (steps that a sweep will i

n

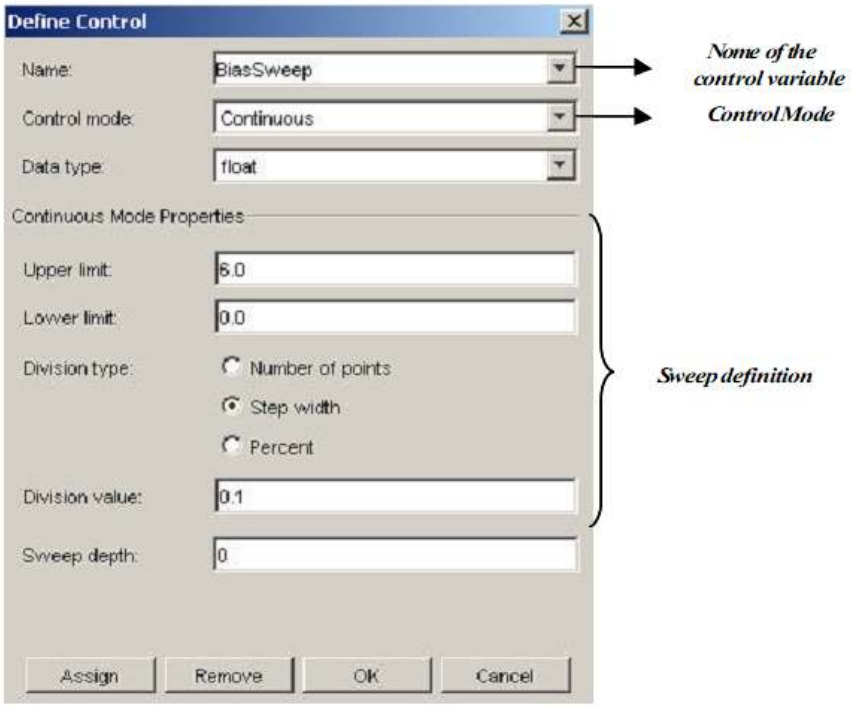

Figure 20. Define Continuos Control window

Once defined, the controls must be assigned to parameters. This assignment is done through the "Assign Control" window activated by clicking on the "Assign" button.

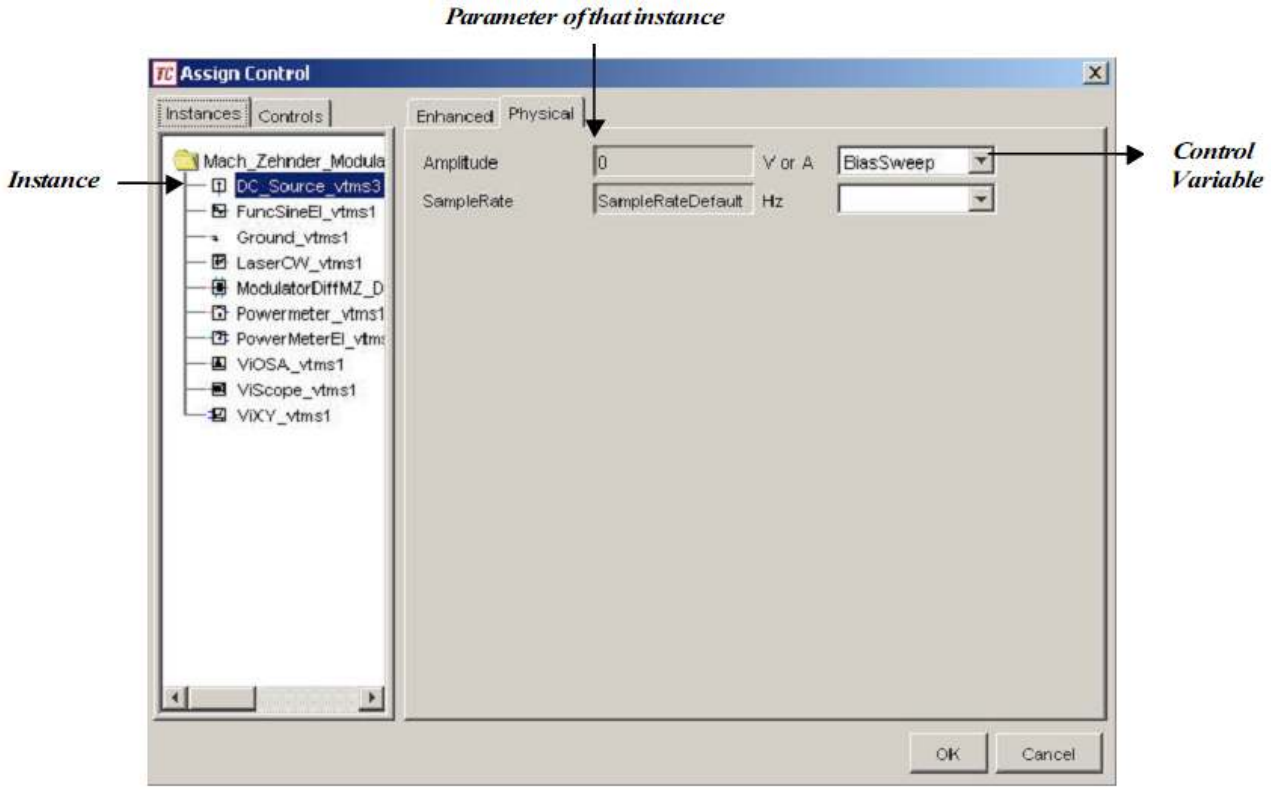

Figure 21. Assign Control window

Finally, from *"Assign Control"* window we go to the *"Master Control Panel*" which is the interface for interactive simulation from where the simulation can be run (Figure 22).

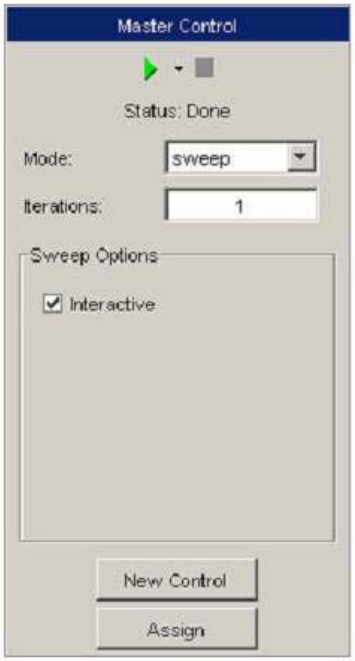

Figure 22. Master Control Panel

4.2 Modulus and Phase comparison between Matlab and VPI

In this section we show the modulus and the phase of MZI Optical Filter obtained with these programs. The final result will be that the modulus obtained with Matlab will be compared with the modulus obtained with VPI. The same for the phase.

First of all we have to take the same frequencies sweep In both programs We decide to use the frequencies sweep of the VPI Simulator as the values vector which determines the simulation range.

4.2.1. Modulus transfer function

4.2.1.1 Matlab (analytical model)

We start with Matlab . Now we present the most important parameters used in order to explain the characteristics of the Optical Filter

The frequency range used

```
f_vpi=[1.92412532469615E14 ;…; 1.92448442469615E14]
```

The value of alpha used, which is the coupler factor, i.e. it refers to the part of input power which is divided into the two arms, is

```
a=0.47;              % coupler factor
```

The value of the delay between the two paths of the Optical Filter is

```
tau=115e-12;          % delay factor
```

We show the part of file which allows us to calculate the modulus of our filter

```
P = ((1-a)* exp(-j.*omega0*tau)-a)

y=abs(P).^2;
plot(f_vpi,abs(P).^2)

figure(2);
semilogy(f_vpi,y)
```

So the modulus with linear axes and with logarithm axe respectively are presented in Figure 23 and 24

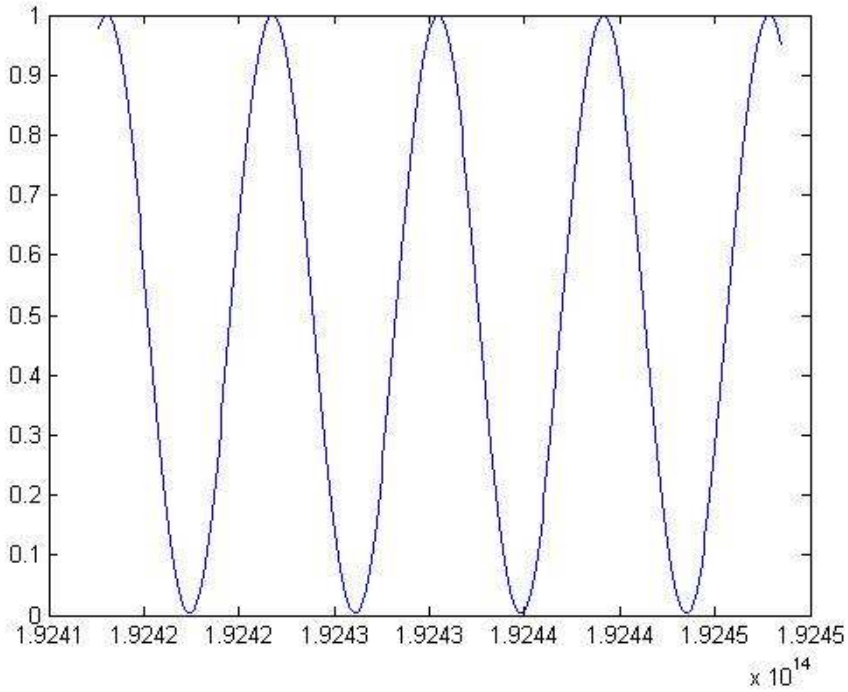

Figure 23. Optical Filter Modulus obtained with Matlab

and

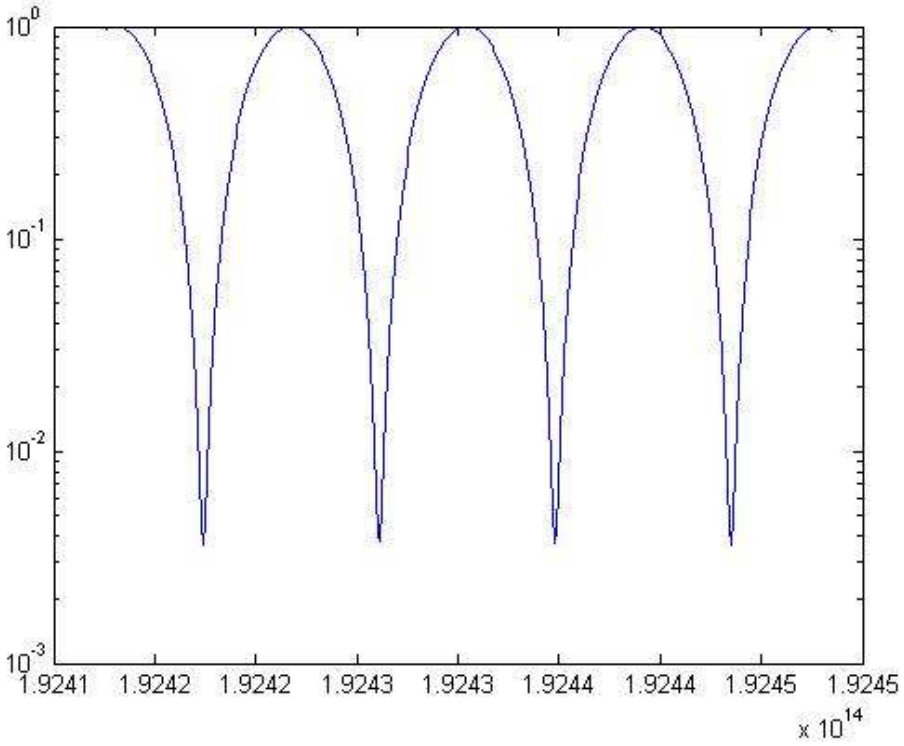

Figure24. Optical Filter Modulus (in dB) obtained with Matlab

4.2.1.2 VPI (numerical simulation of standard measurement setup)

Now we move on to use the VPI Simulator. The measurement system is presented in Figure 25.

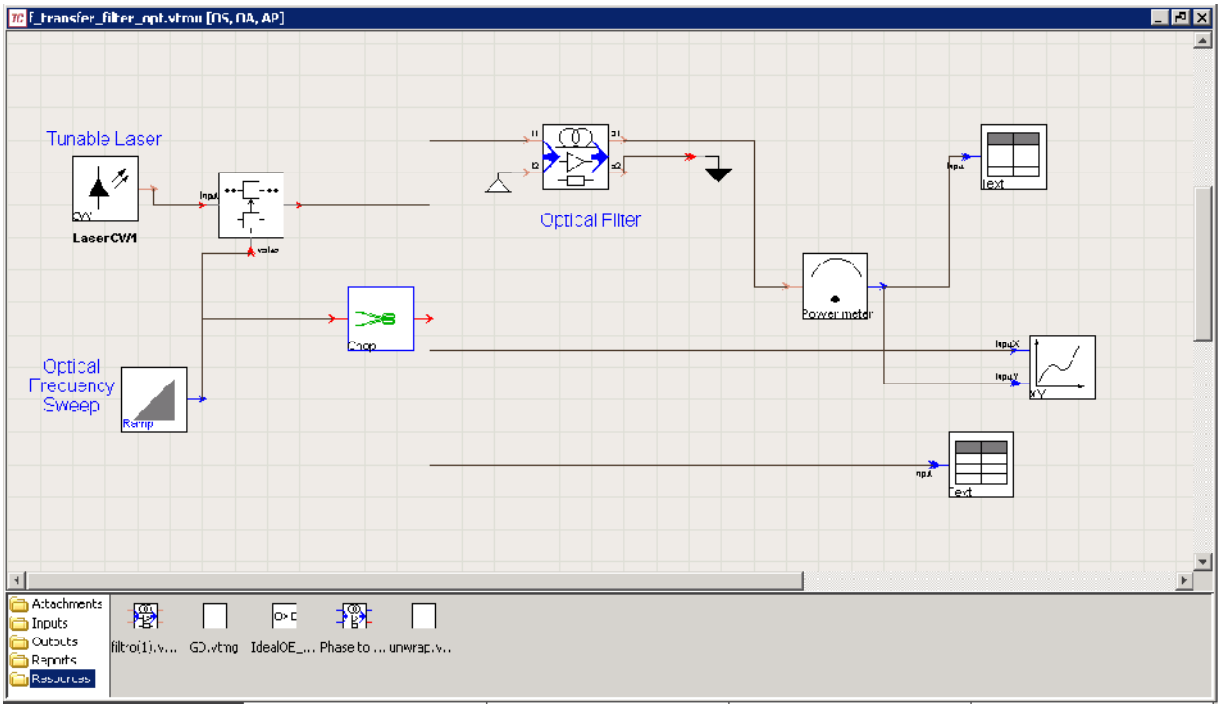

Figure 25. Optical Filter Modulus scheme with VPI

The base of this analysis is the frequency sweep, which gives us the frequency values used for the simulation with Matlab and with VPI. In order to obtain this frequency sweep, in VPI we need two blocks; one of them is the *Ramp* which produces a ramp waveform. It presents two parameters which are *Optical_Frequency_Start* and *Optical_Frequency_Step* which we can plan in the *General Parameter.* The other lock is *Chop* which, on each execution, reads a block of *nread* particles and writes them to the output with the given offset.

We now describe the most important parameters used for the above simulation. We start with the global parameters, i.e. the values which are used in all the blocks, and the general parameters, which are shown in the Figure 26.

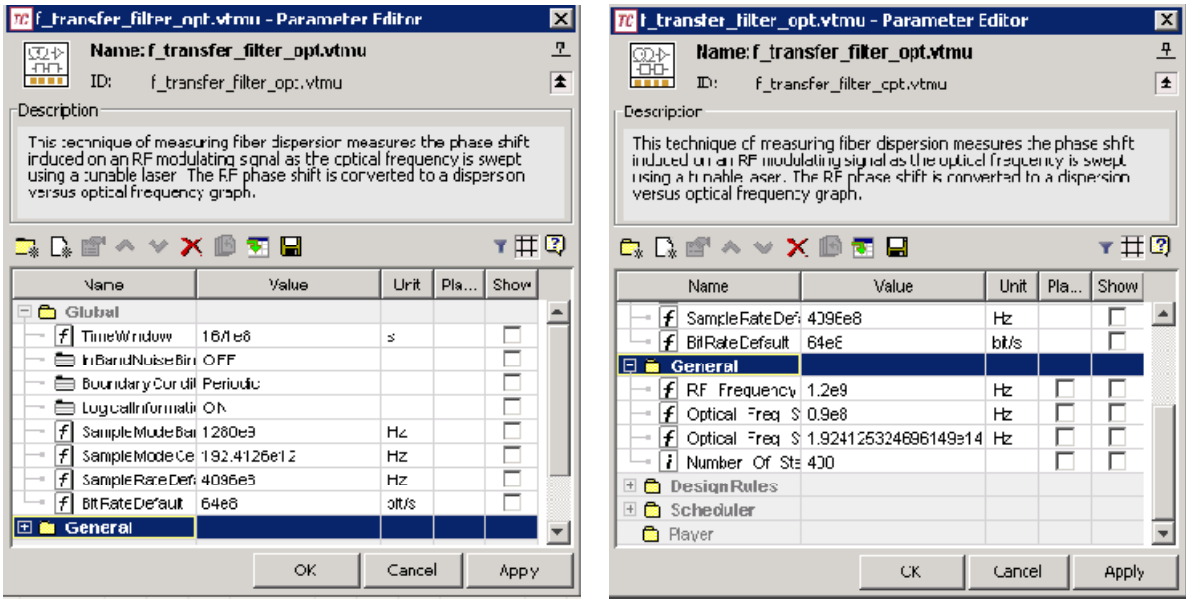

Figure 26. Parameter Editor of Optical Filter Modulus (VPI)

Now we present in detail the most important components of the system and their characterization.

In Figure 25 we see the light comes out from a CW laser which we used with the default parameter setup, see Figure 27.

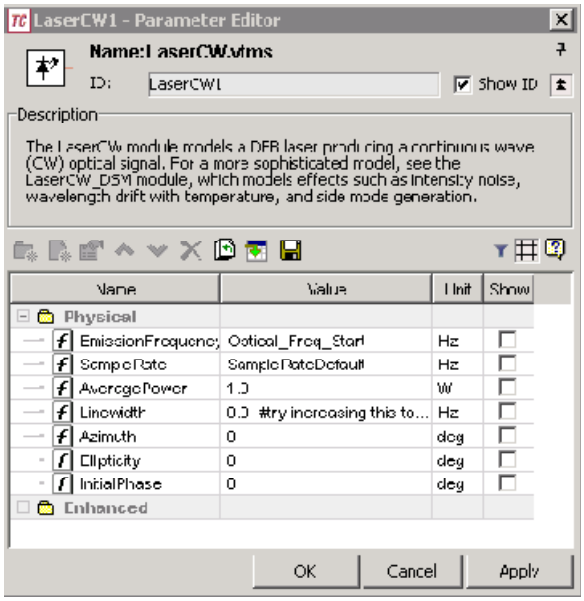

Figure 27. Laser source Parameter Editor

The laser module together with the ramp module and Chop module; they simulate the function of a tunable laser injecting a sweep of optical frequencies into the MZI Filter. The configuration of these modules is as given in Figure 28

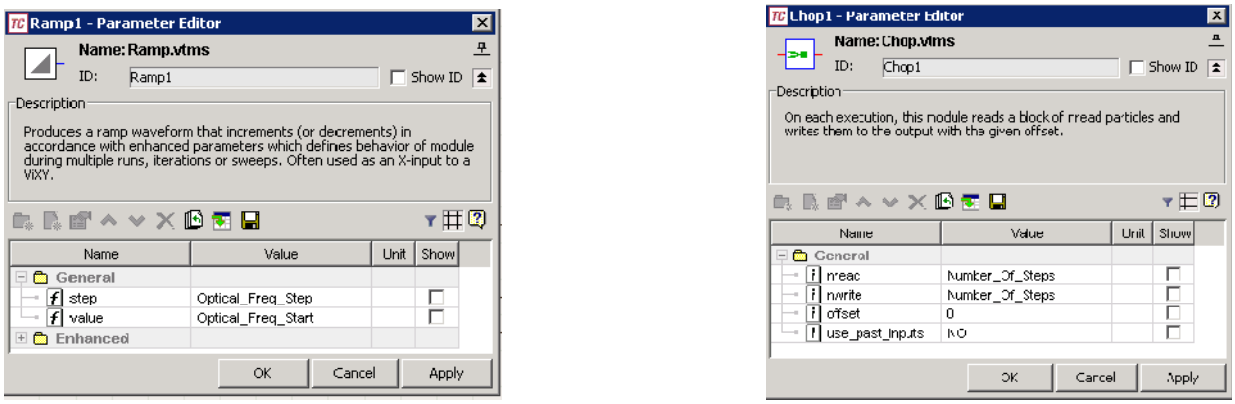

Figure 28. Ramp and Chop *Parameter Editor*

The MZI filter module is a galaxy with the following internal composition (right-click and Look-inside option), Figure 29.

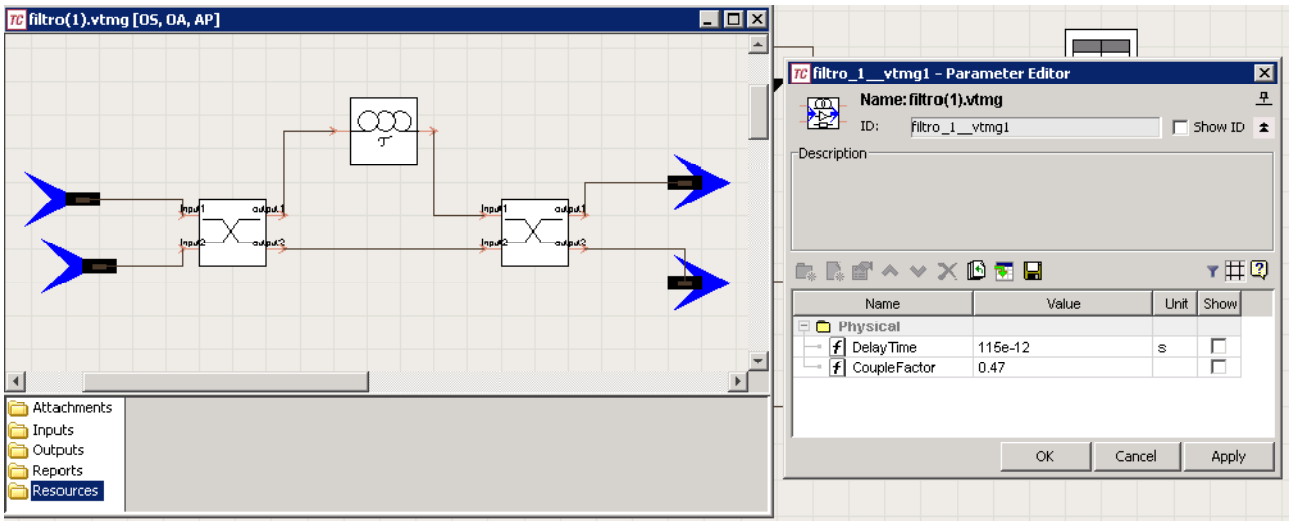

Figure 29. Optical filter block and its Parameter Editor

To study in details the filter we can see the Chapter 2.

Then we can see the blocks: *Power Meter, ViXY* and the *Text*. The first calculates the power of an optical signal. It Includes options for bandwidth limitation, polarization, output units, and switchable detection of different signal types. The second one displays input data in an X/Y plot. The last can be used to display output data textually in a table format.

Now we are ready for simulate. Once the *Run* button is clicked the result is as shown in Figure 30.

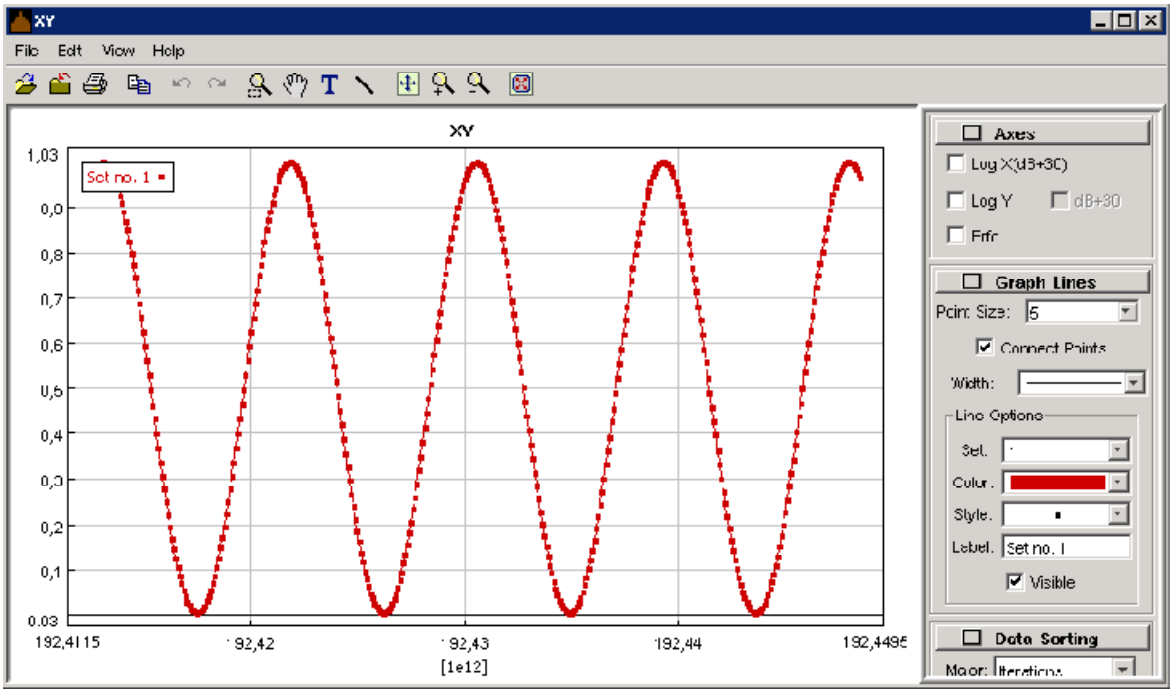

Figure 30. Result of VPI simulation: Modulus of the Optical Filter

After the Filter an optical power meter records the detected power for every optical frequency in the sweep.

The next step is to compare the two modulus obtained. In order to do this we copy the vector values of frequency and power in Matlab. The *Text* block helps us because it recovers the values, so we can take them and bring them in the other program. We plot with Matlab the modulus of Optical Filter with VPI values and we overlap the two different graphics.

The following commands refer to the Modulus obtained by VPI values and plotted with Matlab; then we have the figure which presents the overlap between the Modulus obtained with Matlab and VPI

```
figure(3)
plot(f_vpi,P_vpi);

figure(4)
plot(f_vpi,P_vpi,'r');
hold on
plot(f_vpi,abs(P).^2);
```

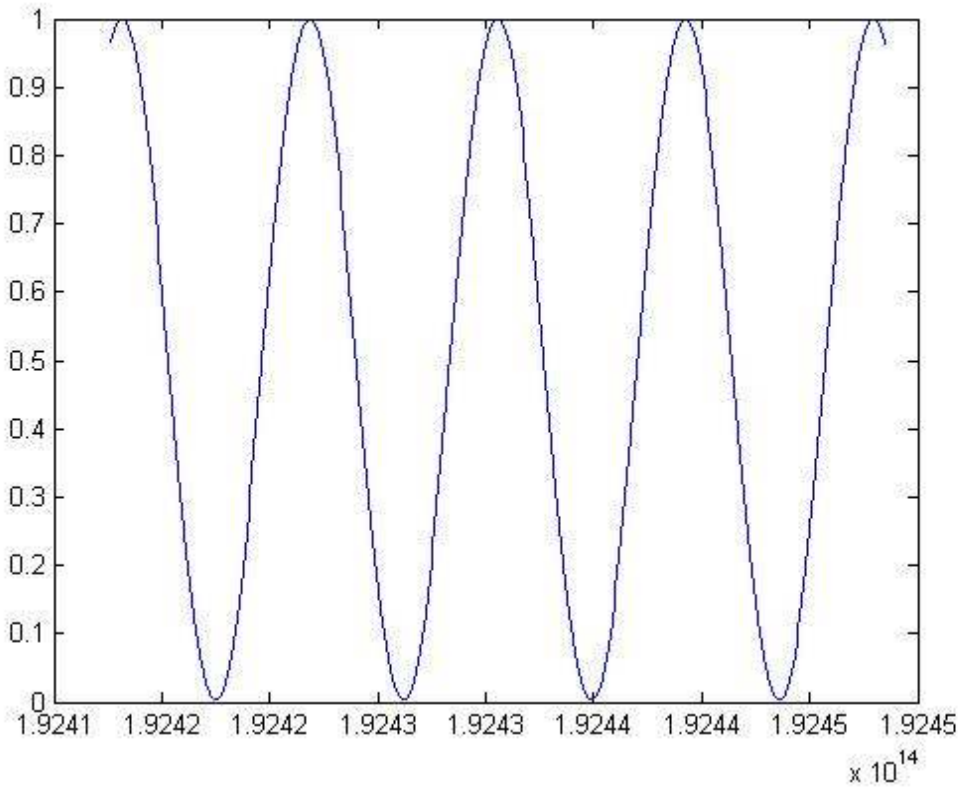

Figure 31. Modulus of Filter obtained by VPI with Matlab

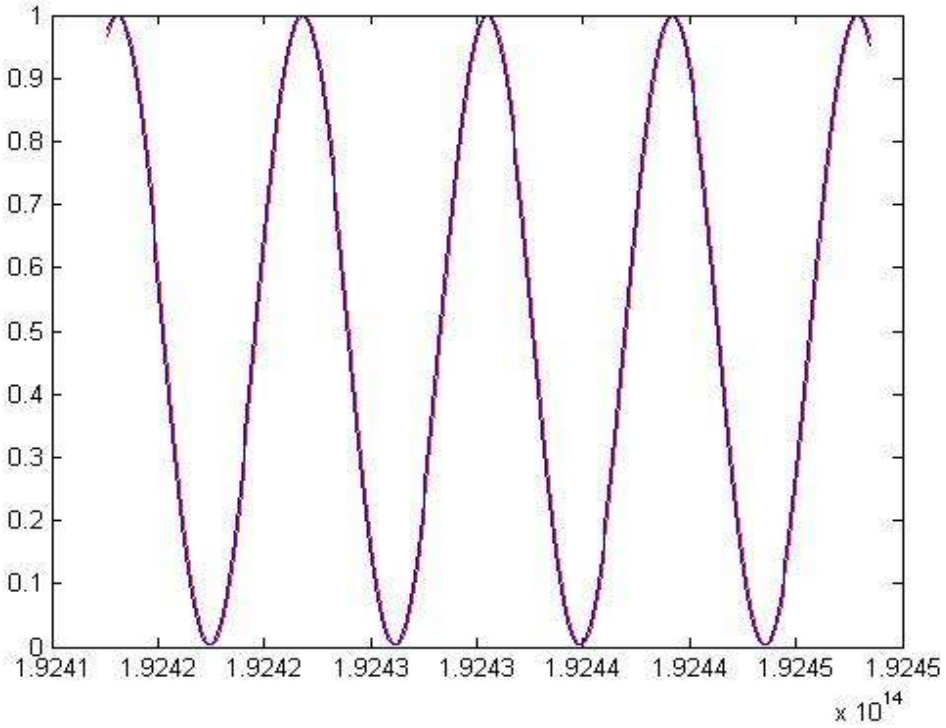

Figure 32. Overlap between the Modulus obtained with Matlab and VPI

From this last figure we can demonstrate that the result of VPI simulation agrees with the graphic of Matlab.

4.2.2. Phase transfer function

Now we concentrate on the Optical Filter phase.

4.2.2.1 Matlab (analytical model)

Now we determine the phase obtained with Matlab; we use the command

```
fase_mat=atan2(-(1-a)*sin(2*pi*f_vpi_ph*tau),(1-a)*cos(2*pi*f_vpi_ph*tau)-a);
```

which uses the cosine and sine, but in this case they are obtained with the parameters de coupler factor and delay which we insert manually through the Matlab.

4.2.2.2 VPI (numerical simulation of standard measurement setup)

In this case the process has two steps. First we built in VPI a measurement setup where we place the MZI filter into an interferometric onfiguration where we get the cos and sin components of the optical phase function to latter get using Matlab the optical phase spectrum.

With Matlab the commands are:

```
fase_vpi=atan2(senfase,cosenofase) % expression of phase determined with VPI


figure(5)
plot(f_vpi_ph,1/2*unwrap(2*fase_vpi)); % with VPI

hold on

fase_mat=atan2(-(1-a)*sin(2*pi*f_vpi_ph*tau),(1-a)*cos(2*pi*f_vpi_ph*tau)-a);
plot(f_vpi_ph,unwrap(fase_mat),'r'); % with Matlab
```

The first command shows the phase obtained with VPI through the vector of phase `fase_vpi` which is the result of two VPI files. `fase_vpi` is the tangent obtained with a file which refers to cosine and with the other which refers to sine. The figures which follow shows the two systems explained before.

The first represents the cosine

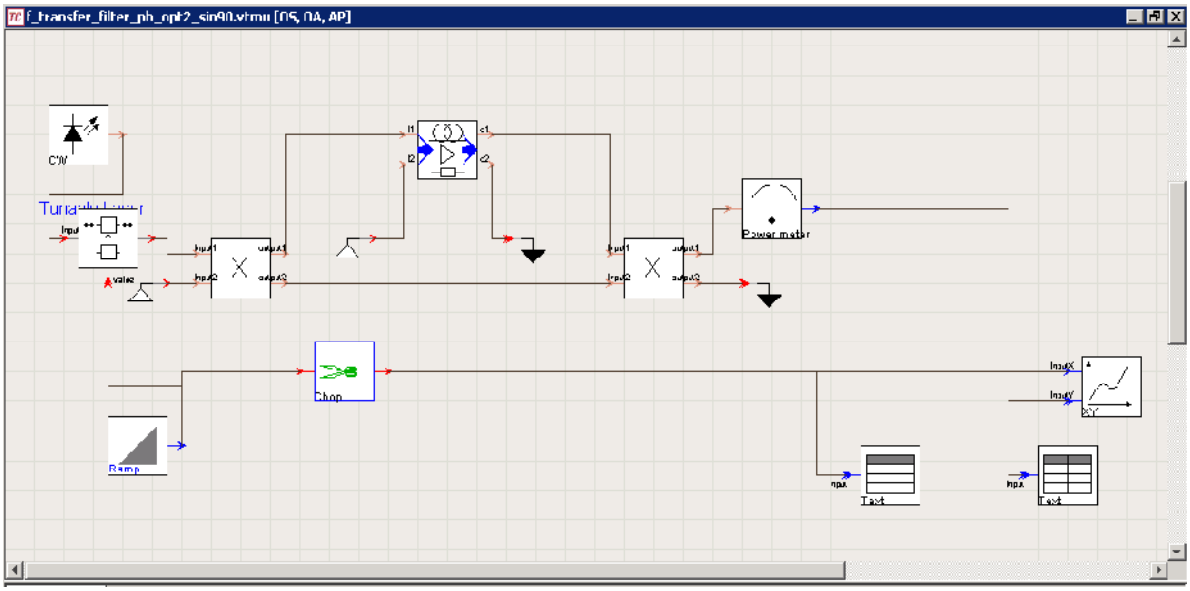

Figure 33. Cosine scheme with VPI

At the output the graphic is

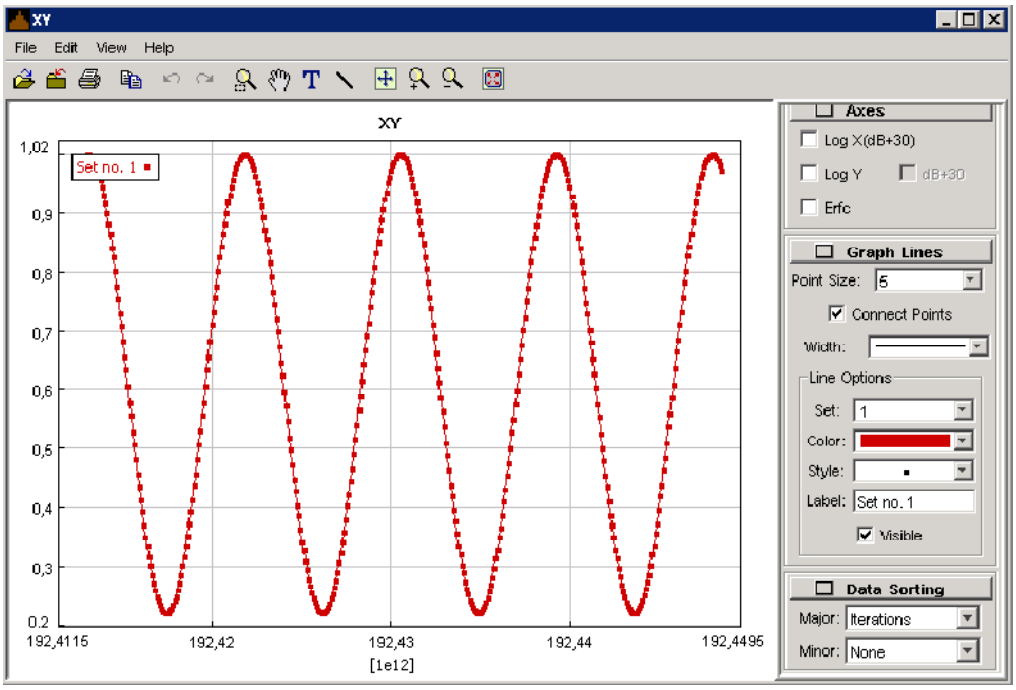

Figure 34. Output of cosine file

Here we present the code matlab to obtain the cosine from the system of the Figure above

```
omega1_cos=f_ph_cos*2*pi;

A1=sqrt((1-const)^2+const^2-2*const*(1-const)*cos(omega1_cos.*tau)); %A1=abs(P)
A2=(1-const)^2+const^2-2*const*(1-const)*cos(omega1_cos.*tau);    % A2=abs(P).^2

cosenofase=(A2+1-4*p_ph_cos)./(2*A1);
```

The parameters A1 and A2 became form the expression of the optical filter

```
P=((1-a)*exp(-j.*omega0*tau)-a);
```

Now we analyze the sine

```
A1=sqrt((1-const)^2+const^2-2*const*(1-const)*cos(omega1_sin.*tau)); %A1=abs(P)
A2=(1-const)^2+const^2-2*const*(1-const)* cos(omega1_sin.*tau);    % A2=abs(P).^2

senfase=(A2+1-4*p_ph_sin)./(2*A1);

fase_vpi=atan2(senfase,cosenofase)
```

The expressions for the sine are similar to the ones of the cosine. The output graphic is shown in the following figures

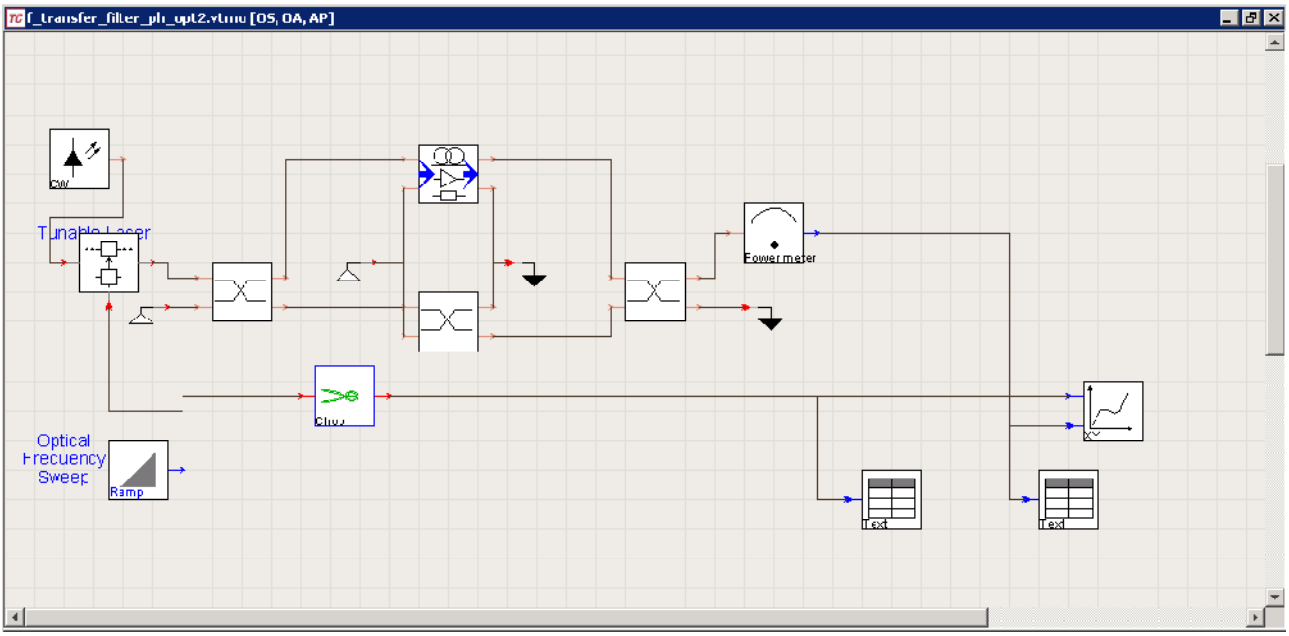

Figure 35. Sine scheme with VPI

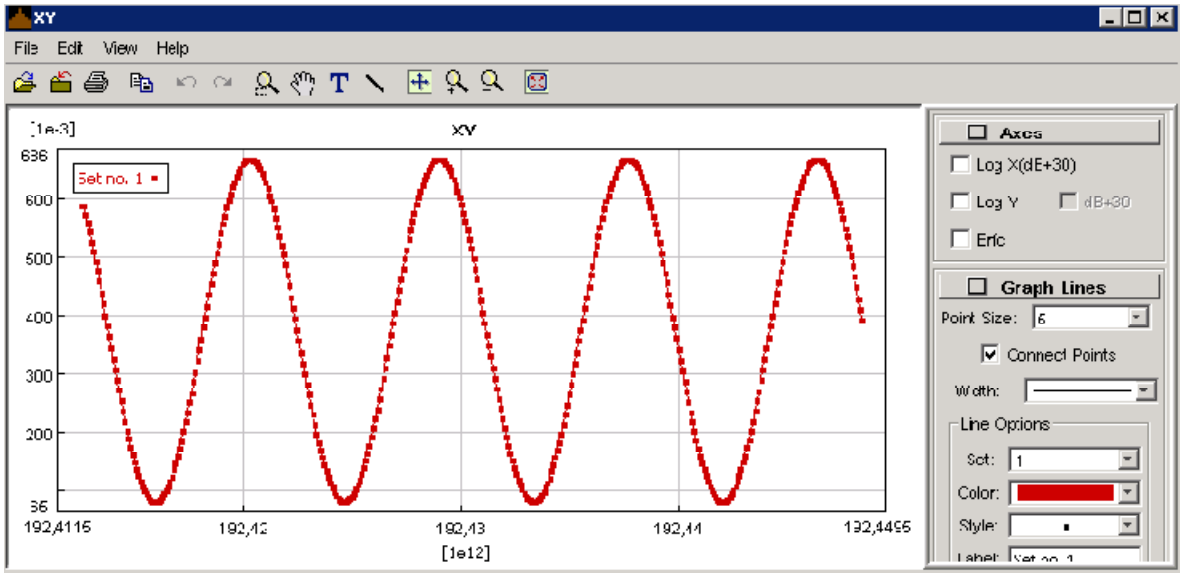

Figure 36. Output of sine file

The final result is the overlap of the two phases calculated with different program as we can see in the Figure above.

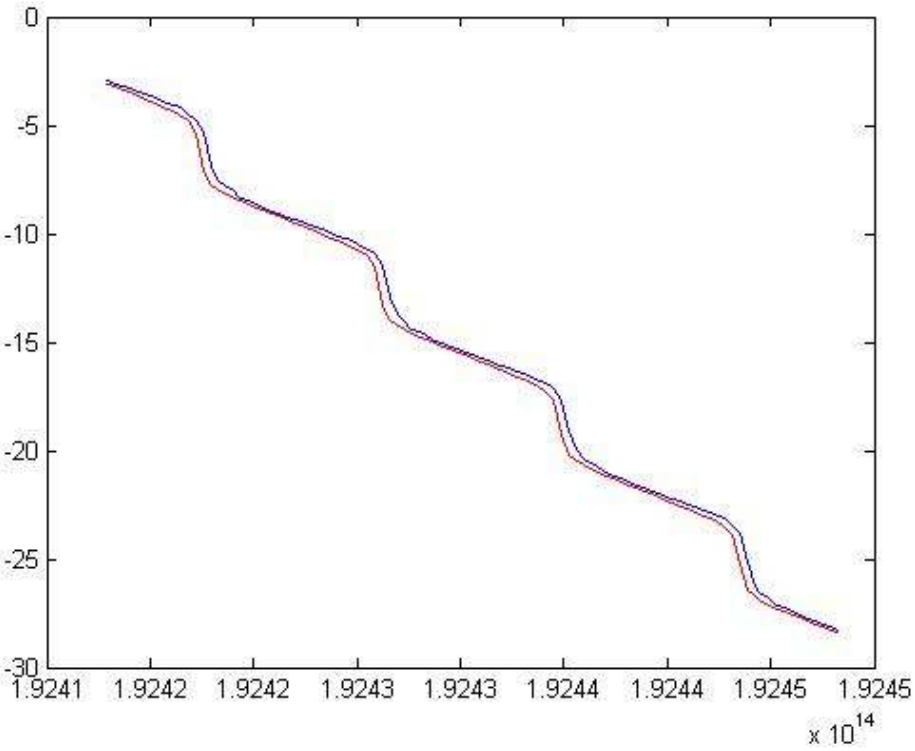

Figure 37. Overlap between the phase obtained with Matlab and VPI

4.3 Simulation of the method RF scan

In this section we simulate, in VPI, the method explained in the section 3.8.

First of all, we built the block systems for our scheme with DUT and without DUT.

With DUT we have

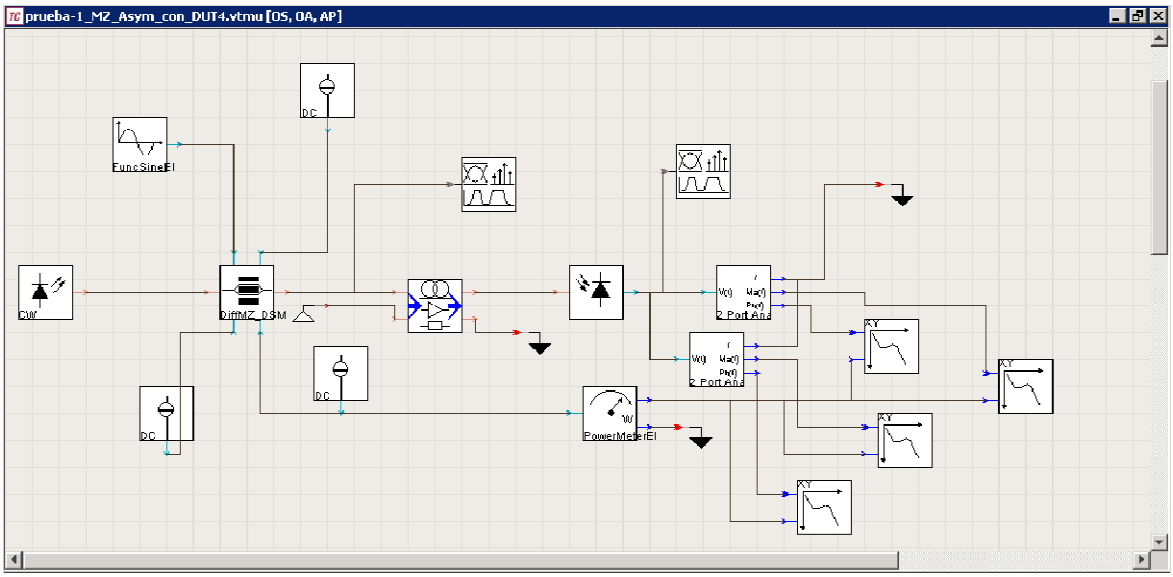

Figure 38. Scheme of the system under simulation

In this scheme we see the device we use:

The modulating signal source, with a frequency of 2.2 GHz

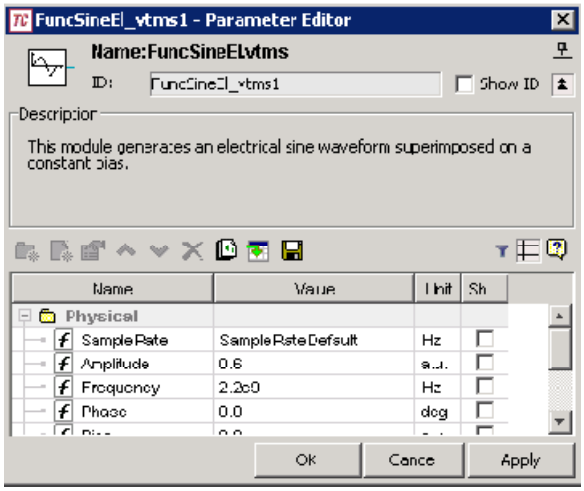

Figure 39. RF signal Parameter Editor

the laser source which emits a frequency of 1.924125324696149e14 Hz.

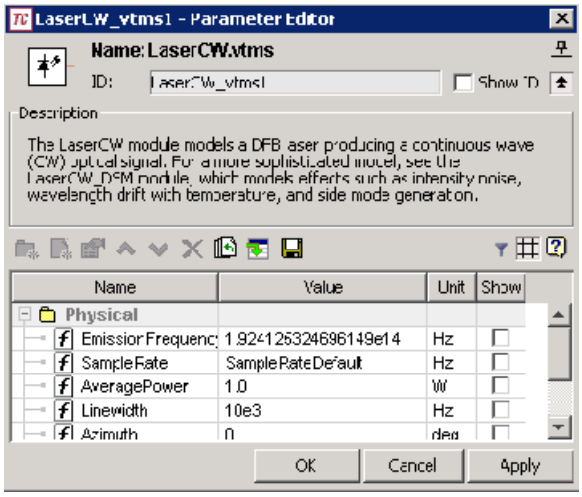

Figure 40. Source Laser Parameter Editor

From the laser, the signal goes to the Modulator MZI in asymmetric configuration

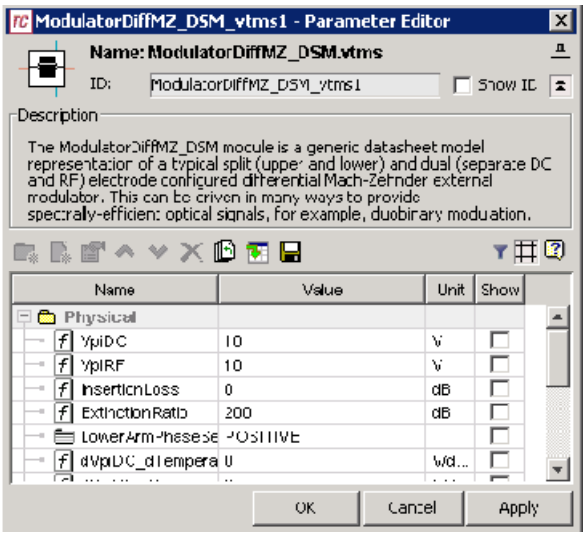

Figure 41. Modulator Parameter Editor

The modulator is taken ideal, a high ER is used, and the values of VpiDC and VpiRF are 10 V.

Then we have the MZI Optical filter, which is the same used in previous sections.

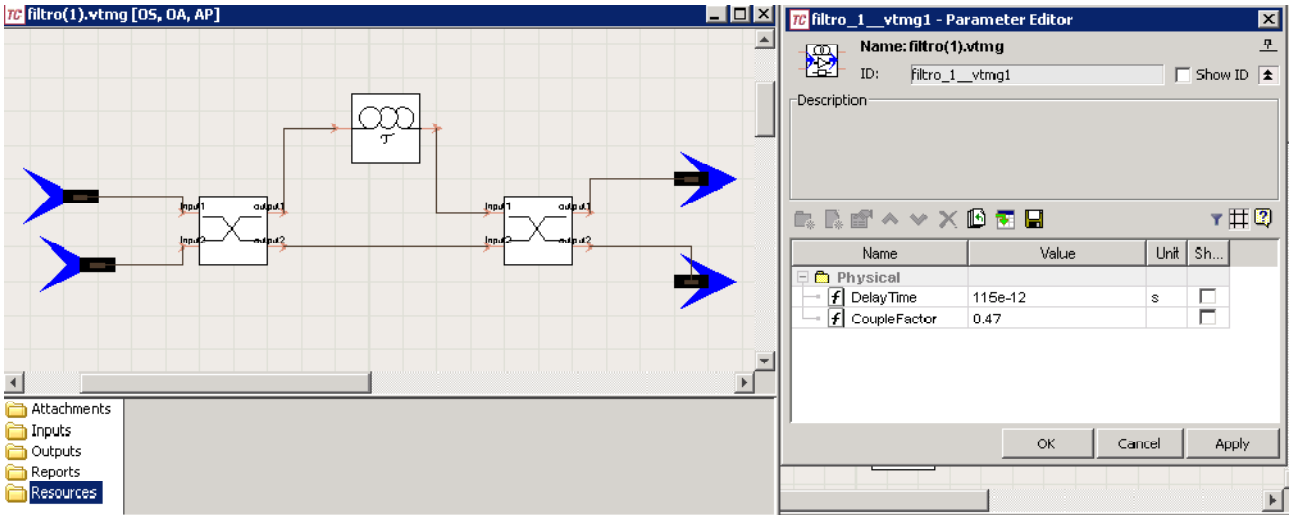

Figure 42. Look inside of the Optical Filter

There are two Electrical Analyzersat the detector's output; one of them is for the first harmonic, the other is for the second harmonic. In the case of the Figure (43) we have a detection frequency of 2.2GHz

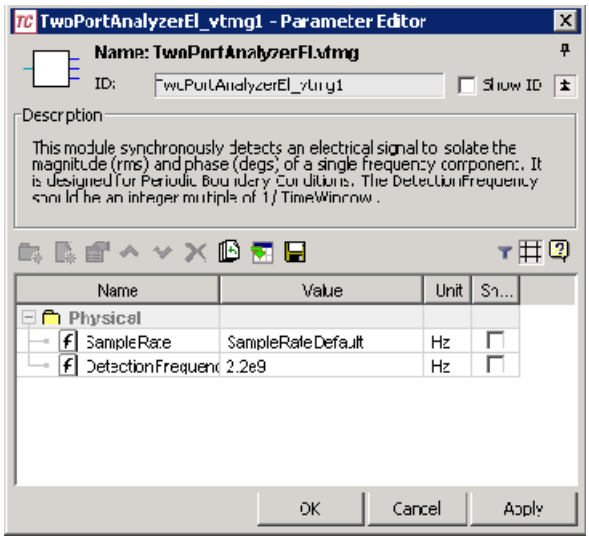

Figure 43. Network Analyzer Parameter Editor

A device which is important for our analysis is the PhotoDetector which brings the signal, from the optical field to the electrical field; in this way the Network Analyzer can detect the frequency we need.

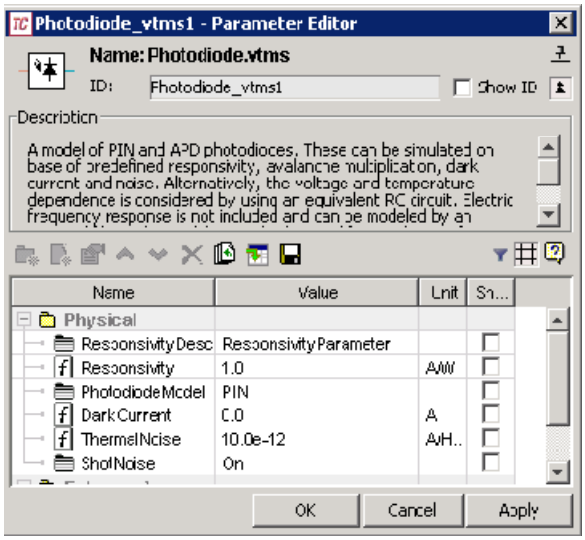

Figure 44. Photodiodo Parameter Editor

Before running the program we need to plan the Global Parameters and the General Parameters.

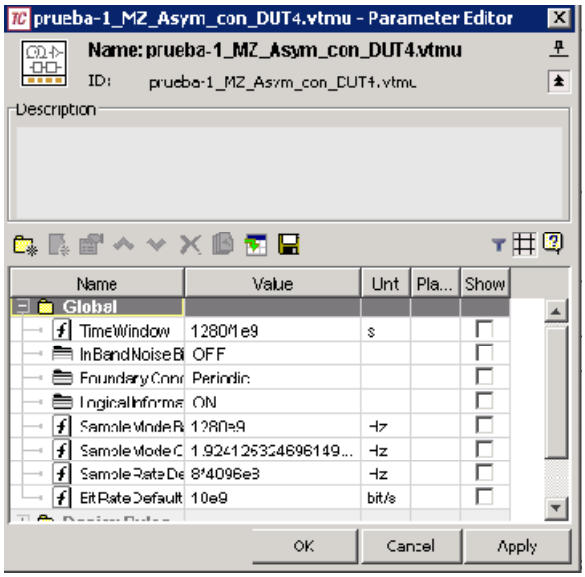

Figure 45. Parameter Editor of the system

The *Time Window* and the *SampleRate* are important to display the graphics with a good resolution. These values require a long simulation time; therefore we have to wait afew hours to see the results.

Once we hit run we get four graphics which represent the amplitude and the phase for the first harmonic and for the second harmonic.

The first figure is for the amplitude of primer harmonic

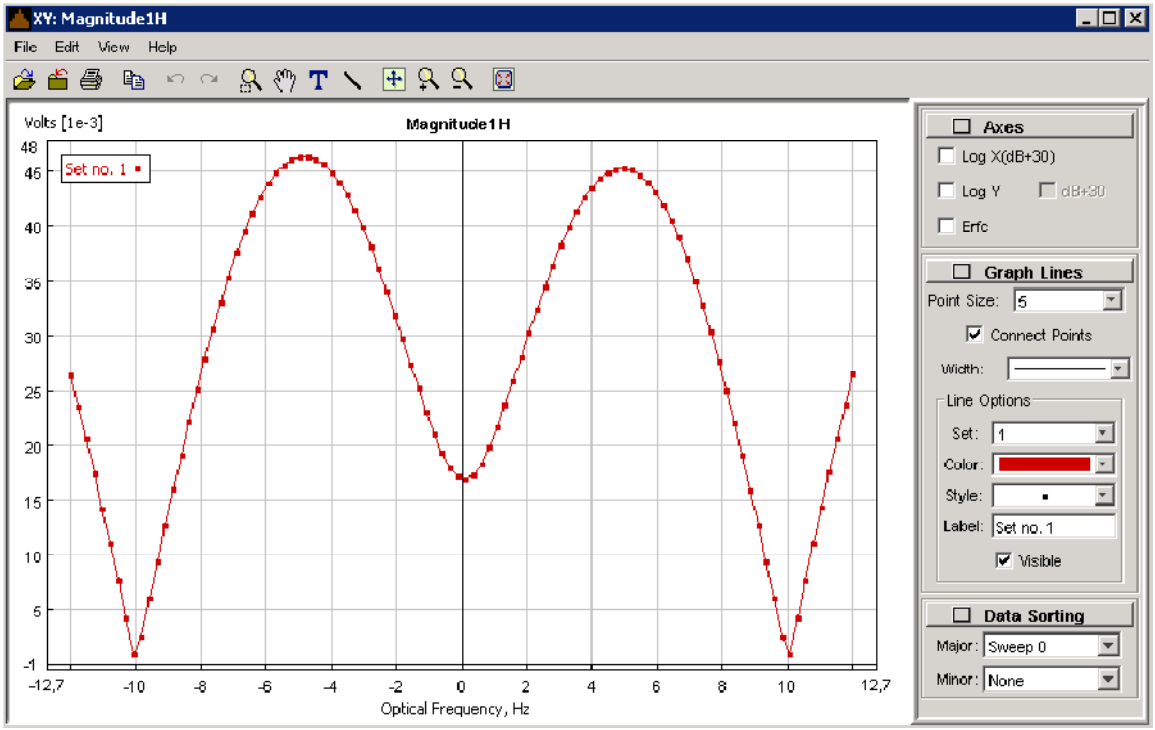

Figure 46. Amplitude graphic of the primer harmonic

The second is for the phase of first harmonic

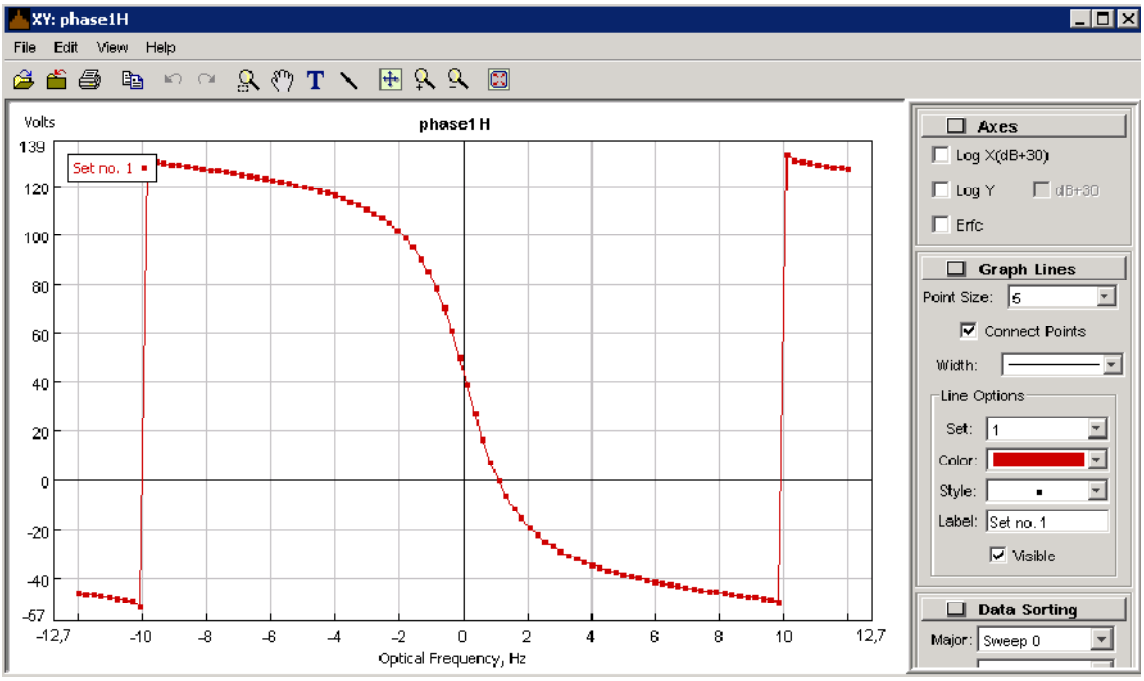

Figure 47. Phase graphic of the primer harmonic

The third is for the amplitude for the second harmonic

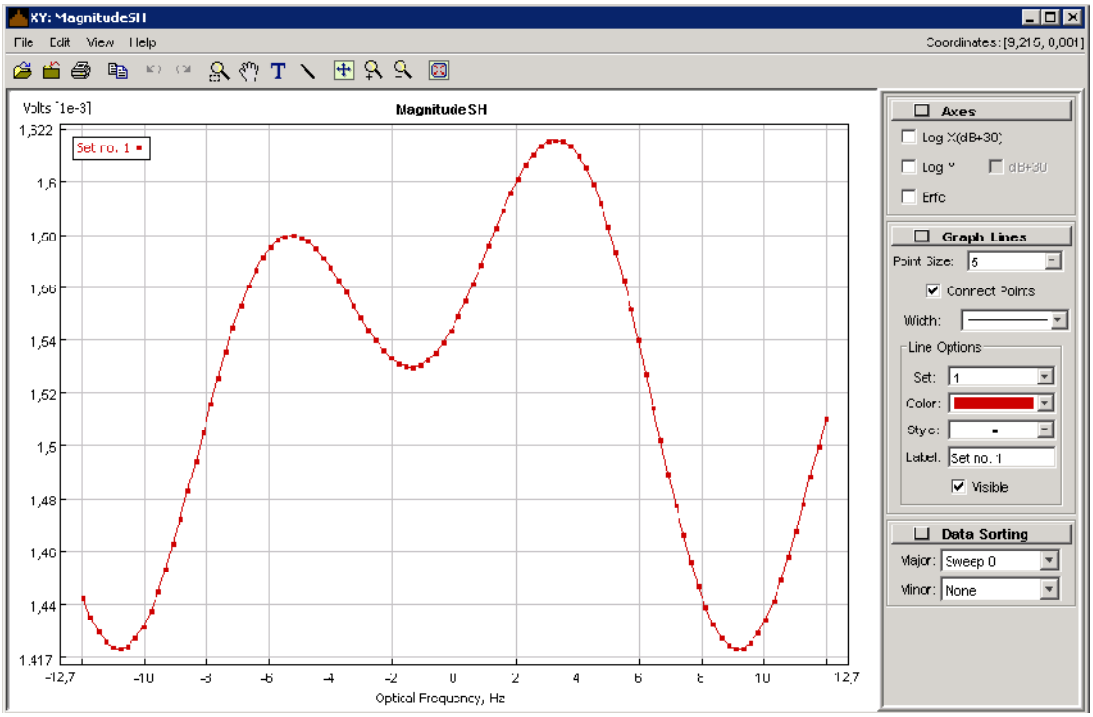

Figure 48. Amplitude graphic of the second harmonic

The fourth one is for the phase of second harmonic

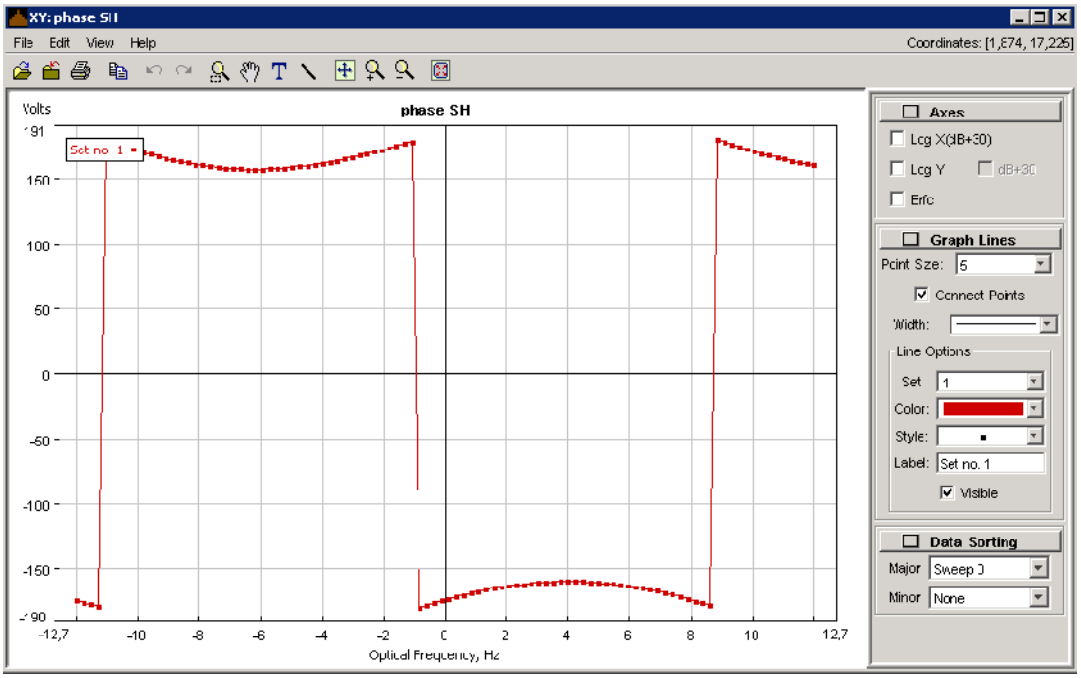

Figure 49. Phase graphic of the second harmonic

Now the next step is to take the values we need from these graphics and verify that these values can be obtained also with the MZI analytical model in matlab.

Well, we start putting the values in a table

Simulation frequency = 2.2 GHz	MATLAB	VPI
$\sum\phi$ in A_{1H}	$V_b(\sum\phi) = 79e-3V$	$V_b(\sum\phi) = 80e-3V$
$\Delta\phi$ in PH_{2H}	171.38°	171.39°
A^+A^- in A_{2H}	0.4591 V	0.4577 V
$\frac{A^+}{A^-}$ in PH_{1H}	1.455	1.446

Figure 50. Parameters values obtained with Matlab and VPI with f=2.2 GHz

The values of the VPI column can be obtained by the graphics; the values with Matlab need the following commands:

```
% frf=2.2e9
fo=1.924125324696149e14;
fp=fo+2.2e9;
fm=fo-2.2e9;
```

```
phi_mas=atan2((a-1)*sin(2*pi*fp*tau),(1-a)*cos(2*pi*fp*tau)-a);
phi_menos=atan2((a-1)*sin(2*pi*fm*tau),(1-a)*cos(2*pi*fm*tau)-a);
phi_cero=atan2((a-1)*sin(2*pi*fo*tau),(1-a)*cos(2*pi*fo*tau)-a);

suma_phi=phi_mas+phi_menos-2*phi_cero;  %calculo suma_phi
suma_phi_final=suma_phi-2*pi;           % quito el periodo 2pi
Vb_suma=(suma_phi_final)*10/pi;         % unwrap

delta_phi=(phi_mas-phi_menos)-2*pi;   %calculo delta_phi


Amas=sqrt((1-a)^2+a^2-2*a*(1-a)*cos(2*pi*fp*tau));
Amenos=sqrt((1-a)^2+a^2-2*a*(1-a)*cos(2*pi*fm*tau));
Ao=sqrt((1-a)^2+a^2-2*a*(1-a)*cos(2*pi*fo*tau));

AmasporAmenos=Amas*Amenos;                      %calculo producto de amplitud

AmasdivididoAmenos=Amas/Amenos;
```

Now we change the RF frequency and take f=2 GHz and run the system. So the table is

Simulation frequency = 2 GHz	MATLAB	VPI
$\sum\phi$ in A_{1H}	$V_b(\sum\phi) = 59.5e-3V$	$V_b(\sum\phi) = 60e-3V$
$\Delta\phi$ in PH_{2H}	-179.1°	-179.25°
A^+A^- in A_{2H}	1.659 V	1.659 V
$\frac{A^+}{A^-}$ in PH_{1H}	1.391	1.391

Figure 51. Parameters values obtained with Matlab and VPI with f=2 GHz

We do this for different RF frequencies and load these values on a excel file, which is in the annex [5]. In this file we put all the calculations: in a sheet we put, for the system with DUT, the bias value of the amplitude in the first harmonic , the phase for the first harmonic, the amplitude and the phase for the second harmonic; we do this for a set of six frequencies. In the next sheet we put, for the system without DUT, the same previous values. Then a sheet is dedicated to the phase and amplitude difference and to the phase and amplitude sum.

We have verified that the optical phase and amplitude values obtained through the RF scan at frequencies within a modulating frequency of the optical carrier agree with the values obtained in the previous sections.

V. CONCLUSIONS AND FUTURE LINES

In this master thesis we have presented a study about the dispersion phenomenon which limits the information capacity of the fibre, limiting the digital bit rate. Dispersion is defined in terms of the differences in group delay between optical wavelengths.

We studied a basic dispersion measurement system composed, mainly, of two devices which are the MZI Modulator and the MZI Optical Filter. We described these devices, with their possible configurations and with their transfer functions. The MZI Optical Filter, in particular, was our Device Under Test, which introduced phase and amplitude distortion on the signal which travels along the system.

Based on the same basic scheme, we studied different methods to measure the dispersion; each of them needed a certain configuration of the MZI Modulator. The MPSM used the Modulator in push-pull configuration and it recovers the semi difference between the optical phase shifts at each of the RF-generated optical sidebands at each side of the carrier as the electrical phase detected at the modulating frequency using a Vectorial Network Analyzer. IWe presented the mathematical analysis for this method with its final detected power expression. The same setup is good for Peucheret's method, which instead of measuring the detected signal's phase, bases the analysis on the amplitude term. By considering distortion in the amplitudes we have seen that while the Peucheret's method can still determine the dispersion value when the amplitudes get distorted, the MPSM introduces an error which is dependent on the amplitude difference imposed between the sidebands.

Then we showed the mathematical analysis of MZI Modulator in Asymmetric configuration, from which we obtained, firstly, the detected power expression with DUT, then without DUT contribution. In this analysis we considered only phase distortion. This allowed us to introduce the MZSM (Modulation Zero Shift Method). To explain this method we used the expression of power detected using the MZI in Asymmetric configuration. We worked with the amplitude, i.e. we measured the amplitude of detected signal (the modulus of S21) and we looked for the bias value which defined the zero in this amplitude. We also showed that this method is robust against amplitude distortions.

The main characteristics of all the methods to measure dispersion were organized in a summary table (Figure 99)

After this, we introduced a method which allowed us to scan the optical spectrum using a single optical carrier and a scan of modulating frequencies which we called RF-scan. It consisted of using, together, the MPSM with Asymmetric configuration and MSZM. Since the MPSM is affected by amplitude distortions this RF-scan method was vulnerable to amplitude distortions.

We laid the mathematical basis of a new method that allows to determine both the optical phase and amplitude spectra of the DUTs transfer function through RF-scan. The new method is based on MZ modulator in asymmetrical configuration and adds to the previous RF-scan method, information coming from the detected second harmonic which comes from the beating of the upper and lower optical sidebands in the absence of optical carrier (by using minimum transmission point biasing in the MZ modulator).

This method was verified with a simulation through the VPI program.

We used the analytical expression of the MZ Filter transfer function calculated in Matlab and that using a simulated standard measurement setup in VPI to test the validity of the method.

We also built a blocks system in VPI which represented the setup of the new RF-scan method. We set up the parameters of every device following the analysis done in the third chapter. With this simulation we obtained the graphics of the electrical amplitude and phase of the first and of the second harmonic as they would be obtained in a Vectorial Network Analyzer, and from these using the analysis in chapter 3 we determined the phase and amplitude spectrum of the MZI through calculations which we organized in an excel sheet.

We organized the simulation as follows: we chose six modulating frequencies, which represented the RF scan and for every frequency we carried out an asymmetric modulator bias value sweep measuring for every bias value the detected amplitude and phase of the first and second harmonic as measured in a vectorial network analyzer (using a frequency divider in the case of second harmonic).

From the VPI outcome we selected: the bias which brought the amplitude of the first harmonic to a minimum, the amplitude and phase of the second harmonic at the Asymmetric Modulator minimum transmission point and the phase of the first harmonic at the quadrature point. We inserted these in an excel file where following the results in the mathematical analysis of the new method we were able to get the values of the optical amplitude and phase transfer function of the MZI filter at frequencies located within an RF frequency of the optical carrier The results have shown agreement with those obtained from the analytical model of the MZI filter and also with those in a VPI setup simulating standard measurement systems of the optical phase and amplitude MZI filter transfer function.

Who wants to continue my work can, first of all, increase the number of modulating frequencies in order to have an RF scan with a high number of frequencies allowing for a broader optical frequency bandwidth. Another future line can be to study how to derive information in the frequency band close to the carrier because we have noticed a blind-zone there that cannot be resolved using our RF-scan. Since the electrical scan will always be limited in range, to combine it with an optical scan (i. e. use a tunable laser to change the carrier and apply again an RF scan) could be a good solution to cover extended optical bandwidths with high resolution. The laser frequency jumps could be broad in order to obtain good stability from the tunable laser while the RF-scan around every optical carrier could provide a good spectral resolution. In this sense we envision that it will be useful to cover with one optical carrier the blind-zone of the neighboring carrier.

Still in the simulation stage, there also remains to see how the method performs when the system setup is not as ideal as the one we used. To test it against a finite extinction ratio in the MZ modulator and other limitations due to poor performance of equipment in order to see if the method can work with low-cost equipment.

Obviously in order to complete the study about my method it is necessary an analysis in the laboratory with real instruments. In this way real problems coming from a practical implementation can be observed and solved.

ANNEX

1. Modulus with Matlab (Values obtained through VPI)

```
a=0.47;              % factor de acoplamiento mejor
c=3e8;               % velocidad de la luz
tau=115e-12;         % factor de retarso del filtro
omega0=f_vpi*2*pi;   % valores de omega

P=((1-a)*exp(-j.*omega0*tau)-a);     % el resultado tiene que ser las dos
graficas
y=abs(P).^2;                         % de la amplitude con matlab y vpi que se
solapan.
plot(f_vpi,abs(P).^2);               % El range de frecuencia es lo mismo, sacado
con
                                     % el vpi.


figure(2);
semilogy(f_vpi,y)                    % grafica de la amplitud (Matlab) con eje
logaritmico

figure(3)
plot(f_vpi,P_vpi);                % grafica de la amplitud con Vpi

figure(4)                         % Las dos amplitudes en la misma grafica
plot(f_vpi,P_vpi,'r');            %
hold on                           %
plot(f_vpi,abs(P).^2);            %
```

2. Phase with Matlab (values obtained through VPI)

```
%% Fase del MZ con Matlab y VPI


tau=115e-12;      % factor de retardo entre los caminos opticos

const=0.47;


omega1=f_vpi_ph*2*pi;


figure(5)
plot(f_vpi_ph,1/2*unwrap(2*fase_vpi)); %unrap de pi griego
hold on
fase_mat=atan2(-(1-a)*sin(2*pi*f_vpi_ph*tau),(1-a)*cos(2*pi*f_vpi_ph*tau)-a);
plot(f_vpi_ph,unwrap(fase_mat),'r');
```

3. Cosine determination

```
% Calculo cos(fase) sin acoplador "abajo" del filtro

const=0.47;
tau=115e-12;
omega1_cos=f_ph_cos*2*pi;

A1=sqrt((1-const)^2+const^2-2*const*(1-const)*cos(omega1_cos.*tau)); %A1=abs(P)
A2=(1-const)^2+const^2-2*const*(1-const)*cos(omega1_cos.*tau);    % A2=abs(P).^2

cosenofase=(A2+1-4*p_ph_cos)./(2*A1);


omega1_sin=f_ph_sin*2*pi;

A1=sqrt((1-const)^2+const^2-2*const*(1-const)*cos(omega1_sin.*tau)); %A1=abs(P)
A2=(1-const)^2+const^2-2*const*(1-const)*cos(omega1_sin.*tau);    % A2=abs(P).^2

senfase=(A2+1-4*p_ph_sin)./(2*A1);
        % matrix dimensions must agree
fase=atan2(senfase,cosenofase)
```

4.Determination of Dispersion parameters

```
%% Calculo de la suma_phi, delta_phi, A1*A2, A1/A2

% frf=2.2e9
fo=1.924125324696149e14;
fp=fo+2.2e9;
fm=fo-2.2e9;

phi_mas=atan2((a-1)*sin(2*pi*fp*tau),(1-a)*cos(2*pi*fp*tau)-a);
phi_menos=atan2((a-1)*sin(2*pi*fm*tau),(1-a)*cos(2*pi*fm*tau)-a);
phi_cero=atan2((a-1)*sin(2*pi*fo*tau),(1-a)*cos(2*pi*fo*tau)-a);

suma_phi=phi_mas+phi_menos-2*phi_cero;  %calculo suma_phi
suma_phi_final=suma_phi-2*pi;           % quito el periodo 2pi
Vb_suma=(suma_phi_final)*10/pi;         % unwrap

delta_phi=(phi_mas-phi_menos)-2*pi;   %calculo delta_phi


Amas=sqrt((1-a)^2+a^2-2*a*(1-a)*cos(2*pi*fp*tau));
Amenos=sqrt((1-a)^2+a^2-2*a*(1-a)*cos(2*pi*fm*tau));
Ao=sqrt((1-a)^2+a^2-2*a*(1-a)*cos(2*pi*fo*tau));

AmasporAmenos=Amas*Amenos;                      %calculo producto de amplitud
x=10*log10(AmasporAmenos);
AmasdivididoAmenos=Amas/Amenos;                 % calculo division de amplitud
y=10*log10(AmasdivididoAmenos);

% frf=2e9
clear all
a=0.47;
tau=115e-12;
fo=1.924125324696149e14;
fp_1=fo+2e9;
fm_1=fo-2e9;

phi_mas_1=atan2((a-1)*sin(2*pi*fp_1*tau),(1-a)*cos(2*pi*fp_1*tau)-a);
phi_menos_1=atan2((a-1)*sin(2*pi*fm_1*tau),(1-a)*cos(2*pi*fm_1*tau)-a);
phi_cero=atan2((a-1)*sin(2*pi*fo*tau),(1-a)*cos(2*pi*fo*tau)-a);

suma_phi_1=phi_mas_1+phi_menos_1-2*phi_cero;  %calculo suma_phi
suma_phi_final_1=suma_phi_1-2*pi           % quito el periodo 2pi
Vb_suma_1=(suma_phi_final_1)*10/pi;         % unwrap

delta_phi_1=(phi_mas_1-phi_menos_1)-2*pi   %calculo delta_phi


Amas_1=sqrt((1-a)^2+a^2-2*a*(1-a)*cos(2*pi*fp_1*tau));
Amenos_1=sqrt((1-a)^2+a^2-2*a*(1-a)*cos(2*pi*fm_1*tau));
Ao=sqrt((1-a)^2+a^2-2*a*(1-a)*cos(2*pi*fo*tau));

AmasporAmenos_1=Amas_1*Amenos_1;                    %calculo producto de
amplitud
x1=10*log10(AmasporAmenos_1);
AmasdivididoAmenos_1=Amas_1/Amenos_1;
y1=10*log10(AmasdivididoAmenos_1);
```

5.Results of the simulation

Without DUT

frecuencia RF	θbz	PH(1H)	A2H	PH(2H)
1 GHz				
1,2 GHz	0 V	-35,95	3,1312e-3 V	-90
1,4 GHZ	0 V	-167,96	3,1315e-3 V	-90
1,6 GHz	0 V	27,22	3,1313e-3 V	-90
1,8 GHz	0 V	94,38	3,132e-3 V	-90
2 GHz	0 V	148,26	3,1312e-3 V	-90
2,2 GHz	0 V	165,88°	3,1312e-3 V	-90

With DUT

frecuencia RF	θbz	PH(1H)	A2H	PH(2H)
1 GHz	10e-3 V	69,14	2.6357e-3 V	-134,1
1,2 GHz	20e-3 V	65,195	2,4764e-3 V	-142,99
1,4 GHz	20e-3 V	61,64	2,29419e-3 V	-151,94
1,6 Ghz	33.3e-3 V	-122,905	2,0946e-3 V	-160,947
1,8 GHz	40e-3 V	-127,45	1,8816e-3 V	-170,04
2 GHz	60e-3 V	-131,4	1,659572e-3 V	-179,25
2,2 GHz	80e-3 V	-135,5°	1,43316e-3V	171,38°

3A

frecuencia RF	suma_amplitud	delta_amplitud
1,2 GHz	-1,0202	0,7493
1,4 GHz	-1,3513	0,8971
1,6 Ghz	-1,7454	1,0577
1,8 GHz	-2,2088	1,2347
2 GHz	-2,7502	1,4332
2,2 GHz	-3,3809	1,6599

3PH

frecuencia RF	suma_phi	delta_phi
1,2 GHz	0,005	-0,925
1,4 GHz	0,0072	-1,0811
1,6 Ghz	0,01	-1,2383
1,8 GHz	0,0136	-1,3969
2 GHz	0,0184	-1,5575
2,2 GHz	0,0248	-1,7207

4PHdiff+

(delta_phi2_1)plus	(delta_phi3_2)plus	(delta_phi4_3)plus	(delta_phi5_4)plus	(delta_phi2_1)plus
-0,07695	-0,0772	-0,0775	-0,0779	-0,0784

5PHdiff-(delta_phi2_1)menus	(delta_phi3_2)menus	(delta_phi4_3)menus	(delta_phi5_4)menus	(delta_phi6_5)menus
0,07915	0,08	0,0811	0,0827	0,0848

4Adiff+

(delta_amp2_1)plus	(delta_amp3_2)plus	(delta_amp4_3)plus	(delta_amp5_4)plus	(delta_amp6_5)plus
-0,09165	-0,11675	-0,1432	-0,17145	-0,202

5Adiff-

(delta_amp2_1)menus	(delta_amp3_2)menus	(delta_amp4_3)menus	(delta_amp5_4)menus	(delta_amp6_5)menus
-0,23945	-0,27735	-0,3202	-0,36995	-0,4287

6PH+

phi_zero	0
delta_phi1	-0,925
phi1_plus	-0,925
phi2_plus	-1,00195
phi3_plus	-1,07915
phi4_plus	-1,15665
phi5_plus	-1,23455
phi6_plus	-1,31295

7PH-

phi_zero	0
delta_phi1	-0,925
phi1_menus	0,925
phi2_menus	1,00415
phi3_menus	1,08415
phi4_menus	1,16525
phi5_menus	1,24795
phi6_menus	1,33275

6A+

amp_zero	0
amp_phi1	0,7493
amp1_plus	0,7493
amp2_plus	0,65765
amp3_plus	0,5409
amp4_plus	0,3977
amp5_plus	0,22625
amp6_plus	0,02425

7A-

amp_zero	0
amp_phi1	0,7493
amp1_menus	-0,7493
amp2_menus	-0,98875
amp3_menus	-1,2661
amp4_menus	-1,5863
amp5_menus	-1,95625
amp6_menus	-2,38495

Ringraziamenti

Per la realizzazione di questa tesi vorrei ringraziare le persone che mi sono state vicine: mia madre, che non mi ha mai fatto mancare nulla; i miei fratelli, che mi hanno dato forza nei momenti più difficili; la mia compagna, che mi ha incoraggiato in questa esperienza all'estero e che mi ha dato preziosi consigli.

Inoltre vorrei rivolgere un saluto a tutte quelle persone che ho incontrato e conosciuto in Spagna; compagni di università di nazionalità diverse che non dimenticherò mai.